

**EUROPEAN SCHOOL OF MOLECULAR MEDICINE  
SEDE DI NAPOLI  
UNIVERSITA' DEGLI STUDI DI NAPOLI "FEDERICO II"  
Ph.D. in Molecular Medicine – Ciclo III/XXI  
Human Genetics**



**“The Alzheimer’s Amyloid precursor protein APP and the adaptor protein Fe65: their role in the cellular response to DNA damage”**

**Tutor:  
Prof. Tommaso Russo**

**Internal Supervisor:  
Prof. Alfredo Fusco**

**External Supervisor:  
Prof. Christopher C. J. Miller**

**Coordinator:  
Prof. Francesco Salvatore**

**Ph.D. student:  
Dr. Maria Stante**

**Academic Year: 2008-2009**

<b>Index</b>	<b>pag. 1</b>
<b>Abstract</b>	<b>pag.5</b>
<b>Introduction</b>	<b>pag. 7</b>
1. Familial and sporadic Alzheimer's disease	pag. 7
2. Pathological features of Alzheimer's disease	pag. 9
3. APP proteolytic processing: focusing on $\gamma$ -secretase complex activity	pag. 12
4. Gain of function versus loss of function hypothesis in AD: learning from mouse model	pag.21
5. The APP function	pag. 25
6. The adaptor protein Fe65	pag. 30
7. Neurodegeneration and DNA damage response	pag. 33
8. The aims of the thesis	pag. 37
<b>Materials and Methods</b>	<b>pag. 38</b>
1. Generation of Fe65 knock out mouse embryonic fibroblast (MEFs)	pag. 38
2. DNA damaging agents treatment and irradiation of mice	pag. 38
3. Comet Assay	pag. 39
4. Cell culture conditions and transfection of shRNAs and siRNAs	pag. 39
5. Generation of the recombinant constructs in pRcCMV vector	pag. 40
6. Immunofluorescence	pag. 42
7. Immunoprecipitation, western blot and antibodies	pag. 42
8. Histone association assay	pag. 43
9. Chromatin immunoprecipitation	pag. 44
10. MNase assay	pag. 46
11. Cloning of mutants in p-Babe-puro retroviral vector	pag. 46
12. Retroviral production and infection	pag. 47
13. Generation of NIH-GS cells and measurement of DNA repair efficiency	pag. 47
14. FACS analysis	pag. 49

<b>Results</b>	pag. 50
1. Fe65 KO MEFs are highly sensitive to DNA damage	pag. 50
2. Fe65 knock down (KD) cells have the same phenotype of KO MEFs	pag. 53
3. Fe65 should be present in the nucleus to rescue the hypersensitivity of Fe65 KO MEFs to genotoxic stress	pag. 55
4. Fe65 KO and KD cells show high level of phosphorylated H2AX and p53 under genotoxic stress condition	pag. 58
5. ATM activation and NBS phosphorylation seem to be normal in Fe65 KO MEFs upon DNA damage induction	pag. 60
6. Effects of DNA damage in Fe65 KO mice	pag. 62
7. Fe65 associates with intact and damaged chromatin and undergoes rapid phosphorylation in response to DNA damage	pag. 64
8. Fe65 association with chromatin determines its degree of condensation	pag. 69
9. Fe65 mutants lacking the WW and the PYB1 domains or carrying C655F point mutatin are unable to rescue the Fe65 KO MEFs phenotype	pag. 72
10. Generation of DR-GFP/ISceI-ER system to study Fe65 involvemet in chromatin remodelling during DNA repair	pag. 76
11. Fe65 suppression prevents the recruitment of Tip60/TRRAP at DNA Double strand breaks	pag. 79
12. The $\Delta$ PTB1 mutant overexpression decreases Tip60 recruitment and Istone H4 acetylation at DNA breaks.	pag. 82
13. The $\Delta$ PTB1 dominant negative effect depends on its interaction with chromatin	pag. 84
14. Fe65 is necessary for efficient DNA repair	pag. 87
15. APP processing is induced by genotoxic stress in a $\gamma$ -secretase Dependent manner	pag. 92
16. The interaction with APP is required for Fe65 function in DNA repair	pag. 94
17. The dominant negative effect of C655F mutant dependes in its ability to interact with chromatin	pag. 98
18. Fe65 interaction with APP is essential for its association with chromatin and in turn for its proper function in DNA repair.	pag. 100

**Discussion**

pag. 104

**References**

pag. 112

## ABSTRACT

Fe65 interacts with the cytosolic domain of the Alzheimer's amyloid precursor protein (APP). The functions of the Fe65 and of the Fe65/APP complex are still unknown. To address this point we generated Fe65 knock out mice. These mice do not show any obvious phenotype, however, when fibroblasts (MEFs), isolated from Fe65 KO embryos, were exposed to low doses of DNA damaging agents, such as etoposide or H<sub>2</sub>O<sub>2</sub>, an increased sensitivity to genotoxic stress, compared to wild type animals, clearly emerged. Accordingly, brain extracts from Fe65 KO mice, exposed to non-lethal doses of ionizing radiations, showed high levels of  $\gamma$ -H2AX and p53, thus demonstrating a higher sensitivity to X-rays than wild type mice. Nuclear Fe65 is necessary to rescue the observed phenotype and, few minutes after the exposure of MEFs to DNA damaging agents, Fe65 undergoes phosphorylation in the nucleus. With a similar timing, the proteolytic processing of APP is rapidly affected by the genotoxic stress: in fact, the cleavage of the APP C-terminal fragments by  $\gamma$ -secretase is induced soon after the exposure of cells to etoposide, in a Fe65-dependent manner. These results demonstrate that Fe65 plays an essential role in the response of the cells to DNA damage. Moreover we found that Fe65 is a chromatin bound protein that determines the degree of chromatin condensation both in basal and under genotoxic stress conditions. Fe65 association with chromatin is required during DNA damage repair. Indeed a known partner of Fe65 is the histone acetyltransferase Tip60. Considering the crucial role of Tip60 in DNA repair, we explored the hypothesis that the phenotype of Fe65 null cells was dependent on its interaction with Tip60. We demonstrated that Fe65 knockdown impaired recruitment of Tip60-TRRAP complex to DNA double strand breaks and decreased histone H4 acetylation. Accordingly, the efficiency of DNA repair was decreased upon Fe65 suppression. To explore whether APP has a role in this mechanism, we analyzed a Fe65 mutant unable to bind to APP. This mutant failed to rescue the phenotypes of Fe65 null cells; furthermore, APP/APLP2

suppression results in the impairment of recruitment of Tip60-TRRAP complex to DNA double strand breaks, decreased histone H4 acetylation and repair efficiency. On these bases, we propose that Fe65 and its interaction with APP play an important role in the response to DNA damage by assisting the recruitment of Tip60-TRRAP to DNA damage sites.

# INTRODUCTION

## **1. Familial and sporadic Alzheimer's disease**

A century ago, Alois Alzheimer first described the neurological disease that bears his name. He described typical clinical characteristics with memory disturbances and instrumental signs, and he detailed two characteristic pathological features that are observed post mortem: amyloid plaques, and neurofibrillary tangles in the cerebral cortex and limbic system, which we today know as the hallmarks of the disease. Alzheimer's disease (AD) is a slowly progressive disorder, with insidious onset and progressive decline in cognitive and functional abilities as well as behavioral and psychiatric symptoms leading to a vegetative state and ultimately death. AD is the most common cause of dementia, accounting for 50–60% of all cases (Moller and Graeber 1998). The prevalence of dementia is below 1% in individuals aged 60–64 years, but shows an almost exponential increase with age, so that in people aged 85 years or older the prevalence is between 24% and 33% in the Western world. AD is very common and thus it is a major public health problem. In 2001, more than 24 million people had dementia, a number that is expected to double every 20 years up to 81 million in 2040 because of the anticipated increase in life expectancy (Ferri, Prince et al. 2005). Besides ageing, which is the most obvious risk factor for the disease, epidemiological studies have suggested several tentative associations. Some can be linked to brain trauma (Jellinger 2004), vascular diseases (Mayeux 2003), dietary life style (Luchsinger and Mayeux 2004), but data so far are not conclusive. Although environmental factors might increase the risk of sporadic AD, this form of the disease has been shown to have a significant genetic background. A large population based twin study showed that the extent of heritability for the sporadic disease is almost 80% (Gatz, Reynolds et al. 2006). Alzheimer's disease is a heterogeneous disorder with both familial and sporadic forms. Familial AD is an autosomal dominant

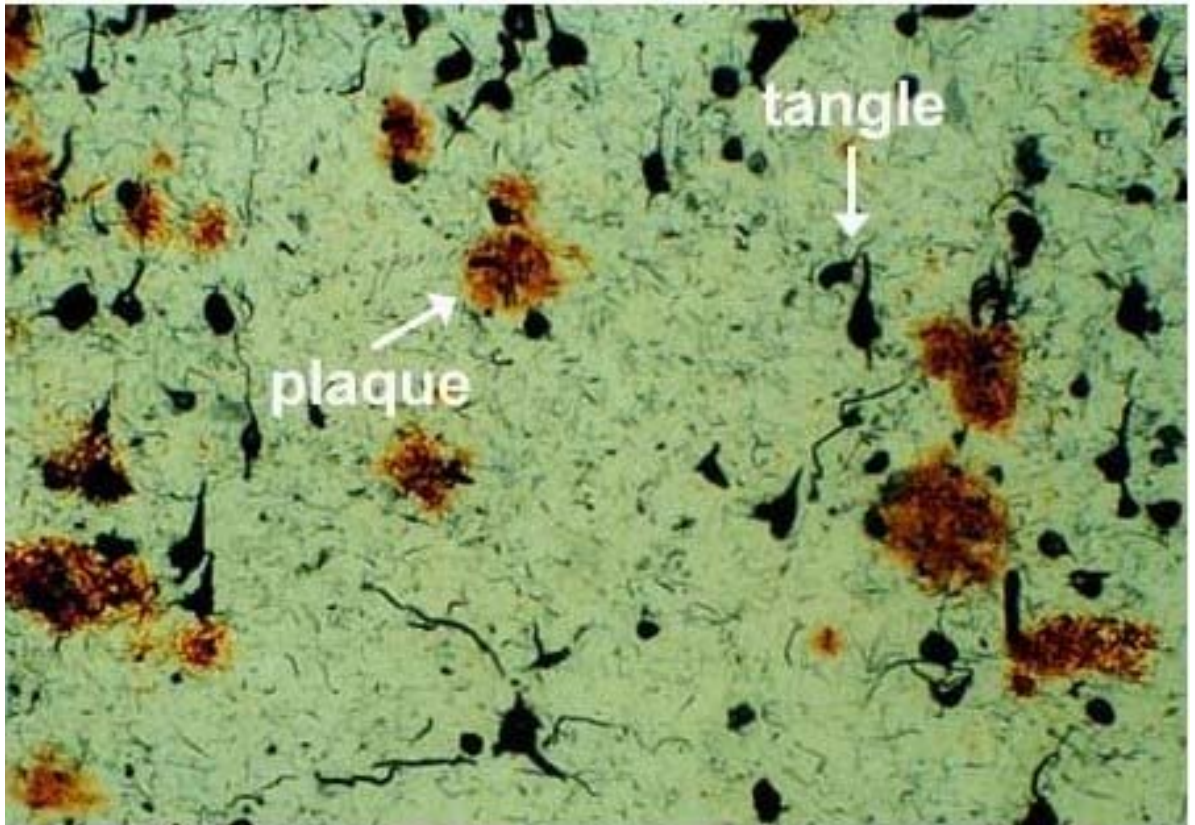
disorder with onset before age 65 years. Four genes have been unequivocally implicated in inherited forms of AD and mutations or polymorphisms in these genes cause excessive cerebral accumulation of the amyloid  $\beta$ -protein and subsequent neuronal and glial pathology in brain regions important for memory and cognition. The first mutation causing the familial form of the disease was identified in the amyloid precursor protein (APP) gene on chromosome 21 (St George-Hyslop, Haines et al. 1990). In 1988, the *APP* gene was found to reside on chromosome 21, which is triplicated in Down syndrome (trisomy 21). Indeed, most Down syndrome patients manifest Alzheimer disease (AD) by the age of 50, and post-mortem analyses of those who die young show diffuse intraneuronal deposits of A $\beta$  in the absence of any tau pathology, suggesting that A $\beta$  deposition is an early event in AD. When investigating other families with the familial disease, several additional APP mutations were found. The recent discovery of an extra copy of the *APP* gene in familial AD (Rovelet-Lecrux, Hannequin et al. 2006) provides further support that increased A $\beta$  production can cause the disease. However, these mutations explain only a few familial cases. Indeed in 1995 mutations in the highly homologous presenilin 1 (PSEN1) and presenilin 2 (PSEN2) genes were also linked with early-onset familial AD (Levy-Lahad, Lahad et al. 1995) (Rogaev, Sherrington et al. 1995) and they account for most cases of familial disease. However, the familial form of the disease is rare, with a prevalence below 0.1%. In 1993, two groups independently reported an association between the apolipoprotein E (APOE)  $\epsilon$ 4 allele and AD (Poirier, Davignon et al. 1993). Meta-analysis showed that the APOE  $\epsilon$ 4 allele increases the risk of the disease by three times in heterozygotes and by 15 times in homozygotes (Dickson, Saunders et al. 1997). The mechanism underlying this increased risk is not completely clear, yet mounting evidence supports the idea that the ability of apoE to interact with the amyloid- $\beta$  peptide and influence its conformation and clearance plays a major role. In vivo, it has been shown that breeding of APP-overexpressing mice with apoE knockout mice completely abolishes

amyloid plaque deposition in the brain of hybrid animals, confirming that apoE favours the extracellular  $\beta$ -amyloid deposition impairing through still unknown mechanisms the  $\beta$ -amyloid clearance. Other susceptibility loci have been identified, but the data so far are unclear.

## **2. Pathological features of Alzheimer disease**

At the microscopic level, the characteristic lesions in Alzheimer's disease are senile or neuritic plaques and neurofibrillary tangles (Figure 1) in the medial temporal lobe structures and cortical areas of the brain, together with a degeneration of the neurons and synapses. These histological lesions can be observed as neuritic plaques or diffuse plaques. Neuritic plaques are microscopic foci of extracellular amyloid deposition and associated axonal and dendritic injury. The plaques are composed primarily of the 39–43-residue amyloid  $\beta$ -peptide ( $A\beta$ ) (Wolfe 2006).  $A\beta$  is released from the amyloid precursor protein (APP) by the sequential action of  $\beta$ - and  $\gamma$ -secretases, with the latter cutting relatively heterogeneously (Esler and Wolfe 2001). Most of the  $A\beta$  produced by  $\gamma$ -secretase is the 40-residue form ( $A\beta_{40}$ ); however, the major  $A\beta$  species deposited in the plaques is the 42-residue variant ( $A\beta_{42}$ ), although this peptide represents only 5–10% of all  $A\beta$  produced. Such plaques contain extracellular deposits of amyloid  $\beta$ -protein ( $A\beta$ ) that occur principally in a filamentous form, i.e., as star-shaped masses of Amyloid fibrils. Dystrophic neurites occur both within this amyloid deposit and immediately surrounding it (Poirier 2003). Such plaques are also intimately associated with microglia expressing surface antigens associated with activation, such as CD45 and HLA-DR, and they are surrounded by reactive astrocytes displaying abundant glial filaments. Diffuse plaques show a finely granular pattern, without a clearly fibrillar, compacted center associated with little or not detectable neuritic dystrophy. It has been suggested that these plaques might represent precursor lesions of neuritic plaques.

**Figure 1 : Plaques and tangles in the cerebral cortex in Alzheimer's disease**



Plaques are extracellular deposits of  $A\beta$  surrounded by dystrophic neurites, reactive astrocytes, and microglia, whereas tangles are intracellular aggregates composed of a hyperphosphorylated form of the microtubule-associated protein tau.

The hypothesis that diffuse plaques represent immature lesions that are precursors to the plaques with surrounding cytopathology arose from two lines of evidence. First, diffuse plaques are the sole form found in the brain regions that largely or entirely lacked neuritic dystrophy, glial changes, and neurofibrillary tangles and are not clearly implicated in the typical clinical symptoms of AD, e.g., cerebellum, striatum, and thalamus. Second, healthy aged individuals free of AD or other dementing processes often show solely diffuse plaques in limbic and association cortices, i.e., in the same regions where Alzheimer patients show mixtures of diffuse and neuritic plaques.

Neurofibrillary tangles are large, non membrane bound bundles of abnormal fibers that accumulate in the perinuclear region of cytoplasm. Electron microscopy reveals that most of these fibers consist of pairs of 10-nm filaments wound into helices (paired helical filaments or PHF), composed of the microtubule-associated protein tau (Brion, Couck et al. 1985) (Kosik, Joachim et al. 1986) (Nukina and Ihara 1986) (Wood, Mirra et al. 1986), which is present in a hyperphosphorylated form. A variety of kinases have been shown to be capable of phosphorylating tau in vitro at various sites (Illenberger, Zheng-Fischhofer et al. 1998), that leads to its apparent dissociation from microtubules and aggregation into insoluble paired helical filaments. The two classical lesions of AD, neuritic plaques and neurofibrillary tangles, can occur independently of each other. Tangles composed of tau aggregates that are biochemically similar to or, in some cases, indistinguishable from those in AD have been described in more than a dozen of less common neurodegenerative diseases, in almost all of which no A $\beta$  deposits and neuritic plaques are present. Conversely, A $\beta$  deposits can be seen in the brains of cognitively normal-aged humans in the virtual absence of tangles (Terry, Hansen et al. 1987).

Genetic and pathological evidence strongly supports the amyloid cascade hypothesis of AD, which states that amyloid- $\beta$ 42, the proteolytic derivative of APP, has an early and vital role in all cases of AD. Indeed APP mutations associated with early-onset dominant

AD are located in and around the A $\beta$  region of the encoded type I integral membrane glycoprotein. These mutations were soon determined to alter the amount of A $\beta$  produced, the ratio of A $\beta$ 42 to A $\beta$ 40 or the amino-acid sequence of A $\beta$  (Selkoe and Kopan 2003). Mutations near the  $\beta$ -secretase cleavage site make APP a better substrate for this enzyme and lead to increased production of all forms of A $\beta$ . Mutations near the  $\gamma$ -secretase cleavage site lead to increases in the more aggregation-prone A $\beta$ 42 relative to A $\beta$ 40, and mutations in the A $\beta$  region itself change the biophysical properties of the peptide to render it more likely to aggregate. These findings provided the first compelling evidence that A $\beta$  might be involved in the pathogenesis of AD rather than simply being a marker. Moreover, the AD-associated mutations of PS1 and PS2 genes, were soon determined to increase the ratio of A $\beta$ 42 to A $\beta$ 40 (A $\beta$ 42/A $\beta$ 40) in mice and humans (Borchelt, Thinakaran et al. 1996) (Citron, Oltersdorf et al. 1992) (Scheuner, Eckman et al. 1996), indicating that presenilins might modify the way in which  $\gamma$ -secretase cuts APP.

### **3. APP proteolytic processing : focusing on $\gamma$ -secretase complex activity**

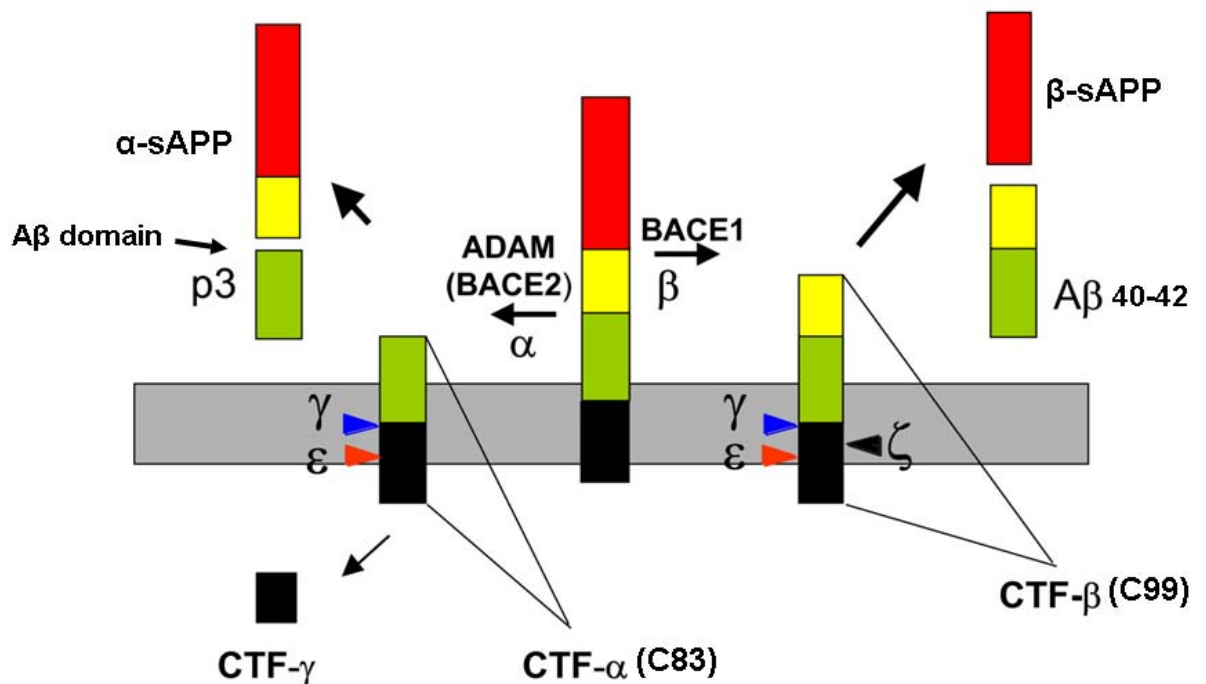
The purification and partial sequencing of the A $\beta$  protein from meningovascular amyloid deposits in AD led to the cloning of the gene encoding the  $\beta$ -APP (Kang, Lemaire et al. 1987). A $\beta$  is derived from its large precursor protein by sequential proteolytic cleavages. APP is an integral membrane protein with a single membrane spanning domain, a large extracellular glycosylated N-terminus and a shorter cytoplasmic C-terminus. A $\beta$  is located at the cell surface (or on the luminal side of ER and Golgi membranes), with part of the peptide embedded in the membrane. APP (Kang et al. 1987) (Goldgaber, Lerman et al. 1987) is a member of an evolutionarily conserved family of type I membrane proteins. Mammals have two APP-like paralogues, APLP-1 and APLP-2 (Wasco, Bupp et al. 1992), which have substantial homology, both within the large ectodomain and particularly within

the cytoplasmic tail, but are largely divergent in the A $\beta$  region. The evolutionary conservation of the APP gene family also extends to invertebrates, with the *Drosophila* gene product known as APPL and the *Caenorhabditis elegans* homologue named APL-1.

APP comprises a heterogeneous group of ubiquitously expressed polypeptides derived from alternatively spliced isoforms, yielding 3 isoforms of 695, 751, and 770 residues. The most abundant form in brain is APP695, that is produced mainly by neurons, and differs from longer forms of APP in that it lacks a kunitz type protease inhibitor sequence in its ectodomain (Hardy and Hutton 1995).

Both during and after its trafficking through the secretory pathway to the cell surface, a subset of APP molecules undergoes specific endoproteolytic cleavages to release secreted derivatives into vesicle lumens and the extracellular space (Figure 2). Enzyme activities involved in cleavage of APP at the  $\alpha$ -,  $\beta$ - and  $\gamma$ -secretase sites are being identified (Annaert, Levesque et al. 1999). The majority of APP is cleaved by  $\alpha$ -secretases within the A $\beta$  sequence thus precluding A $\beta$  generation (Ikezu, Trapp et al. 1998). The identity of  $\alpha$ -secretase remains unclear, although metalloproteases as TACE (an enzyme responsible for cleavage of members of the TNF receptor family at the cell surface) and ADAM9 and ADAM10 are candidates (Hutton, Lendon et al. 1998; Illenberger, Zheng-Fischhofer et al. 1998). This cleavage results in the release of soluble sAPP $\alpha$  and retention of a C83 fragment in the membrane. Cleavage of C83 by  $\gamma$ -secretase results in release of a p3 fragment (approximately 3 kDa) and  $\gamma$ -cleaved C-terminal fragments ( $\gamma$ CTF) also known as the APP intracellular domain (AICD). Amyloidogenic processing of APP involves sequential cleavages by BACE and  $\gamma$ -secretase at the N- and C-termini of A $\beta$ , respectively. Cleavage of C99 by  $\gamma$ -secretase generates the AICD and A $\beta$  peptides including A $\beta$ 40 and the more amyloidogenic A $\beta$ 42 (Selkoe 2001). The concept that missense mutations in APP cause AD via an amyloidogenic mechanism is strongly supported by the fact that all of the

**Figure 2: Proteolytic processing of APP**



APP is a transmembrane protein with a large N-terminal extracellular domain and a short cytosolic tail. In the  $\alpha$ -secretase pathway,  $\alpha$  secretase cleaves APP within the A $\beta$  domain, releasing the large soluble APP fragment ( $\alpha$ -sAPP). The remaining C-terminal fragment (CTF), C83, is cleaved by the  $\gamma$ -secretase releasing the short p3 peptide. The remaining APP intracellular domain (AICD) is metabolised in the cytoplasm. In the  $\beta$ -secretase pathway,  $\beta$ -secretase cleaves APP upstream of the A $\beta$  domain, releasing soluble  $\beta$ sAPP. The remaining CTF, C99, is cleaved by the  $\gamma$ -secretase releasing the free 40 or 42 aminoacid A $\beta$  peptide. Two further cleavage sites of the  $\gamma$ -secretase, termed  $\epsilon$  and  $\zeta$ , are present in the CTF. The remaining AICD is metabolised in the cytoplasm. (Figure modified from Sastre *et al. Journal of Neuroinflammation* 2008 5:25)

known mutations occur within the region encoded by A $\beta$  or immediately adjacent to  $\beta$ - and  $\gamma$ -secretase cleavage sites (Hardy 1997). Indeed, these mutations alter either the properties of A $\beta$  or how much and what type of A $\beta$  is produced. The “Swedish” double mutation found at the P2 and P1 sites for  $\beta$ -secretase causes more efficient processing of APP by this aspartyl protease, resulting in a several-fold increase in the production of both A $\beta$ 40 and A $\beta$ 42 (Citron, Oltersdorf et al. 1992). On the other hand, the several mutations located C-terminal to the  $\gamma$ -secretase site increase the ratio of peptides ending at A $\beta$ 42 to those ending at A $\beta$ 40 (De Jonghe, Esselens et al. 2001) (Suzuki, Cheung et al. 1994) (Scheuner, Eckman et al. 1996). Because the hydrophobic A $\beta$ 42 peptide is more prone to self-assembly (Jarrett, Berger et al. 1993), increases in its relative amount can promote the formation of oligomeric intermediates and, eventually, mature amyloid fibrils. Among the mutations associated with prominent microvascular deposition, the E22Q (“Dutch”) peptide aggregates on the surfaces of smooth muscle and endothelial cells and thus confers local toxicity that could lead to necrosis and vessel rupture (Eisenhauer, Johnson et al. 2000) (Van Nostrand, Melchor et al. 2001) (Wang, Natte et al. 2000). Another major clue to Alzheimer pathogenesis involving APP proteolytic processing, came with the discovery of two related genes, presenilin-1 (PS1) and presenilin-2 (PS2), likewise associated with early-onset disease (Sherrington, Rogaev et al. 1995) (Levy-Lahad, Wasco et al. 1995) (Rogaev, Sherrington et al. 1995). PS1 mutations cause the earliest and most-aggressive form of AD, commonly leading to onset of symptoms in the fifth decade of life and demise of the patient in the sixth. PS2 mutations generally have a slightly later and more-variable age of onset. More than 100 such missense mutations have been identified so far and the vast majority of those examined in detail skew the proportion of A $\beta$  toward the more aggregation-prone 42-residue form (Tanzi and Bertram 2005). Thus, the presenilin mutations change the cleavage site specificity of  $\gamma$ -secretase. The knockout of PS1 in mice was found to markedly reduce  $\gamma$ -secretase cleavage of APP, and follow-up studies showed

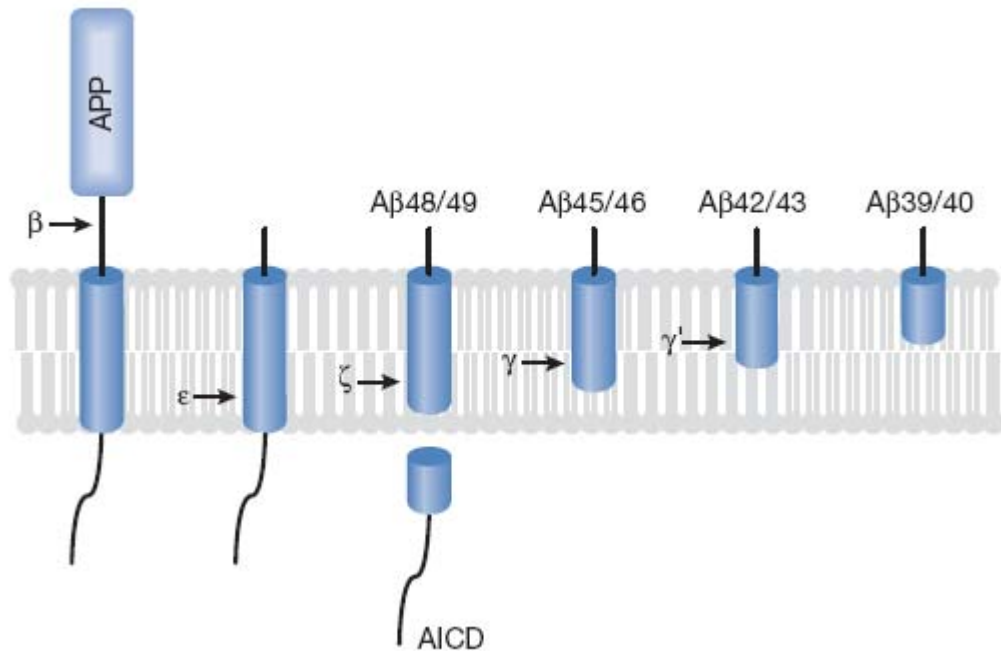
that the knockout of both PS1 and PS2 eliminated  $\gamma$ -secretase cleavage completely (Herreman, Serneels et al. 2000) (Zhang, Goodyer et al. 2000). Presenilins are therefore essential for this proteolytic function. Parallel studies revealed that peptide-substrate mimics with classical aspartyl protease-inhibitory motifs could inhibit  $\gamma$ -secretase, suggesting that the enzyme belongs to this category of proteases (Wolfe, De Los Angeles et al. 1999). This led to the identification of two conserved transmembrane aspartates in presenilin that are essential for  $\gamma$ -secretase activity, and the idea that presenilin is the catalytic component of the enzyme (Wolfe, Xia et al. 1999).

Presenilin mutations occur in the catalytic subunit of the protease responsible for determining the length of A $\beta$  peptides. Presenilin also has non-proteolytic functions (Baki, Shioi et al. 2004) (Huppert, Ilagan et al. 2005), the disruption of which might also contribute to familial AD pathogenesis. However, presenilin and  $\gamma$ -secretase have other substrates besides APP. After interacting with its cognate ligands, the Notch receptor undergoes a series of proteolytic events, in a manner similar to APP, ultimately releasing the intracellular domain that mediates the expression of genes controlling many types of cellular differentiation. We now know that the same  $\gamma$ -secretase cuts the transmembrane domain of the APP and Notch families of proteins, as well as a long list of other type I integral membrane proteins, including neuregulin and its receptor ErbB4, E-cadherins and N-cadherins, CD44, LDL-receptorrelated protein (LRP), nectin-1 and growth hormone receptor.

Cleavage of some of these substrates apparently has a role in cell signalling, but other cleavage events might simply be a means of clearing out membrane-bound stubs after ectodomain shedding (Schroeter, Ilagan et al. 2003). In parallel with the discovery of presenilin as a protease that cleaves APP and Notch, AD-causing mutations in presenilin were found to have reduced proteolytic function. Yankner and colleagues first showed this effect with a range of mutant presenilins by using a Notch-based luciferase-reporter assay

(Song, Nadeau et al. 1999). Several other groups have since noted this phenomenon; for example, De Strooper and colleagues showed that mutations in presenilin reduced its proteolytic function towards several different substrates (Bentahir, Nyabi et al. 2006). These findings raise an apparent paradox, in which AD-causing disease mutations cause both a ‘gain of function’, an increase in A $\beta$ 42/A $\beta$ 40, and a ‘loss of function’, a decrease in proteolytic activity. These seemingly opposing effects have elicited considerable debate over how the presenilin mutations cause AD, with some researchers suggesting that reducing A $\beta$  production with candidate therapeutics might even exacerbate or even cause the disease. To appreciate the resolution of this purported paradox, it should initially be noted that the presenilin-containing  $\gamma$ -secretase complex cuts the transmembrane domain of APP, and other substrates, in at least two positions: the  $\gamma$ -site that produces the carboxyl terminus of A $\beta$  and the  $\epsilon$ -site further downstream that produces the amino terminus of the APP intracellular domain (AICD) (Figure 3) (Evin and Weidemann 2002). Cleavage at the  $\gamma$ -site is heterogeneous, producing A $\beta$  peptides of 39–43 residues, whereas the cut at the  $\epsilon$ -site produces almost exclusively a 50-residue AICD. The same phenomenon occurs with Notch, involving heterogeneous cleavage in the middle of the transmembrane domain (the S4 site) and homogeneous cleavage further downstream (at the S3 site); (Fluhrer, Multhaup et al. 2003). Interestingly, proteolysis at these two sites is affected by AD-causing mutations in *APP* and the presenilins, which lead to an increase in the proportion of A $\beta$ 42 relative to A $\beta$ 40 along with an increase in a new 51-residue AICD relative to the 50-residue product (Sato, Dohmae et al. 2003). These two proteolytic events are therefore not completely independent: a change in the cleavage site in one correlates with a change in the cleavage site of the other. Recent evidence from Ihara and colleagues indicates that the  $\epsilon$ -cleavage might occur before proteolysis at the  $\gamma$ -site. Indeed, analysis of intracellular A $\beta$  reveals a small but significant amount of longer forms of this peptide, up to A $\beta$ 49, which is the proteolytic counterpart to the 50-residue AICD

**Figure 3:  $\gamma$ -secretase cleavage sites and A $\beta$  production**



This model of processive proteolysis of the amyloid precursor protein transmembrane domain by  $\gamma$ -secretase, beginning at the  $\epsilon$ -cleavage site and cleaving every three residues explains how reduction of proteolytic function due to presenilin mutations might lower amyloid  $\beta$ -peptide (A $\beta$ ) production but increase the ratio of A $\beta$ 42 to A $\beta$ 40. Longer forms of A $\beta$ , including most of the hydrophobic transmembrane domain, might be more likely to be retained in the active site of the protease, whereas the shorter forms are more likely to be released. Less catalytically efficient  $\gamma$ -secretase complexes would allow more time for the release of longer A $\beta$  peptides. In addition, Alzheimer disease-causing presenilin mutations shift the initial  $\epsilon$ -cleavage site to produce more A $\beta$ 48, which would lead to A $\beta$ 42. (Figure adapted from Michael S. Wolfe 2007)

(Qi-Takahara, Morishima-Kawashima et al. 2005); by contrast, longer AICDs, for example AICD counterparts to A $\beta$ 40 or A $\beta$ 42, have not been detected. Moreover, expression of A $\beta$ 49 leads to the secretion of A $\beta$ 40 and A $\beta$ 42 in the same proportion that is produced by  $\gamma$ -secretase (Funamoto, Morishima-Kawashima et al. 2004). Swapping tryptophan residues into the  $\gamma$ -site within the APP transmembrane domain prevents  $\gamma$ -cleavage but allows  $\epsilon$ -cleavage; however, swapping tryptophans into the  $\epsilon$ -site leads to proteolysis between the  $\gamma$ -site and  $\epsilon$ -site, at a so-called  $\zeta$ -site (Sato, Tanimura et al. 2005). Installing tryptophans into the  $\zeta$ -site prevents any transmembrane cleavage of APP. Therefore, with these tryptophan swaps,  $\epsilon$ -cleavage can occur without  $\gamma$ -cleavage, but  $\gamma$ -cleavage is not seen without  $\epsilon$ -cleavage or  $\zeta$ -cleavage. Interestingly, longer A $\beta$  peptides resulting from cleavage at the  $\zeta$ -site are seen intracellularly on treatment with one particular  $\gamma$ -secretase inhibitor: a dipeptide analogue called DAPT (Yagishita, Morishima-Kawashima et al. 2006). Finally, a mutation in PS1, M233T, leads to alternative  $\epsilon$ -cleavage, producing the 51-residue AICD and its counterpart A $\beta$ 48 in a cell-free assay with detergent-solubilized membranes (Kakuda, Funamoto et al. 2006).

One way to explain two major cleavage sites would be the presence of two pairs of catalytic aspartates within a presenilin dimer at the core of the  $\gamma$ -secretase complex. Initial proteolysis at the  $\epsilon$ -site leads to the release of AICD, but the long A $\beta$  products (A $\beta$ 49 or A $\beta$ 48) remain in the active site, and are successively cleaved every three residues upstream at the  $\zeta$ -sites and then again at the  $\gamma$ -sites (Qi-Takahara, Morishima-Kawashima et al. 2005). Specifically, they propose that A $\beta$ 49 is processed to A $\beta$ 46, A $\beta$ 43 and A $\beta$ 40, whereas A $\beta$ 48 is trimmed to A $\beta$ 45, A $\beta$ 42 and A $\beta$ 39. This model of processing proteolysis from the  $\epsilon$ -site to the  $\gamma$ -sites elegantly explains how so many presenilin mutations can both reduce proteolytic activity causing a loss of function, and increase the A $\beta$ 42/A $\beta$ 40 ratio, causing a gain of function. Mutant versions of the enzyme that are less proteolytically efficient also cut proportionately more at the alternative  $\epsilon$ -site, producing A $\beta$ 48 (Sato et al,

2003). The slower mutant enzymes allow proportionately more release of A $\beta$ 42 before further trimming to A $\beta$ 39. The net result might be less total A $\beta$ , including less A $\beta$ 40 (Bentahir, Nyabi et al. 2006), but the ratio of A $\beta$ 42 to A $\beta$ 40 is elevated. This proposed mechanism for  $\gamma$ -secretase activity could explain how the reduction of enzymatic activity results in increased A $\beta$ 42/A $\beta$ 40, but on the other hand it should be taken in account that generation of AICD counterpart could be affected. Indeed the very aggressive FAD mutation L166P not only induces an exceptionally high increase of Abeta(42) production but also impairs NICD production and Notch signaling, as well as AICD generation probably leading to the loss of an intracellular still unknown function (Moehlmann, Winkler et al. 2002).

This same mechanism might also account for the changes in A $\beta$ 42/A $\beta$ 40 seen with Alzheimer-causing *APP* mutations that are located near the  $\gamma$ -secretase cleavage sites; in these cases, the mutant substrates might be processed less efficiently by the wild-type protease. The scenario described above, which is supported by numerous reports, also provides an explanation for why the deletion of three out of four presenilin alleles in mice with only one PS1 allele remaining does not result in elevated A $\beta$ 42/A $\beta$ 40 (Lai, Chen et al. 2003) (Refolo, Eckman et al. 1999): the remaining  $\gamma$ -secretase complexes are wild type, have normal proteolytic activity and trim  $\epsilon$ -cleaved A $\beta$  efficiently. This is also consistent with the fact that although more than 100 missense mutations in PS1 and PS2 have so far been associated with AD, none are complete loss-of-function mutations in an allele, for example, complete deletion, loss of expression, mutation of one of the catalytic aspartates or severe truncations. The overexpression of presenilins does not result in increased activity of  $\gamma$ -secretase activity suggesting the presence of possible limiting factors participating to the catalytic activity. Indeed the  $\gamma$ -secretase activity, involves three additional proteins, nicastrin, Aph-1 and Pen-2. The active site of  $\gamma$ -secretase requires the aspartyl protease activity of PS1 conferred by aspartate residues in adjacent

transmembrane domains of the C- and N-terminal cleavage fragments of PS1. Nicastrin, Pen-2 and Aph-1 are each critical components of  $\gamma$ -secretase and each may modify enzyme activity in specific ways and in response to physiological stimuli (Hebert, Godin et al. 2003) (Cervantes, Saura et al. 2004; Nyborg, Kornilova et al. 2004).

More recently, it has been shown that APP is also a substrate for caspase cleavage. Each of the four caspases, 3, 6, 7, and 8, have been shown to cleave APP in in vitro assays, and a major caspase site has been identified at Asp-720 (VEVD), resulting in the release of a fragment containing the last 31 amino-acids of APP (C31) (Lu, Rabizadeh et al. 2000).

#### **4. Gain of function versus loss of function hypothesis in AD : learning from mouse models**

Although many sophisticated mice APP models exist, none recapitulates AD cellular and behavioral pathology. Despite exhibiting a massive and often rapid accumulation of A $\beta$  peptides, none of the examined APP Tg mice, carrying FAD related mutations, replicated the full spectrum of AD pathology. Indeed the morphological resemblance to AD amyloidosis is impressive, but fundamental biophysical and biochemical properties of the APP/A $\beta$  produced in Tg mice differ substantially from those of humans. The greater resilience of Tg mice in the presence of substantial A $\beta$  burdens suggests that levels and forms deleterious to human neurons are not as noxious in these models. Notably, these animals failed to produce dementia-correlated neurofibrillary tangles (NFT) structures. Lack of NFTs and missing neuron loss are the most obvious difference in pathology between APP and APP/PS tg mouse models and the AD brain. This observation shows that mutated human APP and/or PS1/2 overexpression is not sufficient to induce the entire pathological cascade in mice suggests that the presence of A $\beta$  is necessary but not sufficient to induce the tau-involved pathological changes typical of sporadic Alzheimer's disease (SAD) and some familial Alzheimer's disease (FAD) patients (Lamb, Bardel et al.

1999). These limitations may mean that with Tg mice, we are studying the direct effects of A $\beta$  overproduction and deposition, but not AD. Moreover, eliminating amyloid deposits via A $\beta$  immunization (Roher and Kokjohn 2002) may represent a cure in Tg mice, but regardless of the apparent total disruption of senile plaques in immunized patients with SAD, the successful clearance of these structures could neither reverse nor halt the progression of dementia. Indeed transgenic mice were widely used for testing AD therapeutic agents, but unfortunately, clinical trials resulted in unforeseen adverse events or negative therapeutic outcomes. Transgenic mice may suffer proportionately less deleterious effects than do AD patients, and therefore respond to amyloid disruption/removal therapies far better in terms of cognitive function recovery than even minimally demented humans who are contending with a broader scope of pathology.

As a consequence, the preeminence of the amyloid cascade hypothesis as a unique pathogenic factor in AD is being reexamined. The triple Tg (3xTg) mice, carrying the APP Swedish mutation K670N/M671L, the presenilin-1 M146V mutation, and the tau P301L mutation in the C57BL6 mouse background, were developed as an AD model (Oddo, Billings et al. 2004). This widely used Tg model develops intracellular A $\beta$  and extracellular plaque deposits as well as the tau pathology similar to that observed in AD. In addition, these mice demonstrate altered long-term potentiation, synaptic dysfunction, and age-related learning deficits, and may have a role in testing therapeutic interventions against AD (Pietropaolo, Feldon et al. 2008) (Pietropaolo, Sun et al. 2008). One limitation of the 3xTg mouse model is that the key APP/A $\beta$  and tau genes are overexpressed simultaneously by transcriptional forcing methods, whereas tau pathology emerges subsequent to A $\beta$  production in AD. The current status of information from animal models suggest that a major scientific need is to understand the normal function of amyloid- $\beta$  precursor protein (APP) and think how this may relate to the cell death in the disease process. Indeed a major concern about the amyloid hypothesis is that, despite the

fact that it is more than 20 years since the APP gene was cloned (Kang, Lemaire et al. 1987), we have very little idea of its function and almost no idea as to whether A $\beta$  has a function or not. One reason for this lack of knowledge is that APP knockout mice have very little overt phenotype (Heber, Herms et al. 2000).

We also have no idea as to whether A $\beta$  has a function or it is only a metabolic product of APP processing. As mentioned before mutations of the two presenilin-encoding genes, PSEN1 or PSEN2 which contribute to the onset of FAD, lead to an increase in the generation of the more amyloidogenic 42 aminoacid A $\beta$  peptide (A $\beta$ 42). This shift in A $\beta$ 42 abundance, coupled with the fact that A $\beta$ 42 is more amyloidogenic than the predominant A $\beta$ 40 species, is believed to accelerate the pathogenesis of AD. Therefore, inhibition of presenilin-dependent  $\gamma$ -secretase is considered a potential therapy for A $\beta$  lowering and AD intervention according with Amyloid cascade hypothesis but clinical trials based on A $\beta$  immunotherapy, resulted in unforeseen adverse events, or failed to produce clinically beneficial outcomes (Heininger 2000). Nevertheless, it should be taken in account that in addition to cleaving APP, the presenilins are involved in the intramembranous cleavage of numerous type-I integral membrane proteins (Lleo 2008) (Beel and Sanders 2008) (Parks and Curtis 2007) . Following receptor ectodomain shedding, the presenilins are involved in the cleavage of the membrane-tethered carboxylterminus of more that sixty-six membrane proteins, liberating their intracellular domains (ICDs) into the cytosol. In some cases these ICDs translocate to the nucleus and regulate the transcription of target genes, but other cleavage events are proposed to function as a means of clearing redundant protein fragments from the membrane following ectodomain shedding (Kopan and Ilagan 2004). Thus, the presenilins are involved in many signalling events independent of previously reported AD-associated activities. This has lead to the proposal that disruption of one or many of the presenilins activities within signalling complexes may also contribute to the pathogenesis of AD, or other disorders (Thinakaran and Parent 2004) (McCarthy 2005).

Consistent with these hypotheses, inactivation of PSEN1 gene in mice produced severe developmental abnormalities and perinatal lethality (Shen, Bronson et al. 1997) (Wong, Zheng et al. 1997) (Handler, Yang et al. 2000), indicating an essential role for PS1 in development. Indeed presenilins are widely and differentially expressed in mammalian tissues, with a broad cellular distribution suggesting multiple presenilin-dependent functions. They are located at the nuclear envelope, endoplasmic reticulum, Golgi apparatus, early secretory pathway and the plasma membrane. PS1 and PS2 share a high degree of homology (67%) with conservation between some transmembrane domains reaching 95% (Tomita and Iwatsubo 1999). Accordingly, there is significant similarity in their translated structures. Each of the presenilin genes encodes a multi-transmembrane protein and, although it is well over a decade since these proteins were discovered, a consensus has yet to be reached as to their precise topology (Laudon, Winblad et al. 2007) (Kornilova, Kim et al. 2006). Presenilin 1 plays essential roles *in vivo*, including neuronal differentiation and migration during embryonic development (Shen, Bronson et al. 1997) (Handler, Yang et al. 2000) (Wines-Samuels and Shen 2005). However, *PS1* conditional knock-out (*PS1* cKO) mice, in which PS1 inactivation is restricted to the postnatal forebrain, show reduced A $\beta$  generation and only subtle spatial memory impairment (Yu, Kim et al. 2001). Nevertheless, complete inactivation of both presenilins in the adult cerebral cortex results in hippocampal memory and synaptic plasticity impairments, followed by progressive neurodegeneration (Saura, Choi et al. 2004).

The finding that PS1 mutations devoid of  $\gamma$ -secretase activity are associated with fronto-temporal dementia ((Raux, Gantier et al. 2000) (Amtul, Lewis et al. 2002) (Dermaut, Kumar-Singh et al. 2004) also supports a possible link between loss of PS1 function and pathogenic mechanisms of dementia. The requirement of presenilins for synaptic plasticity, memory, and neuronal survival is mediated partly by the regulation of the cAMP response element-binding protein pathway, likely by  $\gamma$ -secretase dependent Notch cleavage and

signalling (Saura, Choi et al. 2004). Therefore, it is unlikely that  $\gamma$ -secretase inhibitors that affect Notch signaling will be useful as potential drugs for AD treatment. The hypothesis alternative to that of “Amyloid cascade hypothesis” is the “presenilin hypothesis” based on several *in vivo* observations. First, conditional inactivation of PS in the adult mouse brain causes progressive memory loss and neurodegeneration resembling AD, whereas mouse models based on overproduction of A $\beta$  have failed to produce neurodegeneration. Second, whereas pathogenic PS mutations enhance A $\beta$ 42 production, they typically reduce A $\beta$ 40 generation and impair other PS-dependent activities. Third,  $\gamma$ -secretase inhibitors can enhance the production of A $\beta$ 42 while blocking other  $\gamma$ -secretase activities, thus mimicking the effects of PS mutations. Finally, PS mutations have been identified in fronto-temporal dementia, which lacks amyloid pathology. Based on these and other observations, the partial loss of PS function seems to better explain neurodegeneration in the pathogenesis of AD. Moreover it has been proposed that A $\beta$ 42 may act primarily to antagonize PS-dependent functions, possibly by operating as an active site-directed inhibitor of  $\gamma$ -secretase.

## **5. The APP function**

The normal functions of APP are not fully understood, but increasing evidence suggests it has important roles in regulating neuronal survival, neurite outgrowth, synaptic plasticity and cell adhesion (Mattson 1997). One possible function of full-length APP is as a cell surface receptor that transduces signals within the cell in response to an extracellular ligand (Kimberly, Zheng et al. 2001).

Several functions have been proposed for this protein. For example, the extracellular domain of the protease nexin form of APP (APP751/770) is part of the clotting cascade (Xu, Davis et al. 2005). One possibility is that APPs (and possibly A $\beta$ ) are damage response proteins. While others have argued that A $\beta$  might have some protective role (Lee,

Castellani et al. 2005), this possibility has not been rigorously investigated. The concern is that APP up regulation (and even perhaps A $\beta$  deposition) is an acute response to damage, perhaps vascular damage, (Atwood, Bishop et al. 2002) (Kumar-Singh, Pirici et al. 2005) (Cullen, Kocsi et al. 2006) (Weller, Subash et al. 2008), in line with the role of APP in the regulation of blood clotting (Xu, Davis et al. 2005). However, neither a ligand nor downstream signaling cascades for APP have been clearly established. APP's evolutionary conservation and the existence of APP-like isoforms (APLP1 and APLP2), which lack the A $\beta$  sequence, however, suggest that these might have important physiological functions that are unrelated to A $\beta$  production. The functional redundancy between mammalian APP, APLP-1, and APLP-2 became clear when it was first shown that APP/APLP-2 (von Koch, Zheng et al. 1997), and subsequently, APLP-1/APLP-2 double knockouts (Heber, Herms et al. 2000) (Wang, Yang et al. 2005), exhibit early postnatal lethality. APP/APLP-2 double knockouts have structurally and functionally defective neuromuscular synapses, with excessive nerve terminal sprouting, reduced synaptic vesicle numbers at the presynaptic compartment, and an observable aberrant apposition of presynaptic markers with postsynaptic acetylcholine receptors. APP/APLP-1 double knockouts are viable, but these also exhibit early postnatal death in conjunction with a haplodeficiency of APLP-2 (Wang, Yang et al. 2005). The triple knockouts are postnatally lethal and exhibit cranial abnormalities. These include cortical dysplasias resembling the phenotype found in human type II lissencephaly and a partial loss of cortical Cajal retzius (CR) cells (Herms, Anliker et al. 2004). These phenotypes of the APP/APLP-1/APLP-2 triple knockout are suggestive of defects in the survival of specific central nervous system cell types and the migration of neuroblasts. It is therefore clear that the APP and APPLs have important developmental and postnatal functions.

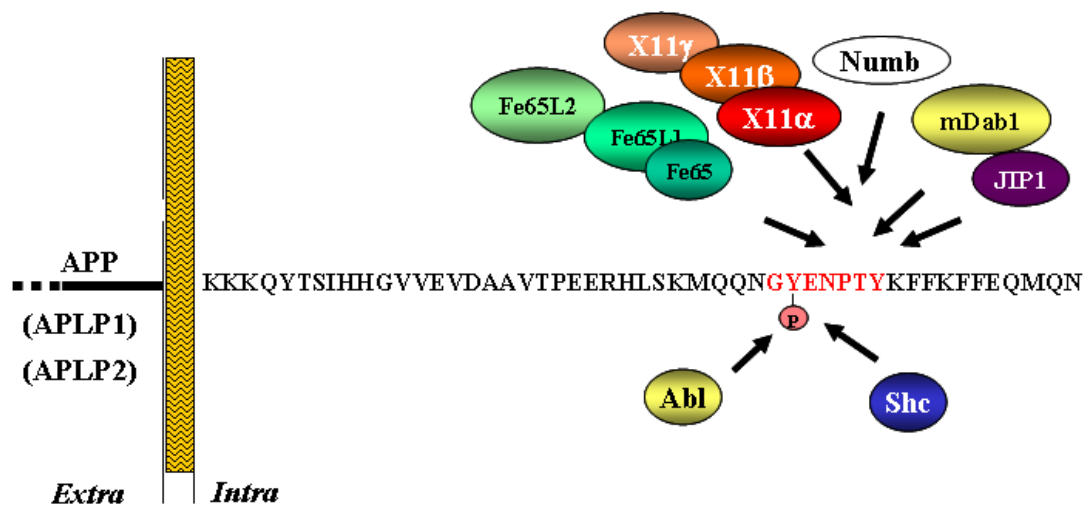
Soluble N-terminal fragments of APP have been known to be neuroprotective. Recent findings have brought to light two possible functions of the APP family in the brain-

regulation of neural progenitor cell proliferation. sAPP $\alpha$ , as does the ectodomain of APLP-2 (Cappai, Mok et al. 1999), has been shown to be able to stimulate the proliferation of neural progenitor cells in vitro (Hayashi, Kashiwagi et al. 1994) (Ohsawa, Takamura et al. 1999) and in vivo in the subventricular zone (SVZ) (Caille, Allinquant et al. 2004). The SVZ is one of two adult CNS sites that harbor neural progenitors that are capable of producing neurons in the adult brain (Conover and Allen 2002; Caille, Allinquant et al. 2004). The results of Caille et al. have important implications for APP and APLP-2 functioning as rather specific growth factors or co-factors for CNS neuroprogenitors. A possible endogenous source of APP or APLP ectodomains at the SVZ has in fact been noted in a subpopulation of cells, which expresses astrocytic markers (Yasuoka, Hirata et al. 2004). However, any specific sAPP $\alpha$  receptor has been identified and the respective proliferative signaling pathways dissected in detail (although MAP kinase activation by sAPP has been demonstrated (Greenberg, Koo et al. 1994). In fact, unlike the cytoplasmic C-terminus of APP, the N-terminus is surprisingly devoid of known specific neuronal interacting proteins. Candidate interacting proteins thus far known include ApoE (Barger and Harmon 1997) and the most recently identified F-spondin (Ho and Sudhof 2004). In this case, F-spondin binding to APP inhibits its proteolytic cleavage by BACE-1 and appears to modulate APP-dependent transactivation of Tip60-mediated transcription. F-spondin has been shown to promote neurite outgrowth of both CNS (Feinstein, Borrell et al. 1999) and peripheral nervous system neurons (Burstyn-Cohen, Frumkin et al. 1998), as well as functioning in developmental axonal pathfinding and neuronal regeneration (Burstyn-Cohen, Tzarfaty et al. 1999) (Feinstein and Klar 2004).

Although biochemical interaction studies have identified a plethora of molecules that interact with the APP intracellular domain (AICD), concrete evidence for a physiological significance of these interactions is often lacking. The cytoplasmic domain of APP is characterized by the GYENPTY motif, which is 100% conserved from *C. elegans* to

humans supporting the notion of its importance. This motif contains the consensus sequence for clathrin-coated pit internalization. Deletion of the cytoplasmic tail impairs internalization of cell surface APP and decreases A $\beta$  secretion into conditioned medium by precluding endosomal–lysosomal APP processing (Essalmani, Macq et al. 1996) (Koo and Squazzo 1994) (LeBlanc and Gambetti 1994). The GYENPTY sequence is also a consensus motif for the binding of adaptor proteins that possess a phosphotyrosine binding domain (PTB), such as those in the X11, Fe65, and JIP families (Figure 4). These proteins bind the AICD in a phosphotyrosine independent manner and may affect the APP processing. Fe65 is an adaptor protein highly expressed in neurons (Fiore, Zambrano et al. 1995) and is the first PTB-containing protein identified as ligand of the GYENPTY motif of the intracellular domain of APP and its orthologues APLP1 and APLP2. Fe65 and its orthologues Fe65L1 and Fe65L2 can modulate the APP processing in distinct ways that may be cell-type dependent, either promoting sAPP and A $\beta$  secretion (Guenette, Chen et al. 1999) (Chang, Tesco et al. 2003) (Sabo, Lanier et al. 1999) either stabilizing immature APP and inhibiting sAPP and A $\beta$  secretion (Ando, Iijima et al. 2001). The same GYENPTY motif is implicated in the binding of X11 and mDab1. X11 is an adaptor protein (Borg, Yang et al. 1998) (Butz, Okamoto et al. 1998) that inhibits A $\beta$  secretion (King, Perez et al. 2003), likely via impaired trafficking of APP to subcellular compartments containing active  $\gamma$ -secretase complex (King, Cherian et al. 2004), because has no inhibitory effect on  $\gamma$ -cleavage activity in a cell-free system. Indeed, human X11 $\alpha$  and human APP<sup>swe</sup> double transgenic mice reveal a significant decline in A $\beta$ <sub>40</sub> levels in brain homogenates and rescue of age-dependent amyloid plaque deposition in brain compared to age-matched human APP<sup>swe</sup> transgenic control mice (Lee, Lau et al. 2003). Disabled-1 (Dab1), which plays a role in neuronal development (Homayouni, Rice et al. 1999) (Howell, Lanier et al. 1999) has not clear effect on APP processing. Other proteins has been shown to interact may with the APP C-terminus, but little is known of their

**Figure 4: APP Intracellular Domain (AICD) ligands.**



The cytosolic tail of APP is reported with the GYENPTY motif in red. Some of the PTB-containing proteins that interact with AICD are shown. It is represented the Tyr residue phosphorylated by Abl and involved in the binding with activated Abl and Src tyrosine kinases.

potential modulatory effects on its processing or the in vivo significance of their interaction, such as the JNK-interacting protein 1 (Jip1) (Matsuda, Yasukawa et al. 2001; Scheinfeld, Roncarati et al. 2002), Shc (Russo, Dolcini et al. 2002; Tarr, Roncarati et al. 2002), Numb (Roncarati, Sestan et al. 2002), ARH (Noviello, Vito et al. 2003), Grb2 (Zhou, Noviello et al. 2004) and AIDA (Gherzi, Vito et al. 2004).

In our lab it has been shown that the proteolytic processing of APP is induced by activated PDGF receptor through a pathway involving the activation of Src and Rac1 (Gianni, Zambrano et al. 2003). This mechanism can be modulated by APP interactors. Infact, overexpression of Fe65 and Shc induce an increase of the APP processing, but via two different mechanisms. Fe65 induces the cleavage by caspase and Shc induce the g-secretase cleavage.

## **6. The adaptor protein Fe65**

Yeast two-hybrid screens using the APP C-terminus as bait identified the adaptor protein Fe65 (Fiore, Zambrano et al. 1995) (Russo, Faraonio et al. 1998) (Zambrano, Buxbaum et al. 1997). Fe65 is expressed at high levels in neurons (Bressler, Gray et al. 1996). Human and mouse *Fe65* genes have an alternatively spliced isoform with an exon present only in the neuron-specific transcript (Hu, Hearn et al. 1999). In adult mouse brain Fe65 is highly expressed in neurons in the hippocampus, cerebellum, thalamus, and midbrain, with some expression in a subset of astrocytes in the hippocampus. Fe65 expression is also developmentally regulated, with levels declining after embryonic day 15 and increasing again progressively from postnatal day 10 to adulthood (Simeone, Duilio et al. 1994) (Kesavapany, Banner et al. 2002).

Fe65 is a member of a protein family consisting of Fe65, Fe65-like (Fe65L or Fe65L1) (Guenette, Chen et al. 1996) and Fe65L2 (Duilio, Faraonio et al. 1998). The members of

the Fe65 family share a high grade of sequence homology in the three functional domains and all of them can bind the APP family members cytosolic tail although the Fe65-APLP1 interaction is the most affine.(Guenette, Chen et al. 1996; Duilio, Faraonio et al. 1998). A difference between the members of Fe65 family is in the tissue specificity. Fe65 is highly expressed in neurons; Fe65L1 is ubiquitously expressed; and Fe65L2 is very abundant in testis and brain (Duilio, Zambrano et al. 1991; Simeone, Duilio et al. 1994; Guenette, Chen et al. 1996). Genetic models suggest a redundant function of the Fe65 family members. Fe65 knock out mice appear normal, but double mutants Fe65<sup>-/-</sup>/Fe65L1<sup>-/-</sup> show cortical dysplasia, mislocalization of CR neurons, disruption of basal membrane, with a phenotype similar to that observed in the triple knock out mice of the APP family and to the PS1 knock out. A possible explanation of the overlapping phenotype is the impairment of a  $\gamma$ -secretase-dependent signalling involving the APP-Fe65 interaction, thus implying a role of APP-Fe65 signaling as effector of normal neuronal positioning in brain development.

The Fe65 protein contains three protein interaction domains: a WW domain in the N-terminus and two PTB domains in the C-terminus, with distinct binding specificities. The PTB domains of Fe65 have distinct features compared to those present in proteins as Shc and IRS-1. They lack a Phe residue, which is conserved in all known PTBs and in Fe65 is replaced by a Cys (Zambrano, Buxbaum et al. 1997) and they can bind the GENPTY motif when the tyrosine is not phosphorylated (Margolis, Borg et al. 1999). The WW domain is one of the smallest protein domain composed of 40 aminoacids, which is found in a wide range of signaling molecules, and binds proteins containing proline-rich motif. The WW domain of Fe65 belongs to the II group of WW domains that recognizes a PPPPLP consensus sequence (Kay, Williamson et al. 2000).

In the literature several partners of the three protein interaction domains of Fe65 have been described. The WW domain interacts with Mena (mammalian enabled), which binds actin and thus links Fe65 and APP to cytoskeletal dynamics and cellular motility and

morphology (Ermekova, Zambrano et al. 1997). Indeed, Fe65 and APP colocalize at synaptic sites and in distal domains of neuronal growth cones, particularly actin-rich lamellopodia (Sabo, Ikin et al. 2003). Another ligand of the WW domain of Fe65 is the active form of the tyrosine kinase c-Abl, which mediates the phosphorylation of Fe65 on tyrosine 547 within its second PTB domain and modulates its nuclear function (Russo, Faraonio et al. 1998). It has been hypothesized that Fe65 might recruit c-Abl to the C-terminus tail of APP to allow the phosphorylation of the tyrosine Y682 by the c-Abl, which can itself bind the phosphorylated AICD through its SH2 domain (Zambrano, Bruni et al. 2001; Perkinson, Standen et al. 2004). As part of my thesis project I described a new complex of Fe65 with the nucleosomal assembly protein SET that requires an overlapping region of the WW domain (Telese, Bruni et al. 2005) and is able to modulate its nuclear function.

The PTB1 domain of Fe65 binds the low density lipoprotein receptor related protein (LRP) which serves as a receptor for ApoE and  $\alpha$ -2 macroglobulin that scavenge secreted A $\beta$  (Trommsdorff, Borg et al. 1998). Recently, it has been reported that Fe65 binds with its PTB1 domain another member of the LRP family, the ApoER2 (Hoe, Magill et al. 2006). The complex between Fe65 and the members of the LDL-related proteins might affect the APP processing. The PTB1 domain of Fe65 also binds the transcription factor complex CP2-LSF-LBP-1c (Zambrano, Minopoli et al. 1998) and this interaction is implicated in the regulation of transcription of GS3K $\beta$  (glycogen synthase kinase-3 $\beta$ ) (Kim, Kim et al. 2003) and thymidilate synthase (Bruni, Minopoli et al. 2002). Another nuclear ligand of the PTB1 domain of Fe65 is the histone acetyl transferase Tip60 (Cao and Sudhof 2001).

The PTB2 domain of Fe65 binds the APP C-terminus. This interaction requires the GYENPTY motif as well as threonine-668, 14 residues N-terminal to the internalization sequence. Phosphorylation of threonine-668 of APP impairs Fe65 interaction, suggesting

that the interaction of Fe65 with APP may be differentially regulated by its phosphorylation–dephosphorylation status (Ando, Iijima et al. 2001).

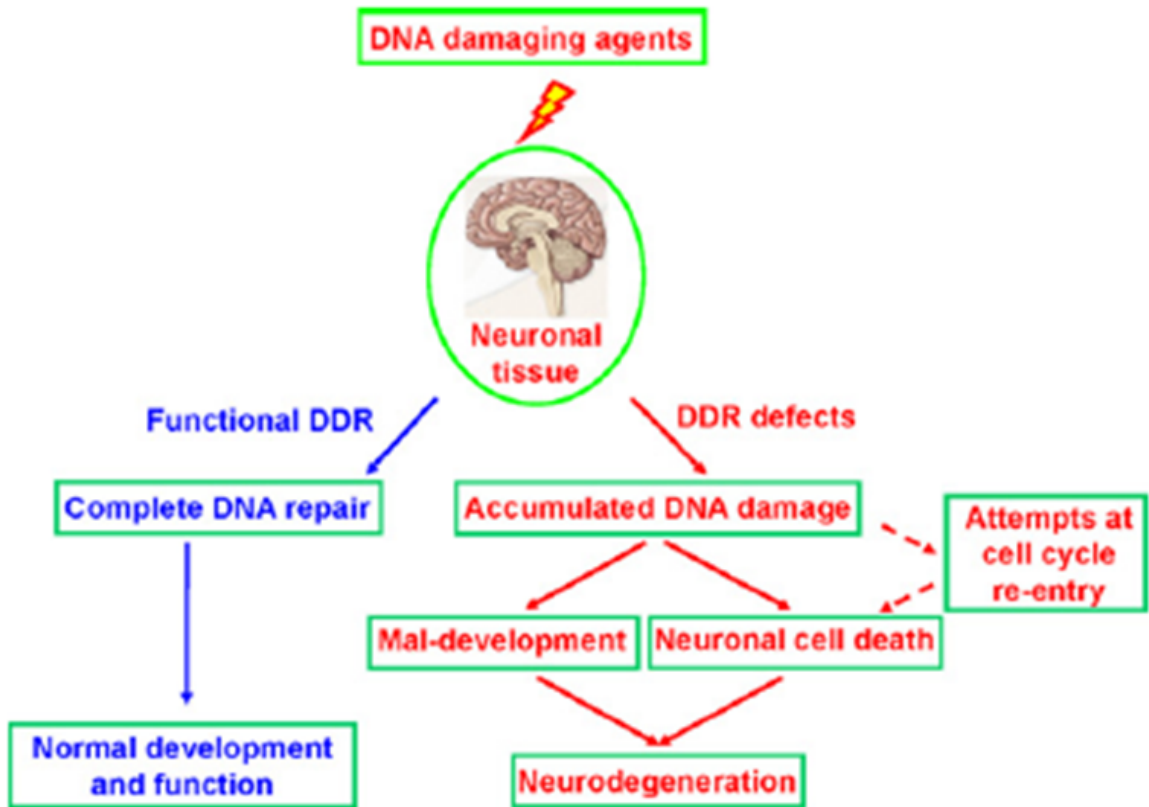
## **7. Neurodegeneration and DNA damage response.**

Neurodegenerative diseases are a group of pathologies affecting the central nervous system whose common feature is the deterioration of neuronal functions. Neuronal cells are fully differentiated post-mitotic cells, highly specialized for the processing and transmission of cellular signals. The maintenance of genomic integrity has crucial meaning for these cells considering their inability to proliferate and substitute damaged cells. Since they are irreplaceable and should survive as long as the organism does, they need elaborate, stringent defense mechanisms to ensure their longevity. Neurons display high rates of transcription and translation, which are associated with high rates of metabolism and mitochondrial activity. The amount of oxygen consumed by the brain relative to its size far exceeds that of other organs. This high activity coupled with high oxygen consumption creates a stressful environment for neurons: damaging metabolic by-products, primarily reactive oxygen species (ROS), are constantly attacking neuronal genomic and mitochondrial DNA (Barzilai, Biton et al. 2008) (Katyal and McKinnon 2007) (Fishel, Vasko et al. 2007) (Weissman, de Souza-Pinto et al. 2007) (Halliwell 2006) (LeDoux, Druzhyna et al. 2007) and (Ryter, Kim et al. 2007). Neurons ensure their longevity and functionality in the face of these threats by elaborate mechanisms that defend the integrity of their genome. The DNA damage response is a key factor in the maintenance of genome stability. It is now clear that diverse mechanisms encompassing cell cycle regulation, repair pathways, many aspects of cellular metabolism, and cell death are inter-linked and act in concert in response to DNA damage. One of the most powerful activators of the DDR is the double strand break (DSB) in the DNA (Helleday, Lo et al. 2007). Eukaryotic cells employ two major mechanisms to repair DSBs: nonhomologous end-joining (NHEJ), an

error-prone ligation mechanism, and a high-fidelity process based on homologous recombination (HR) between sister chromatids that operates in the late S and G2 phases of the cell cycle (van Gent and van der Burg 2007) (Wyman and Kanaar 2006). But, the overall cellular response to DSBs goes far beyond repair. This broad, powerful signaling network works to affect chromatin organization and a large number of cellular systems (figure 5) (Bakkenist and Kastan 2004) (Shiloh 2003) (Harrison and Haber 2006) (Shiloh 2006). One of its hallmarks in proliferating cells is the activation of cell cycle checkpoints that temporarily halt the cell cycle while damage is assessed and processed (Jeggo and Lobrich 2006) (Bartek and Lukas 2007). Defects in the DNA damage response in proliferating cells can lead to cancer while defects in neurons result in neurodegenerative pathologies (Figure 5). In animal models, ectopic expression of oncogenes in terminally differentiated cells, including neurons, has been shown to induce apoptosis rather than proliferation. For instance, mice transgenic for the SV40 T antigen, which is normally oncogenic in cycling cells, show progressive degeneration of Purkinje neurons to which transgene expression was targeted (Klein, Longo-Guess et al. 2002). Other genetic models suggest that cell-cycle reactivation in neurons precedes or is at least coincident with neuronal apoptosis.

The cell cycle in a normally cycling cell proceeds through four distinct phases, whereas cell-cycle reactivation in a post-mitotic neuron (by a stimulus such as excitotoxicity, growth factor withdrawal or overwhelming DNA damage) leads to apoptosis. Several genetic deficiencies in enzymes that detect or repair DNA damage can induce the apoptosis of specific neuronal populations or further sensitize them to genotoxic stresses. A good link between defects in DNA repair, malignancy and neurodegeneration are seen with loss-of-function mutations in ataxia telangiectasia-mutated (ATM), a member of the phosphatidylinositol-3 (PI3) kinase superfamily with multiple functions and protein targets. ATM can activate repair proteins such as the Rad50–Mre11–Nsb1 complex in response to

**Figure 5: Effects of defective DDR pathways on the central nervous system (CNS).**



Neurons are characterized by elaborate structure and function, perhaps more than any other cell type. The combination of their critical function, post-mitotic nature, finite number and high oxygen consumption demands a robust DNA damage response. Reduction in DNA repair proteins has been associated with various neurodegenerative pathologies such as typical late onset, chronic diseases like Alzheimer’s disease (AD) and Parkinson’s disease (PD) or monogenic disorders such as the genomic instability syndromes, Ataxia telangiectasia, Nijmegen breakage Syndrome, Cockayne’s syndrome (CS) and Trichothiodystrophy (TTD)

DNA double-strand breaks created, for instance, by ionizing radiation, but when the DNA repair machinery is overwhelmed, ATM can also activate p53 and Chk1 to induce cell-cycle arrest or apoptosis. In mouse models deficiency of ATM causes a progressive apoptosis of nigral dopamine neurons followed by degeneration of striatal projection neurons (Eilam, Peter et al. 2003) (Eilam, Peter et al. 1998). The neurodegenerative phenotype early in the human disease ataxia-telangiectasia is restricted to Purkinje and granule cells of the cerebellum but broadens considerably with age and may extend to the basal ganglia (Gibb and Lees 1989) (Agamanolis and Greenstein 1979). ATM and ATM-related protein (ATR) function at a nexus of neurodevelopmental and DNA repair activities; specific biallelic defects in these lead not only to cerebellar degeneration but also to microcephaly (Seckel syndrome) and, in conjunction with p53 inactivation, tumors of the central nervous system such as medulloblastoma (Lee and McKinnon 2007).

A convergence of biochemical, genetic and epidemiologic data has implicated certain genes in both oncogenesis and neuronal dysfunction. These include the tumor suppressors ATM and PTEN and possibly parkin. Typical late onset, chronic diseases are Alzheimer's disease (AD) and Parkinson's disease (PD), while monogenic disorders such as the genomic instability syndromes are characterized by early onset and acute manifestation. There are common denominators between these two groups of diseases, and accumulation of DNA damage is one of them (Fishel, Vasko et al. 2007) (Halliwell 2006) (Rutten, Schmitz et al. 2007) (Rutten, Korr et al. 2003) (Cotman and Su 1996) (Itzhaki 1994) (Robbins 1987). All of these disorders impair "brain functionality" to various degrees, defined by total input and output of the brain's neuronal circuits. Neurodegenerative disorders deregulate the activity of specific circuits, affecting their organization, cell numbers, cellular functionality, and interactions between cells and circuits. It is reasonable to assume that DDR components that affect early onset neurodegenerative diseases can also be involved in late onset neurodegenerative diseases such as PD or AD. Increased

oxidative stress; accumulation of oxidative damage; reduced NHEJ; accumulation of DSBs and SSBs; reduction in MRN complex components; activation of cell cycle program. It will be of clinical interest to determine which of these genes and their molecular partners would be useful biomarkers or therapeutic targets and at what stage of disease such applications would be most effective. In addition, determining which aspects of cell-cycle control in normal neuronal development are recapitulated in neurodegeneration and which are unique to each process may help optimize conditions for regenerative therapies based on stem-cell differentiation and transplantation.

### **The aims of the thesis**

Fe65 is a nuclear protein interacting with Tip60, SET, c-Abl and CP2/LSF. Among these nuclear partners Tip60 and SET are involved in chromatin remodelling. The high sensitivity to genotoxic stress induced by the Fe65 suppression both *in vitro* and *in vivo* led us to investigate the involvement of Fe65 in chromatin remodelling during DNA repair. This hypothesis was supported by the fact that the histone acetyl-transferase Tip60 is a component of NuA4 complex involved in the early steps of chromatin decondensation during DNA repair. To this aim I investigated the role of Fe65 and its main interactor APP in the cellular response to DNA damage. Most of the data shown in this thesis have been published in the following papers: (Stante, Minopoli et al. 2009) (Minopoli, Stante et al. 2007).

## **MATERIALS AND METHODS**

### **1. Generation of Fe65 knock out mouse embryonic fibroblasts (MEFs)**

For generation of mouse embryo fibroblast lines, E13.5 embryo bodies devoid of heads and liver were trypsinized and plated in DMEM (Invitrogen) supplemented with 10% Newborn Calf Serum (HyClone), 1% penicillin and streptomycin, 1% MEM-non-essential amino acids (Invitrogen), 1.6 mM 2-mercaptoethanol. Immortalized lines were obtained following spontaneous recovery of the primary cultures from proliferation crisis. These lines were cultured in DMEM supplemented with 10% fetal bovine serum.

Three Fe65 knock out (KO) immortalized lines (# 3, # 8 and # 9) were obtained from three independent Fe65 KO mice.

### **2. DNA damaging agents treatment and irradiation of mice**

Etoposide (VP-16, Calbiochem, 100 mM stock in DMSO) was added to the medium at final concentration of 15  $\mu$ M for comet assay analysis or 40  $\mu$ M for western blot analysis. Cells were then incubated at 37°C and 5% CO<sub>2</sub> for 30 minutes before comet assay or for 2 hours before lysis and protein extraction. H<sub>2</sub>O<sub>2</sub> was diluted from a 30 % w/w (8.8 M stock) aqueous solution (Sigma) immediately before cell treatment in complete conditioned medium at the final concentration of 10 $\mu$ M.

Cells were incubated at 37°C and 5% CO<sub>2</sub> for 30 min or 1 hour before Comet Assay. To induce genotoxic stress in mice, these were exposed to 0.5 or 1 Gy doses of 6 MV X-ray from a linear accelerator (Primus, Siemens).

### **3. Comet assay**

The neutral comet assay was carried out according to manufacturer's recommendations (Trevigen, Gaithersburg, MD). After treatment described before cells were trypsinized and resuspended in cold PBS at  $10^6$  cells/ml. All passages were done on ice.

For each point 10  $\mu$ l of resuspended cells were added to 100  $\mu$ l of melted agarose (37°C) and rapidly spread on slides. Agarose was allowed to solidify for 30 min. at 4°C and then slides were incubated for 30 min in lysis buffer and for 40 min in alkaline solution (pH>13). Comet tails were generated by a 10 min electrophoresis in TBE buffer at 20 V at room temperature. Slides were stained with Syber Green and DNA migration was analyzed by fluorescence microscopy (Leica DMS 4000B). Tail moment and tail length were calculated using the software CometScore™ (TriTek Corporation). A minimum of 50 cells per experiment was analyzed. All the experiments were done in triplicate. The Student's t-test was used to measure statistical significance.

### **4. Cells culture conditions and transfection of shRNAs and siRNAs**

NIH3T3, Hepa 1-6 and murine neuroblastoma cell line N2A were cultured under standard conditions and transfected with lipofectamine 2000 (Invitrogen) according to manufacture instructions. Fe65 silencing was obtained by transfecting pSM2 retroviral shRNAmir vectors (Open Biosystems, cat #RMM1766-9351830) or siRNAs (Dharmacon, cat#LQ-042929); APP and APLP2 silencing was obtained by transfecting siRNAs (Dharmacon, cat#L-043246 and L- 042937, respectively), following the manufacturer's instructions. Non-silencing siRNAs were used as a control (Dharmacon, cat#D-001810-10-20). 48 hours upon transfection of Fe65 shRNA or non silencing shRNA cells were selected with puromycin at final concentration of 5  $\mu$ g/ml for 2-3 days until cells in non transfected control plate were died to enrich the pool of transfected cells.

Puromycin resistant cells were then plated at desired confluence to perform following experiments. siRNAs transfected cells were used for following experiments 48 hours upon transfection. Transfection was carried out using the siRNAs at final concentration of 100nM using 1:1 Lipofectamine : siRNAs ratio. In all cases the silencing of proteins was evaluated by western blot analysis with specific antibodies.

## **5. Generation of the recombinant constructs in pRcCMV vector**

pRC-CMV-NES-myc and pRC-CMV-mutNESmyc vectors were obtained by cloning in the pRC-CMV (Invitrogen) the sequence of NESmyc and mutNES-myc using NotI / ApaI restriction sites. NES-myc and mut NES-myc ds DNA were obtained by annealing synthetic oligonucleotides (see sequence below) using the following annealing buffer : 100mM NaCl, 50 mM Hepes pH 7.4.

3 $\mu$ g of forward oligo and 3 $\mu$ g reverse oligo were added to the annealing buffer in a final volume of 50  $\mu$ l and incubated in a thermal cycler as follow:

90° C 4 min.

70° C 10 min.

37° C 20 min.

20° C 10 min.

The Fe65-NES and Fe65-NESm constructs were obtained by cloning into the pRC-CMV-NESmyc and pRC-CMV-mutNES-myc vectors, respectively, the FE65 cDNA amplified by PCR with the primers listed below and digested with appropriate restriction enzymes. All the Fe65 mutants were cloned in the pRcCMVmutNES-myc vector using HindIII and NotI restriction sites. The sequences of the oligonucleotide primers used in this work to build recombinant constructs were:

**NES-myc**

**Forward**

5'GGCCGCGCCCTACAGAAGAAGCTGGAAGAAGTGGAACTGGACGAATTCGGCCCGCGGGGCG  
AGCAGAACTCATCTCTGAAGAGGATCTGTAGGGGCC3'

**Reverse**

5'CCTACAGATCCTCTTCAGAGATGAGTTTCTGCTCGCCCCGCGGGCCGAATTCGTCCAGTTCCA  
GTTCTTCCAGCTTCTTCTGTAGGGCGC3'

**mutNES-myc**

**Forward**

5'GGCCGCGCCGCACAGAAGAAGGCAGAAGAAGCAGAAGCAGACGAATTCGGCCCGCGGGGCG  
AGCAGAACTCATCTCTGAAGAGGATCTGTAGGGGCC3'

**Reverse**

5'CCTACAGATCCTCTTCAGAGATGAGTTTCTGCTCGCCCCGCGGGCCGAATTCGTCTGCTTCTG  
CTTCTTCTGCCTTCTTCTGTGCGGGCGC3'

The following primers were used to amplify the wild type Fe65 cDNA and the point mutation mutants ( C655F and YYW->AAA) using respectively the wild type template or constructs carrying the specific mutations.

**Fe65-HindIII for** : 5'CCCAAGCTTAAGGCCATGTCTGTTCCATCATCCC3'

**Fe65-NotI rev** : 5'CCCGCGGCCGCTGGGGTCTGGGATCCTAG3'

Deletion mutants were amplified using Fe65-NotI rev primer and the following forward primers:

**ΔupWW Hind III for: 5'CCCAAGCTTAAGGCCATGTCCGATCTACCGGCTG3'**

**ΔWW Hind III for: 5'CCCAAGCTTAAGGCCATGCAGGGGAACAGTCCC3'**

The ΔPTB1 mutant was amplified by overlapping PCR using the following primers:

**ΔPTB1 Hind III for: 5'CATGCCAGCCCATCGTCAGCCGCTGCTTGGTAAATGGACTC3'**

**ΔPTB1 Hind III for: 5'GAGTCCATTTACCAAGCAGCGGCTGACGATGGGCTGGGCATG3'**

The ΔPTB2 was amplified using Fe65 HindIII for primer and

**ΔPTB2 Not I rev: 5'CCCGCGGCCGCCCTTTGGTGCTGGGAATTC3'**

## **6. Immunofluorescence**

Cells were fixed in 4% paraformaldehyde for 10 min, permeabilized for 10 min in 0.2% Triton X-100, and blocked in 10% BSA for 1 h at room temperature. The slides were incubated with primary antibody for 1 h, washed in PBS, and incubated with Alexa Fluor conjugated secondary antibodies (Molecular Probes, Eugene, OR) for 1 h at room temperature. Cells were washed in PBS and mounted using Vectashield mounting medium with DAPI (Vector Laborator). Images were captured with an inverted microscope (DMI4000, Leica Microsystems).

## **7. Immunoprecipitation , western blot and antibodies**

For the preparation of the cellular extracts, monolayer cultures were harvested in cold phosphate-buffered saline and sonicated in lysis buffer (50 mM Tris·HCl, pH 7.5, 150 mM NaCl, 0.5% Nonidet P-40, 10% glycerol, 0.4 mM EDTA, 50 mM NaF, 1 mM sodium vanadate, 1 mM phenylmethylsulfonyl fluoride, and protease inhibitor tablets). The extracts were clarified by centrifugation at  $16,000 \times g$  at 4 °C, and the protein concentration was determined by the Bio-Rad protein assay according to manufacturer's

instructions. For immunoprecipitations, appropriate amount of antibodies was incubated with 1.5 mg of protein lysates for 2 h at 4 C, followed by a 1 hour incubation with Protein A–Sepharose. Immunoprecipitates were washed three times in lysis buffer. Proteins released by boiling in SDS sample buffer were separated by Novex Bis–Tris 4–12% polyacrylamide gels (Invitrogen) and analysed by specific antibodies. 50 µg (or the indicated amounts) of each extract were electrophoresed on 4-12% SDS-polyacrylamide gradient gel under reducing conditions. Western blot experiments were carried out as described (Zambrano et al. 1998). For p-ATM western blot, proteins were separated on 5% low bis acrylamide gels (acrylamide:bis ratio 5:0,17). The antibodies used and their dilutions were: anti-H2AX (Bethyl Laboratories, Inc., 1:1000); anti-p53 (Ab-1) (Upstate Biotechnology, 10 µg/ml), antiphospho- p53 (Cell Signaling, 1:1000), anti-Fe65 (9); anti-γH2AX (Ser139) (Cell Signalling Technology, 1:1000); anti- phospho ATM (Ser 1981) (Cell Signaling, 1:1000), anti-APP C-term (A8717 Sigma, 1:4000), anti-NBS (Santa Cruz, 1:500), anti-lamin B (Santa Cruz, 1:250), anti-β- actin (Sigma, 1:1000), anti-myosin (Santa Cruz, 1:1000), anti-tubulin (Sigma, 1:1000) APLP2 (Calbiochem 1:5000). Horseradish peroxidase-conjugated goat polyclonal anti-rabbit and anti-mouse IgG were purchased from GE Healthcare. The rabbit polyclonal anti-FE65 antibody was described in (Duilio, Faraonio et al. 1998)

## **8. Histone Association Assay**

This procedure is a modification of the earlier described CHIP protocol (Liu, Wang et al. 2008). Cells were treated with formaldehyde at a final concentration of 1% for 15 min. The reaction was quenched with the addition glycine to a final concentration of 125 mM. Nuclei were prepared as described in Zambrano et al. 1998, lysed in CHIP lysis buffer (50mMHepes-KOH pH 7.5, 150 mMNaCl, 1 mMEDTA, pH 8.0, 1% Triton X-100, 0.1%

sodium deoxycholate and protease inhibitors) and chromatin was sheared by sonication to 200–500 bp. The extract was centrifuged for 5 min at 20,000  $\times$  g at 4 °C. For each histone H3 immunoprecipitation, 1 mg of nuclear extract (as measured by the Bradford assay) was incubated with 8  $\mu$ g of rabbit polyclonal histone H3 antibody (Upstate). Equal amount of Rabbit IgG (Sigma) was used as negative control. Samples were incubated overnight at 4 °C with shaking. 20  $\mu$ g of single-stranded herring sperm DNA and 25  $\mu$ L of protein A Sepharose beads were added and incubated at 4 °C with shaking for 90 min. The beads were washed twice in ChIP lysis buffer, once in ChIP lysis buffer with 500 mM NaCl, once in ChIP washing buffer (10 mM Tris pH 8.0, 0.25 M LiCl, 0.5% Nonidet P-40 and 0.5% sodium deoxycholate). The beads were washed once more in ChIP lysis buffer and resuspended in 50  $\mu$ L of Laemmli loading buffer. The input controls and immunoprecipitates were boiled for at least 30 min to reverse the cross-links. Chromatin-associated Fe65 was analyzed by SDS/PAGE and Western blot with Fe65 antibody.

## **9. Chromatin Immunoprecipitation.**

Cells were treated with 1% formaldehyde for 10 min at room temperature and formaldehyde was then inactivated by the addition of 125 mM glycine. Chromatin was then sonicated to an average DNA-fragment length of 200–1,000 bp. Soluble chromatin extracts were immunoprecipitated using Tip60, TRRAP, acetyl-histone H4, Fe65 or myc antibodies and goat or rabbit IgG as a control. Supernatant obtained without antibody was used as input control. The amount of precipitated DNA was calculated by real-time PCR relative to total input chromatin, and expressed as percent of total chromatin according to the following formula:  $2^{-\Delta Ct} \times 10$ , where Ct represents the cycle threshold and  $\Delta Ct = Ct(\text{input}) - Ct(\text{immunoprecipitation})$  (Frank, Heim et al. 2002). All the experiments have been done at least as independent triplicates and the Student's t-test was used to measure statistical

significance. Primer sequences used to amplifying the 0.5, 2 and 10 Kb regions downstream I-SceI site in NIH-GS clones (see below) are:

<b>0.5 Kb F</b>	CCACTACCTGAGCACCCAGTC
<b>0.5 Kb R</b>	GGTCACGAACTCCAGCAGGA
<b>2 Kb F</b>	TCAGGTGCAGGCTGCCTAT
<b>2 Kb R</b>	TTTGTGAGCCAGGGCATTG
<b>10 Kb F</b>	TTCTGATGGAATTAGAACTTGGCAA
<b>10 Kb R</b>	GAACGAGATCAGCAGCCTCTGT

Oligo sequences used to amplifying endogenous loci are listed below:

<b>POLII Start F</b>	5' GATTCTGGGAACGTCGGAGA 3'
<b>POLII Start R</b>	5' AAAGCTGGAGACGGGAAGC 3'
<b>POLII 17Kb up F</b>	5' GCTCAGCCAACCACAGTGATT 3'
<b>POLII 17Kb up R</b>	5' CCTGTCCGAGCGGTGATG 3'
<b>POLII 20Kb down F</b>	5' CCCTTGGCACCTTCTTTGG 3'
<b>POLII 20Kb down R</b>	5' ATCAGAGCTAAAACAGAAAGTGAGTCAA 3'
<b>ALBUMIN Start F</b>	5' TGGCAAATGAAGTGGGTAACC 3'
<b>ALBUMIN Start R</b>	5' CGAAACACACCCCTGGAAAA 3'
<b>ALBUMIN 10 Kb up F</b>	5' GCTCCATTTCTCACTGTAATACCATTT 3'
<b>ALBUMIN 10 Kb up R</b>	5' CCAGTCACCCAGCTAAAACCTTAAAA 3'
<b>ALBUMIN 15 Kb down F</b>	5' CTGGAAGAGGAAACTGGGTGAT 3'
<b>ALBUMIN 15 Kb down R</b>	5' GACCCTTTGACCACGCAACT 3'
<b>GST Start F</b>	5' CACATCTAAGCGGTCCTGGTCTA 3'
<b>GST Start R</b>	5' TGAGACTGAAGCACAGAAAAGCA 3'
<b>GST a 5Kb down F</b>	5' CCTTCCTCCACTTTTGAGTCTGA 3'
<b>GST a 5Kb down R</b>	5' TCCCTACGGTCATGTCAATCC 3'
<b>GST Start F</b>	5' CACATCTAAGCGGTCCTGGTCTA 3'
<b>GST Start R</b>	5' TGAGACTGAAGCACAGAAAAGCA 3'

All primers were used to a final concentration of 4  $\mu$ M in a 20  $\mu$ l Real Time reaction containing 10  $\mu$ l of Syber Green 2X ( Applied Biosystems) and 1  $\mu$ l DNA.

## **10. MNase ASSAY**

Micrococcal Nuclease Digestion was performed as described in ref. 1. Briefly, 10<sup>6</sup> cells were Dounce homogenized in RSB buffer (10 mM Tris\_HCl pH 7.4, 10 mM NaCl, 3 mM MgCl<sub>2</sub>, 0.5% Nonidet P-40) containing 1 mM phenylmethylsulfonyl fluoride, 1 mM Na<sub>3</sub>VO<sub>4</sub>, 1 mM DTT and protease inhibitors mixture, and incubated on ice for 15 min. Samples were washed twice with RSB buffer and digested with 2.5 units of micrococcal nuclease (USB) in digestion buffer (15 mM Tris\_HCl pH 7.5, 60 mM KCl, 15 mM NaCl, 1 mM CaCl<sub>2</sub>, 3 mM MgCl<sub>2</sub>, 20% glycerol, 15 mM β-mercaptoethanol) for the indicate times. Digestion was stopped by adding 1 volume of stop solution (50mMTris pH 7.5, 150mMNaCl, 50mMEDTA, 0.3% SDS). DNA was phenol/chloroform extracted, precipitated with isopropyl alcohol and separated using 1.2% agarose gel electrophoresis.

## **11. Cloning of mutants into p-Babe-puro retroviral vector**

p-Babe puro retroviral vector was modified by destroying the Hind III restriction site and by inserting an artificial polylinker sequence (p-Babe-puroM7). To destroy the original HindIII site, the vector was linearized with Hind III restriction enzyme and the sticky ends were filled in by using the Klenow large fragment before the ligation reaction with T4 DNA ligase to obtain a p-Babe-puro NO HINDIII vector. The artificial polilynker containing the HindIII and ApaI restriction sites was obtained by annealing in vitro the following oligonucleotides :

### **poliBamHI forward :**

5'-GATCCACCTGCAGCAAGCTTCTCGAGACGCGTGGGCCCTCGCGAG-3'

### **poliEcoRI reverse :**

5'-AATTCTCGCGAGGGCCACGCGTCTCGAGAAGCTTGCTGCAGGTG-3'

and was cloned into the p-Babe-puro NO HINDIII vector BamHI/EcoRI digested, to obtain a p-Babe-puro NO HIND III/poli vector. The resulting vector was used to clone into

HindIII/ApaI sites the Fe65 wt and mutants DNA fragments obtained by HindIII/ApaI digestion of correspondent pRC-CMV-mutNES-myc constructs described before.

## **12. Retroviral production and infection**

Fe65wt and Fe65 mutants retroviral vectors were transfected into LinX packaging cell line (Catalog #: LNX1500) by using calcium phosphate method. 48 hours after transfection viral supernatants were collected, filtered, supplemented with 8 µg/ml polybrene, and combined to infect early Fe65 KO Mefs. Infection was performed twice to ensure high efficiency. Incubation of cells with retrovirus containing supernatant was carried out for 5-6 hours at 37°C and 5% CO<sub>2</sub>.

Cells were then incubated with fresh medium and reinfected 24h after the first infection. 48 hours after the first infection, cells were selected with puromycin (2.5 µg/ml) for 4 days and used for following experiments. Effective infection was confirmed by Western blot analysis.

## **13. Generation of NIH-GS cells and measurement of repair efficiency.**

To obtain the NIH-GS clones, NIH3T3 cells were transfected with pDRGFP plasmid (SI ref. 2). 48 hours after transfection, cells were selected with puromycin (3 µg/ml) for 5 days. Puromycin-resistant colonies were pooled and amplified under puromycin selection to obtain NIH3T3-G stable clones. The latter were then transfected with the I-SceI-ER vector (see below). 48 hours after transfection, cells were selected for 9 days with 900µg/ml G418 and 2µg/ml puromycin. Double resistant colonies were pooled and amplified.

To generate the inducible I-SceI-ER construct, the ER sequence was amplified with following primers

**5glyER-For-HindIII:**

5'-CCCAAGCTTGGAGGTGCAGGAGGTCGAAATGAAATGGGTGCTTCAGGAG-3'

**ER-rev-NotI:**

5'-AAGGAAAAAAGCGGCCGCTCAGATCGTGTGGGGAAGCCCTCTGCTTCC-3'

using as template the pBSKS+ER vector kindly provided by Caterina Missero and inserted into the HindIII/NotI sites of  $\beta$ -actin promoter vector (Parisi, Passaro et al. 2008) to obtain the an ER-  $\beta$ -actin promoter vector.

The Sce-I cDNA was amplified from pC $\beta$ ASce plasmid kindly provided by prof. Avvedimento using the following primers:

**SceI BamHI forward:**

5'-CCCGGATCCAAGGCCATGGGATCAAGATCGCCAAAAAAG-3'

**SceI no stop SmaI reverse:** 5'-CCCCCGGGCTTTCAGGAAAGTTTCGGAGGAG-3'

and was cloned in frame into the BamHI/HindIII filled ER- $\beta$ -actin promoter vector, to obtain a Sce-ER plasmid.

Sequences of the oligonucleotide pairs used in ChIP experiments are reported before (see Chromatin Immunoprecipitation). NIH-GS cells were exposed to 1  $\mu$ M 4-OH-tamoxifen for 6 hours before ChIP experiments. For FACS analysis NIH-GS cells were exposed to 1  $\mu$ M 4-OH-tamoxifen for 48 hours to allow cells growth upon I-SceI-ER induction. In both cases vehicle was used to treat control plates.

## **14, FACS analysis**

For FACS analysis NIH-GS clones were transfected with Fe65 or APP+APLP2 siRNAs or control siRNA or with Fe65 constructs. 24 hours from transfection cells were treated with tamoxifen. 48 hours after I-Sce-I-ER induction, cells were harvested, resuspended in PBS at 200,000 cells/ml and GFP positive cells were counted with FACScanto (BD Biosciences, San Jose, CA) instrument. Each experiment was performed at least in triplicate by counting 30,000 events per sample. The Student's t-test was used to measure statistical significance.

## RESULTS

### **1. Fe65 KO MEFs are highly sensitive to DNA damage**

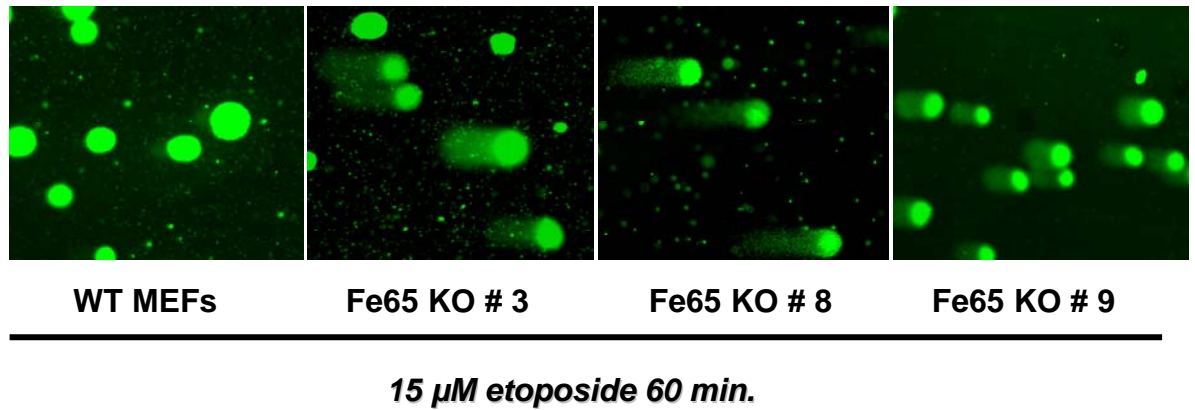
To explore the functions of Fe65 and of the Fe65/APP complex we generated Fe65 knock out mice. These mice do not show any obvious phenotypes up to 12 months of age. The most conceivable explanation of these findings is that Fe65L1 and/or Fe65L2 compensate for the absence of Fe65, thus allowing the animal to develop and live normally. However, we explored whether in stressful conditions the absence of Fe65 protein in Fe65 knock out cells could be not enough to arrange an adequate cellular response and this could result in a defect that unmasks the function of the protein. To this aim we generated mouse embryonic fibroblasts (MEFs) from Fe65 knock out (KO) mice and from wild type (WT) mice as control cell lines. Immortalized cell lines established from them were amplified and used as experimental system to evaluate the cellular response to genotoxic agents such as etoposide or hydrogen peroxide (H<sub>2</sub>O<sub>2</sub>) in the absence of Fe65.

The first experiment we performed on this cell lines was the Comet Assay, also known as Single Cell Gel Electrophoresis, that allows to evaluate the susceptibility to DNA damaging agents by measuring the length of the tail (tail length) and the amount of DNA in the tail (tail moment) in every single cells upon electrophoresis on a solid support and staining with a double-strand DNA binding dye (Sybr Green). In Figure 6A are shown Comet Assay fluorescence microscopy images from WT and Fe65 KO MEFs. The exposure to 15  $\mu$ M etoposide or 20  $\mu$ M H<sub>2</sub>O<sub>2</sub> for 30 minutes, has only marginal effects on wild type MEFs whereas three Fe65 KO MEFs, derived from three independent embryos, showed high levels of damaged DNA. Wild type MEFs show a dose dependent increase of DNA damages upon the exposure for 30 minutes to etoposide or H<sub>2</sub>O<sub>2</sub> indeed the measure of tail moment in the comet assay demonstrated that at concentrations of 15  $\mu$ M, the two agents have only marginal effects on these cells (Figure 6B). On the contrary, three Fe65

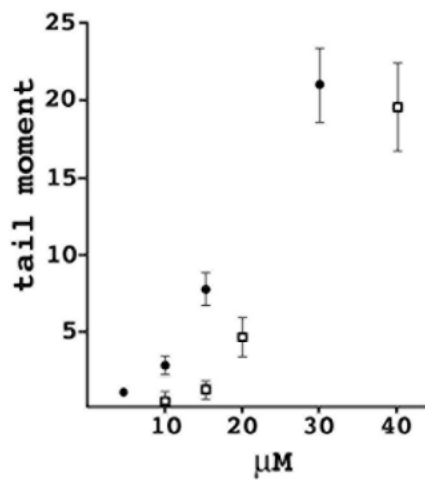
KO MEFs derived from three independent embryos showed at these low concentrations high levels of DNA damage (Figure 6B).

**Figure 6: Fe65 knock MEFs are highly sensitive to DNA damage**

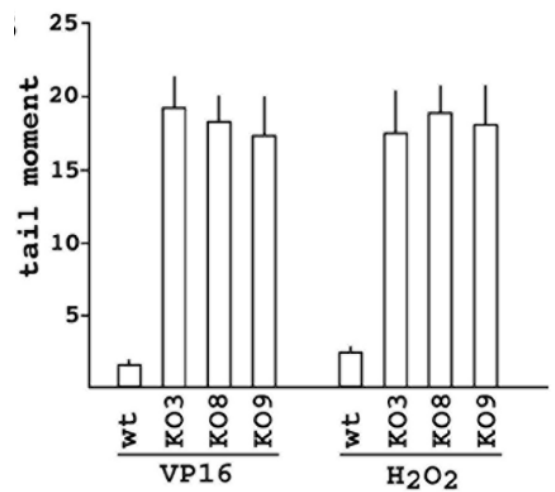
**A**



**B**



**C**



A : Fluorescence microscopy images of cells upon Comet Assay and Sybr Green staining.

B: The extent of DNA damage in wild type MEFs exposed to various doses of etoposide (VP16, squares) or H<sub>2</sub>O<sub>2</sub> (circles) was measured by the comet assay as reported under Materials and Methods. C: WT and Fe65 KO MEFs (cell lines KO3, KO8, KO9) were exposed to 15 μM etoposide or 10 μM H<sub>2</sub>O<sub>2</sub> for one hour; thereafter the extent of DNA damage was measured by the comet assay. Standard error is reported for each point.

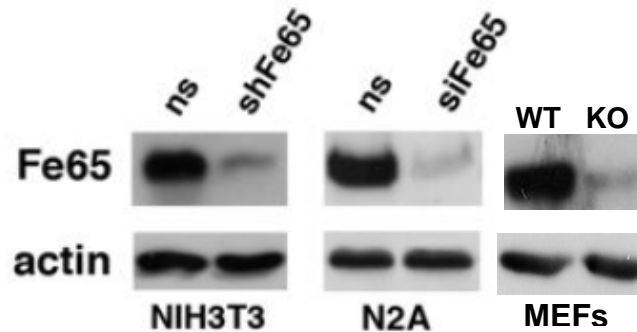
## **2. Fe65 knock down (KD) cells have the same phenotype of KO MEFs**

To confirm the phenotype observed in Fe65 KO MEFs we analyzed the sensitivity to genotoxic stress in other cellular systems in which Fe65 knockdown was obtained by RNA interference strategy. In NIH3T3 cells Fe65 expression was transiently suppressed by transfecting a shRNA-encoding vector targeting Fe65. A non silencing (ns) shRNA was transfected in control cells. As shown in figure 7 the western blot analysis with a specific Fe65 antibody, revealed that Fe65 protein level was reduced of about 80% compared to non silencing transfected cells. These cells were exposed to 20  $\mu$ M etoposide for 1 hour at 37° C and analyzed by Comet Assay.

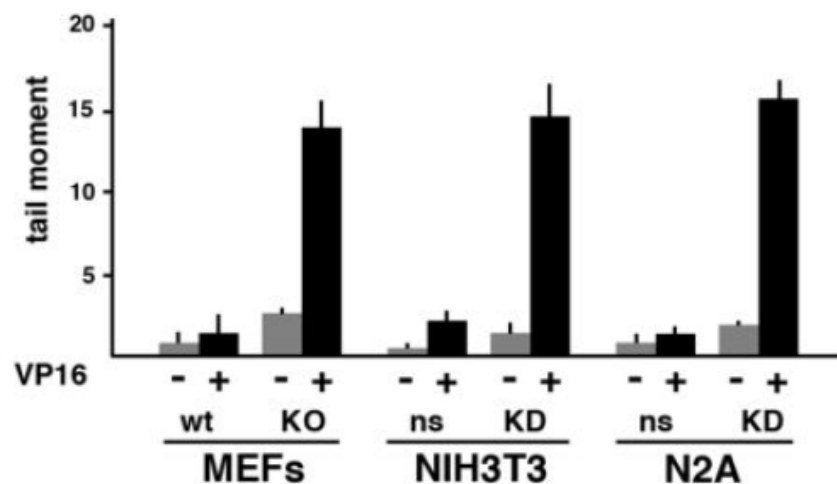
As shown in the graph, the tail moment of NIH3T3 knocked down cells is significantly higher than NIH3T3 non silencing transfected cell similar to what observed in Fe65 KO MEFs. We performed the same experiment in Neuro2A cells (N2A) in which the suppression of Fe65 was obtained by transfecting a pool of Fe65 specific siRNAs. Also in this case the western blot analysis shows an 80% reduction of Fe65 protein level compared to non silencing siRNA transfected cells. The knock down of Fe65 in N2A cells exposed to etoposide, leads to high level of damaged DNA compared to control cells (Figure 7) confirming that the absence of Fe65 in different cellular system results in high susceptibility to DNA damaging agents.

**Figure 7: Suppression of Fe65 by RNA interference results in the same phenotype observed in Fe65 KO MEFs**

**A**



**B**



NIH3T3 or N2A cells were transfected with an shRNA-encoding vector or with siRNAs targeting Fe65, respectively. Western blot analysis demonstrated that the decrease of Fe65 levels due to RNAi was of about 80%, compared to cells transfected with non silencing (ns) shRNA or siRNA. These cells were exposed to 20  $\mu$ M etoposide for 1 hour and analyzed by Comet assay as described under Materials and Methods. The results obtained in NIH and N2A KD cells are compared to those obtained in Fe65 null MEFs exposed to 20  $\mu$ M VP16. A minimum of 50 cells per experiment were analyzed. All the experiments were done in triplicate.

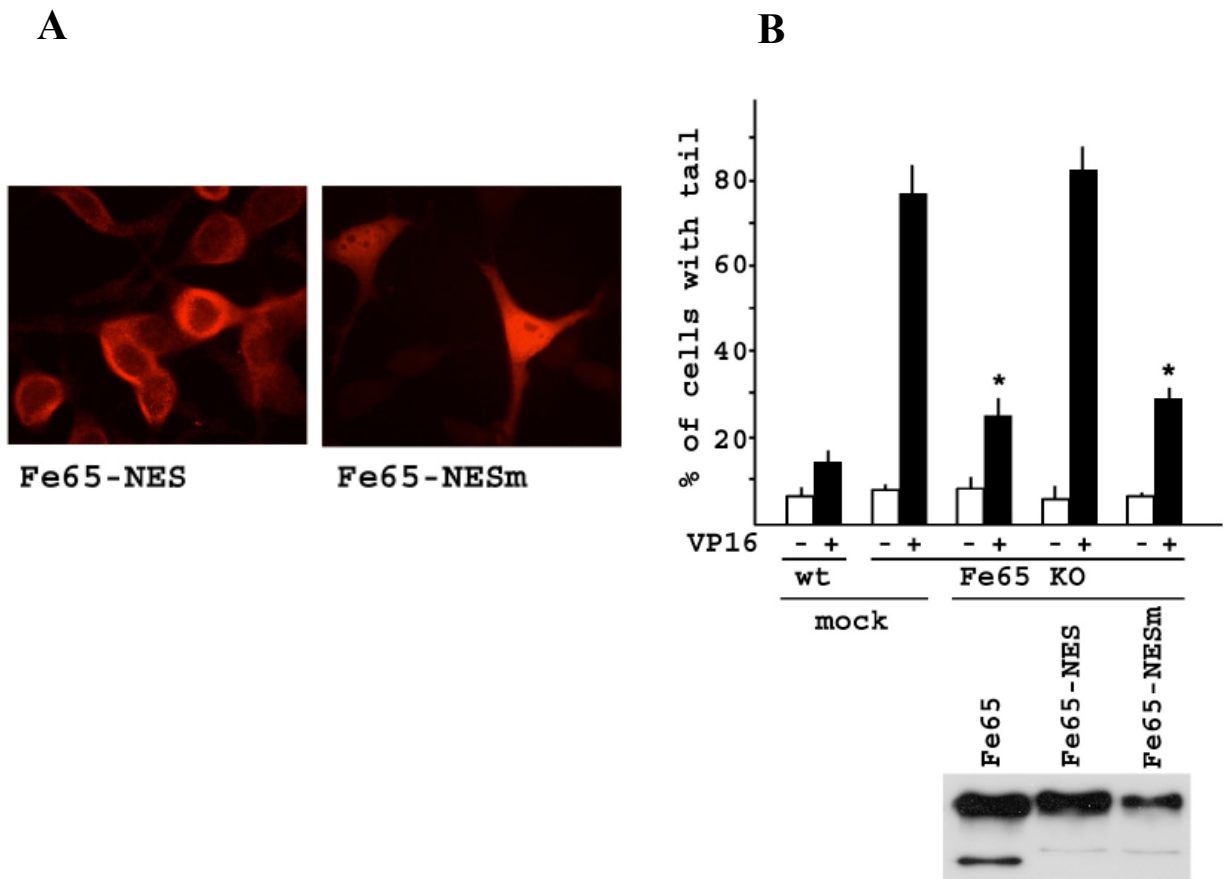
### **3. Fe65 should be present in the nucleus to rescue the hypersensitivity of Fe65 KO MEFs to genotoxic stress**

It was well demonstrated that the overexpression of Fe65 in different cell lines is accompanied by the accumulation of the protein in the nucleus and APP functions as an extranuclear anchor preventing Fe65 nuclear translocation (Cao and Sudhof 2001) (Minopoli, de Candia et al. 2001). Indeed, when overexpressed alone, Fe65 accumulates in the nucleus. Furthermore, the C-terminal fragment of APP resulting from the cleavage catalyzed by  $\gamma$ -secretase was found in the nucleus associated with Fe65 (Kimberly, Zheng et al. 2001). These observations led to the hypothesis that the processing of APP could be involved in the mechanism regulating Fe65 availability in the nucleus. On the other hand, APP cytodomain is phosphorylated at Thr668 and this phosphorylation decreases the affinity of APP for Fe65 (Nakaya and Suzuki 2006), thus suggesting a second mechanism to regulate the nuclear availability of Fe65. Therefore, we addressed the question of whether the phenotype we observed in the Fe65 KO MEFs is related to Fe65 functions requiring its presence in the nucleus. To test this point we generated two expression vectors encoding Fe65 fused at the C-terminus to the nuclear export signal of the MAPKK or Fe65 fused to a mutated, non functional, version of this NES, as previously described in ref. 27. Moreover both fusion proteins were cloned in frame at the C-terminus with the myc tag sequence. Figure 8A shows the immunostaining with an anti-myc monoclonal antibody in cells overexpressing Fe65-NES and Fe65-mutNES. As expected the Fe65 fused to the nuclear export signal accumulates in the cytoplasm and is mostly excluded from the nucleus, whereas the mutant NES sequence allows Fe65 nuclear accumulation. Fe65 KO MEFs transfected with the two recombinant proteins or with a vector encoding the Fe65 protein fused to the C-terminus with the myc tag sequence were exposed to 20 $\mu$ M etoposide and subjected to Comet Assay.

The count of cells with the tail shows that transfection of the Fe65-NES protein was unable to rescue of the phenotype of KO MEFs, while the Fe65 fused to the mutant form of the

NES had the same effect as the wt Fe65-myc fusion protein (Figure 8 B) thus suggesting that nuclear Fe65 is necessary to rescue the high sensitivity to DNA damage observed in KO MEFs.

**Figure 8: Nuclear Fe65 is needed to rescue the phenotype of Fe65 KO MEFs upon genotoxic stress.**



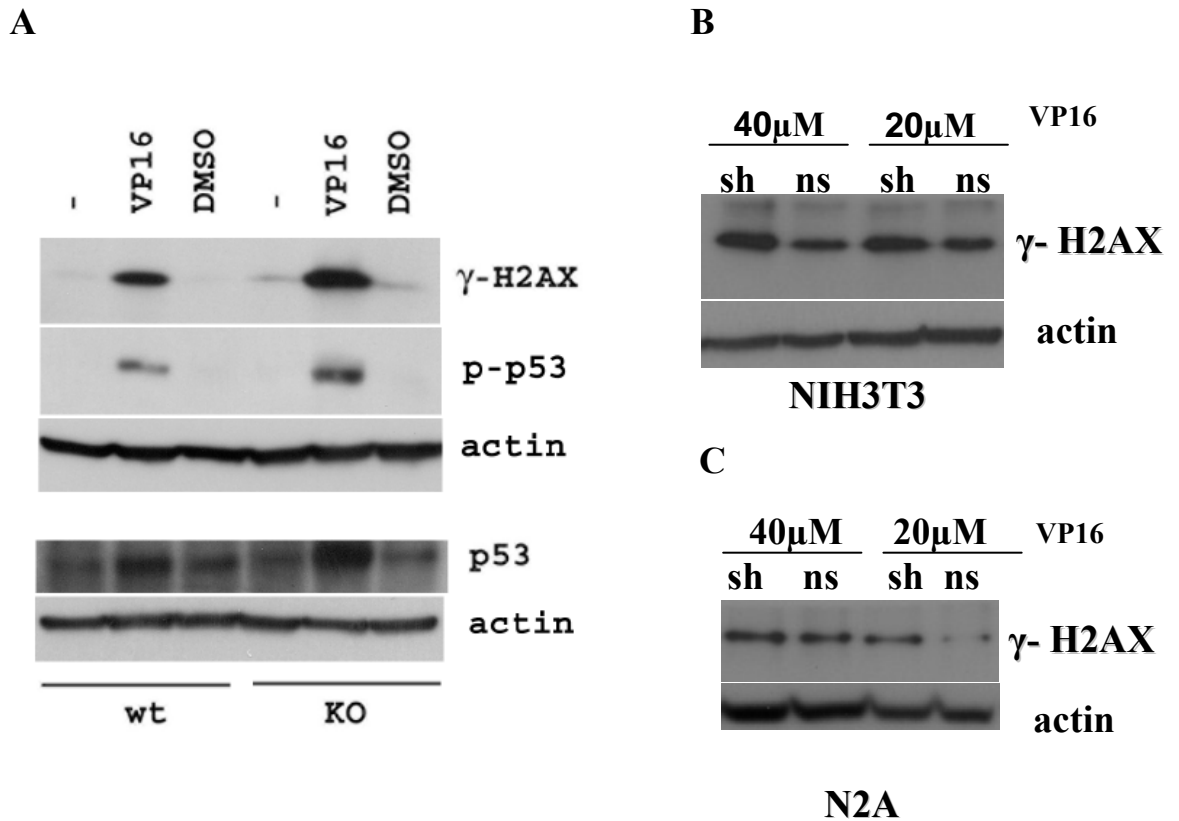
Wild type and Fe65 KO MEFs were transfected with empty vector(mock) or with vectors encoding wt Fe65 or Fe65 fused to the nuclear export signal of MAPK (Fe65-NES) or Fe65 fused to a mutated non-functional version of the NES (Fe65-NESm). Anti-myc immunostaining (A) shows the cellular localization of the two recombinant proteins. 36 hours after transfection, the cells were exposed to 15  $\mu$ M etoposide for one hour and DNA damage was measured by comet assay (B). Expression level of transfected recombinant proteins is shown. Standard deviation is reported for each point. The asterisks indicate that the mean values are significantly different ( $p < 0.01$ ) from that of mock transfected cells.

#### **4. Fe65 KO and KD cells show higher level of phosphorylated H2AX and p53 under genotoxic stress condition**

Comet assay analysis showed that the absence of Fe65 in different cellular systems leads to high sensitivity to DNA damage induced by genotoxic agents like VP16 or H<sub>2</sub>O<sub>2</sub>.

To confirm this phenotype we analyzed the amount of phosphorylated H2AX histone and p53 upon low doses of etoposide treatment in Fe65 KO MEFs. Indeed both protein are early marker of DNA damage response since they are rapidly phosphorylated on specific residues by the serin/ threonine kinase ATM. We performed a Western Blot analysis with an antibody that specifically recognize phosphorylated H2AX on serin-139 (known as  $\gamma$ -H2AX) on total protein extracts obtained from Fe65 KO and WT MEFs. As shown in figure 9A  $\gamma$ -H2AX was undetectable in non treated or DMSO treated WT MEFs, whereas the exposure to etoposide resulted in  $\gamma$ -H2AX accumulation. The amount of  $\gamma$ -H2AX is higher in KO than in WT MEFs after etoposide treatment. Moreover a little amount of  $\gamma$ -H2AX was detectable also in non treated or DMSO exposed Fe65 KO MEFs thus confirming that the absence of Fe65 leads to high sensitivity to DNA damage. As shown in figure 4B also the phosphorylation of p53 on serin15 residue was higher in KO than in WT MEFs as a consequence of a stronger DNA damage response, and according to literature this modification leads to the accumulation of the protein as shown by the Western Blot of total p53.  $\gamma$ -H2AX is a very well known marker of damaged DNA since it accumulates in specific foci representing DNA double strand breaks. We measured the amount of  $\gamma$ -H2AX upon etoposide treatments (20  $\mu$ M and 40  $\mu$ M for 1 hour) in NIH3T3 cells and N2A cells in which Fe65 was knocked down as described before. As shown in figure 9 B and C in both cell lines the absence of Fe65 led to stronger phosphorylation of H2AX histone supporting the idea that the number of etoposide induced double strand breaks is higher in KD than in WT cells.

**Figure 9: Fe65 KO and KD cells show stronger activation of H2AX and p53 than WT under genotoxic stress condition**



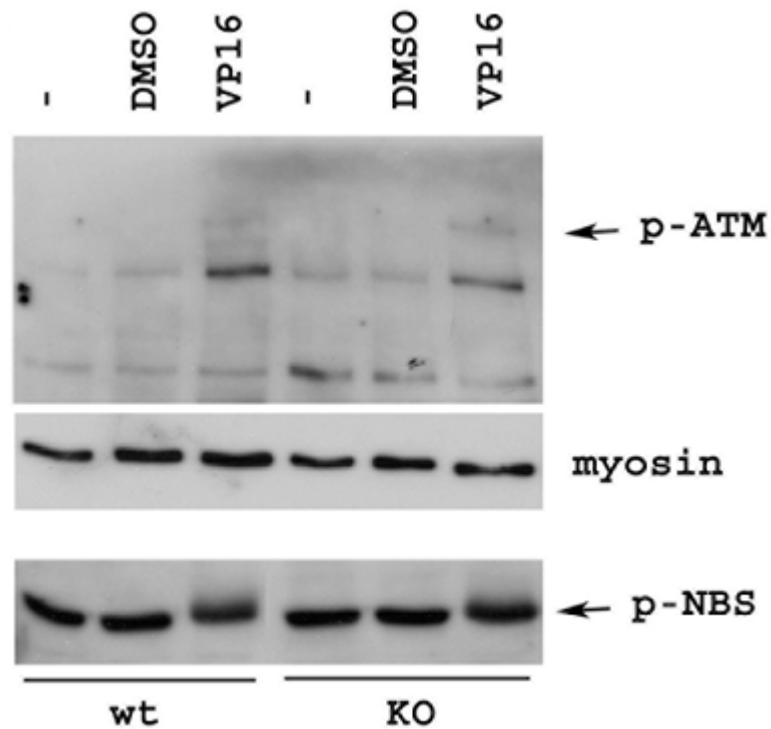
A : Wild type and KO cells were exposed to 15  $\mu$ M etoposide and their sensitivity to DNA damage was explored by measuring  $\gamma$ -H2AX (ser-139) and phospho-p53 (ser15) and the accumulation of total p53, as indicated. The Western blot refers to the experiment made with extracts from KO9 MEF line; extracts from two other lines gave the same results. 100  $\mu$ g of total protein extract were loaded per line. B and C : The phosphorylated form of histone H2AX ( $\gamma$ -H2AX) was measured by Western blot analysis in NIH 3T3 cells transfected with non silencing (ns) or Fe65 targeting shRNA and in N2A cells transfected with an siRNA targeting Fe65 or with non silencing (ns) siRNA as a control. Cells were exposed to two different concentration of VP16 ( 20 and 40  $\mu$ M) for 1 h. Actin was used to normalize the amount of protein in different samples.

## **5. ATM activation and NBS phosphorylation seem to be normal in Fe65 KO MEFs upon DNA damage induction**

It is well known that generation of DSBs results in intermolecular modification within ATM dimers that leads to their activation via autophosphorylation of Ser-1981. Intermolecular phosphorylation subsequently triggers dimer dissociation, and the free monomers can phosphorylate several nuclear proteins for recruitment of DNA damage response proteins, including the MRN complex (Lukas, Falck et al. 2003). Considering that histone H2AX is, possibly, the first protein that is phosphorylated by ATM but also by other members of the ATM family (DNA-PK and possibly ATR), we decide to evaluate the phosphorylation of ATM in our KO MEFs upon etoposide treatment by Western Blot analysis using a ser-1981 phospho specific antibody. As shown in figure 10 the phosphorylation of ATM occurred normally in Fe65 KO MEFs compared to WT suggesting that the upstream events during DNA damage response were unaffected in the absence of Fe65.

To further investigate the proper activation of ATM we analyzed the phosphorylation of NBS1 that is one of the ATM downstream target phosphorylated in response to DSB-inducing agents (Wu, Ranganathan et al. 2000) (Gatei, Young et al. 2000). NBS1 is recruited to damage sites by binding to MRE11 at the C-terminus in an ATM-independent manner, and then recruits/retains the MRN complex by binding to H2AX at the N-terminus in an ATM-dependent manner. The Western Blot with an anti-NBS antibody (figure 10) shows that the phosphorylation of NBS occurred properly in Fe65 KO MEFs upon etoposide treatment as demonstrated by the band migrating slower than unphosphorylated protein.

**Figure 10: ATM activation and NBS phosphorylation are apparently normal in Fe65 KO MEFs compared to WT cells**

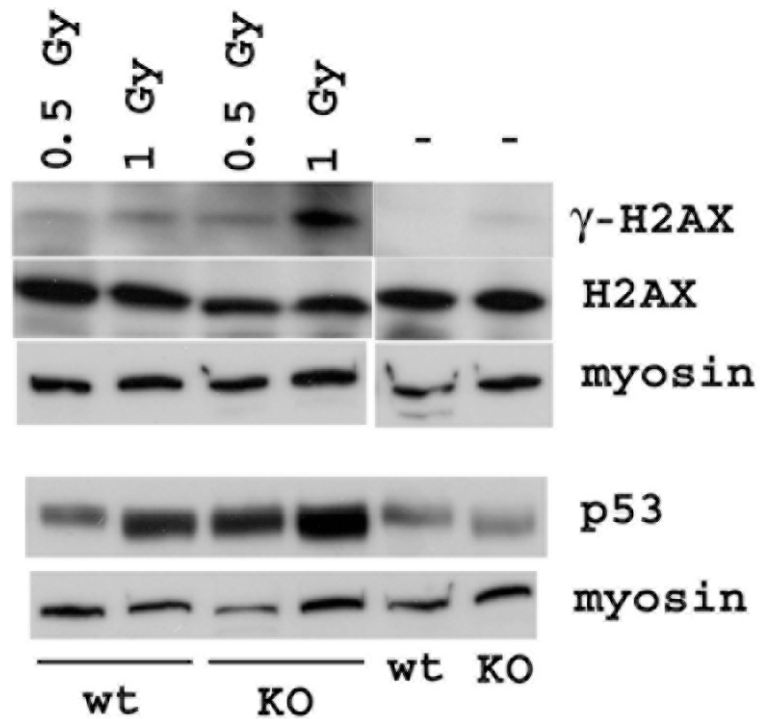


The cell response to genotoxic stress was analyzed in wt and Fe65 KO MEFs exposed to 40  $\mu$ M etoposide by exploring the activation of ATM; active, autophosphorylated ATM (arrow) was analyzed by western blotting with anti-phospho-ATM (ser-1981) of the indicated extracts from untreated, DMSO- or etoposide-treated cells. Phosphorylation of NBS, one of the substrates of ATM, was analyzed by western blotting of the same extracts: NBS phosphorylation is detected as a band migrating slower than the unphosphorylated protein (arrow).

## **6. Effects of DNA damage in Fe65 KO mice**

The differences observed between wild type and Fe65 KO MEFs could imply an abnormal response of Fe65 KO mice to DNA damage. Therefore, we analyzed the sensitivity of our KO mice to X-ray-induced DNA damage. KO male mice of 3 months of age and normal mice, sex and age matched and belonging to the same litter, were exposed to non-fatal, low doses (0.5 and 1 Gy) of ionizing radiations. As shown in Figure 11, 2.5 hours after the exposure to ionizing radiations brain extracts from Fe65 KO mice showed higher levels of phosphorylated  $\gamma$ -H2AX and a higher p53 accumulation compared to those of wild type mice. The latter are clear signs of the high sensitivity of Fe65 KO mice to genotoxic stress, thus confirming what observed in *in vitro* cellular systems.

**Figure 11: Fe65 knock out mice are highly sensitive to DNA damage.**



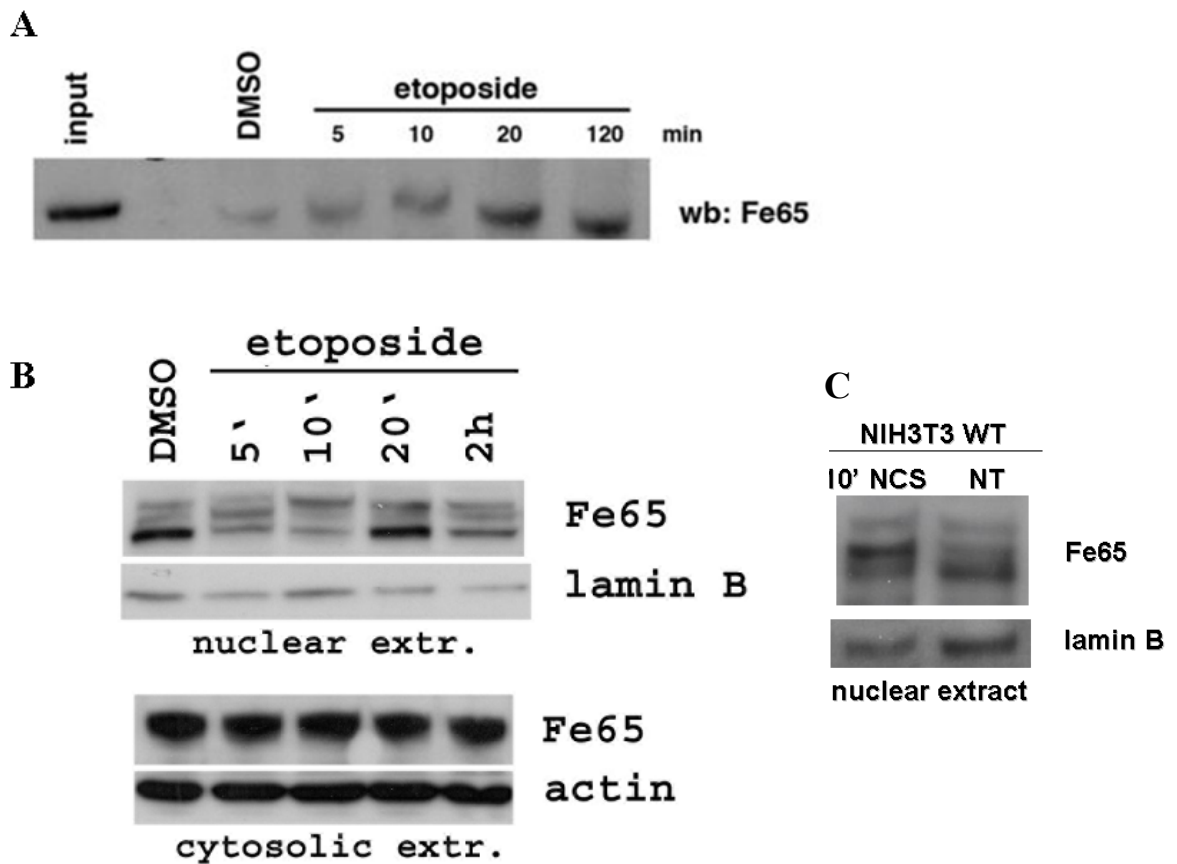
WT and Fe65 KO mice were exposed to 0.5 and 1 Gy of X rays as described under Materials and Methods. 2.5 hours after irradiation the animals were sacrificed and brain extracts were analyzed by western blotting with anti- $\gamma$ -H2AX histone or with anti p53 antibodies. Myosin heavy chain is used as a control of load. Controls experiments from untreated mice are reported in the last two lanes.

## **7. Fe65 associates with intact and damaged chromatin and undergoes rapid phosphorylation in response to DNA damage**

The findings that the absence of Fe65 leads to hypersensitivity to DNA damage and that it should be present in the nucleus to rescue this phenotype suggested us to investigate the possibility that Fe65 is a chromatin bound protein. Therefore we analyzed Fe65 association with chromatin at a global genomic level both in basal conditions and in presence of DNA damage. To this aim, we immunoprecipitated crosslinked chromatin from N2A cells with an histone H3 antibody. This H3 immunoprecipitated chromatin, roughly representing the whole chromatin, was de-crosslinked and analyzed by western blot for the presence of Fe65. Figure 12A shows that Fe65 is indeed associated with intact chromatin and that this association was only slightly increased upon genotoxic stress induced by etoposide. Moreover the western blot revealed that the protein migration was slower in the sample exposed for 10 minutes to etoposide than non treated sample probably as a consequence of protein phosphorylation. To further investigate this possibility, we monitored nuclear Fe65 at various times after the exposure of wild type MEFs to 40  $\mu$ M etoposide (figure 12B). We previously demonstrated that our polyclonal antibody against Fe65 recognizes several bands in nuclear extracts, the slowest migrating ones are erased by the alkaline phosphatase treatment (Zambrano, Minopoli et al. 1998). The etoposide treatment induced a rapid modification of the pattern of the Fe65 bands after 5 and 10 minutes. Thereafter, the basal pattern was restored (20 min) and remained unchanged for several hours. The amount of cytosolic Fe65 was not affected by the etoposide treatment. We performed the same experiment in NIH-3T3 cells exposed to the radiomimetic agent Neocarzinostatin (NCS). As shown in figure 12C the exposure of cells to NCS for 10 minutes resulted in the accumulation of a band with slower migration than non treated cells, supporting the idea that Fe65 phosphorylation is an early event during DNA damage response. The association to chromatin and the rapid modification of Fe65 as a consequence of the exposure of the

cells to DNA damaging agents suggest its involvement in the early steps of the cellular response to the genotoxic stress.

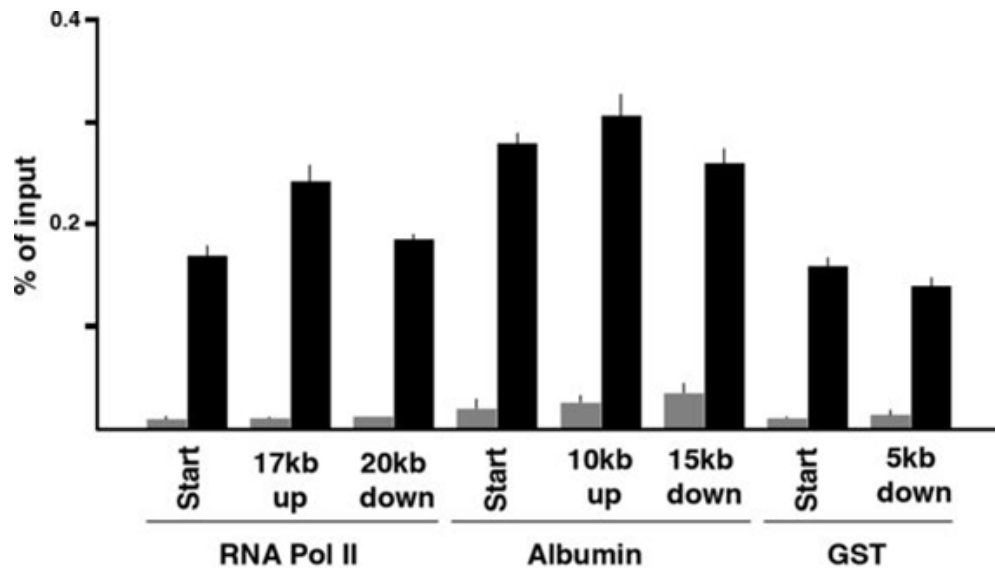
**Figure 12: Endogenous Fe65 associates with chromatin and undergoes rapid phosphorylation in response to DNA damage**



A: N2A cells were treated or not with 100  $\mu$ M etoposide for the indicated times. Crosslinked chromatin was immunoprecipitated with histone H3 antibody. De-crosslinked chromatin was analyzed by western blot with Fe65 antibody. Input indicates the non immunoprecipitated crosslinked extract. B: Normal MEFs were exposed to 40  $\mu$ M etoposide for the indicated times. Nuclear and cytosolic extracts were prepared at the indicated intervals and analyzed by western blot with anti-Fe65 antibody (L12 serum 1:2000). Lamin B and actin were used as control of loading. C: NIH3T3 cells were exposed to neocarzinostatin (NCS) 0.5  $\mu$ g/ml for 10 minutes. Nuclear extracts were prepared from untreated (NT) and treated (10'NCS) cells and analysed as in B

We know that after sequential proteolytic processing of membrane-bound APP and release of AICD into the cytoplasm, Fe65 can translocate to the nucleus to participate in gene transcription events. This role is further mediated by the interactions of Fe65 PTB1 with the transcription factors CP2/LSF/LBP1 and Tip60 and the WW domain with the nucleosome assembly factor SET although none of proposed Fe65 target genes have yet been confirmed. The finding that Fe65 is a chromatin bound protein suggested us to explore the possibility that its association with chromatin preferentially occurs at the genomic regions that are highly transcribed. To explore this possibility we analyzed in NIH3T3 cells, the association of Fe65 with three random genomic loci, i.e. those of RNA polymerase II that is a constitutive gene, albumin that is a tissue specific gene and glutathione-S-transferase that is an inducible gene performing Chromatin Immunoprecipitation (ChIP) experiments. To this aim chromatin from NIH-3T3 cells was immunoprecipitated with an anti-Fe65 antibody or control IgG and immunoprecipitated chromatin was amplified with three different oligo pairs surrounding the transcriptional start site, the upstream and the downstream regions of each locus. As shown in figure 13 the Fe65 antibody was able to immunoprecipitate the endogenous protein at each locus. Moreover this association seems to be independent from transcriptional status of chromatin since Fe65 bound to the same extent the analyzed transcriptional start sites and the distal upstream and downstream regions.

**Figure 13: Fe65 is widely associated to chromatin of randomly selected loci.**



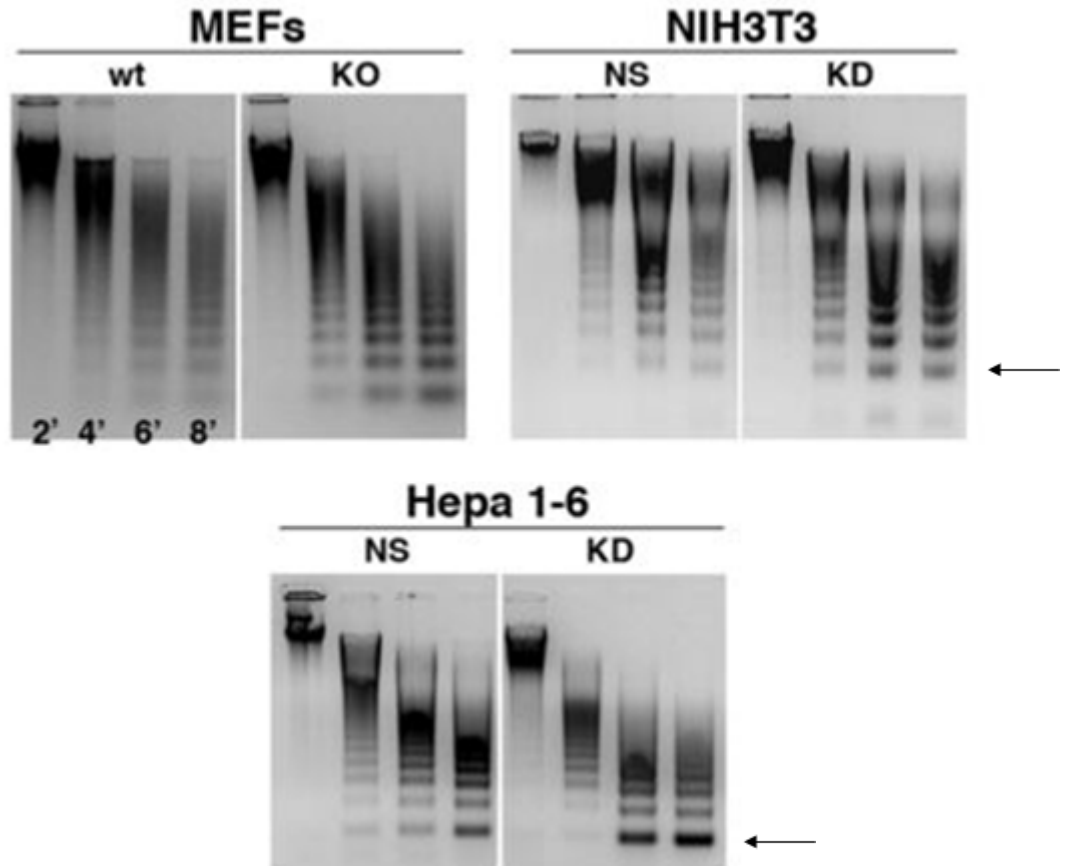
Chromatin from NIH3T3 cells was immunoprecipitated with Fe65 antibody (black bars) or control IgG (grey bars) and amplified with the oligonucleotide pairs reported in SI Table III of (materials and methods) , to explore the presence of Fe65 on three genomic loci. The oligonucleotides were designed to amplify regions of the RNA polymerase II, serum albumin and glutathione-S-transferase genes close to their start sites and at the indicated distances upstream or downstream from the start sites.

## **8. Fe65 association with chromatin determines its degree of condensation.**

The finding that the absence of Fe65 rendered the cells more vulnerable to DNA lesions and that Fe65 associated with chromatin both in basal and under genotoxic stress conditions, suggested us to explore its possible involvement in chromatin condensation state. To this aim we analyzed the accessibility of chromatin to micrococcal nuclease digestion in Fe65 KO and KD cells compared to WT. We found that chromatin from Fe65 KO MEFs or Fe65 KD cells was more accessible to micrococcal nuclease digestion, than chromatin from wt cells (figure14), thus demonstrating that Fe65 suppression leads to a significant degree of chromatin de-condensation. This phenotype was rescued by Fe65 re-expression in KO MEFs (figure 15A).

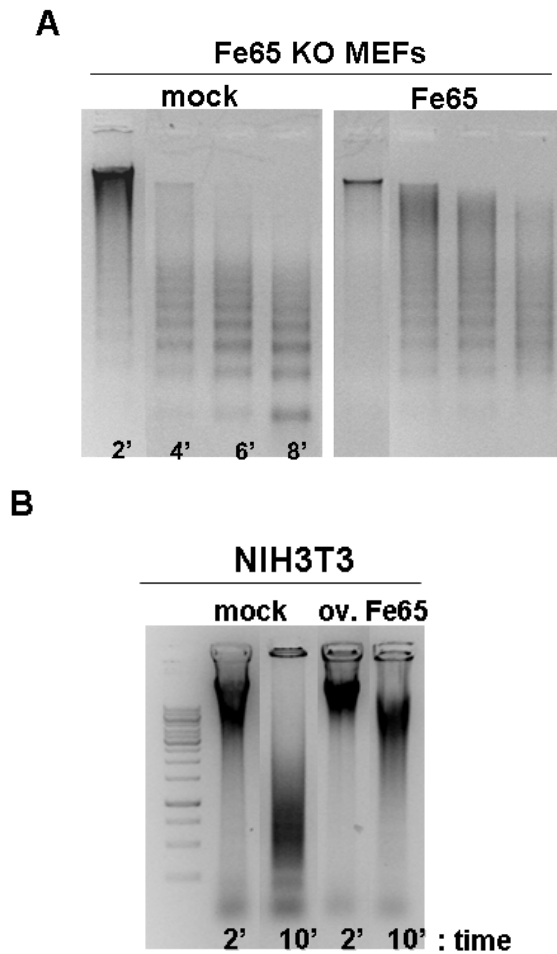
Moreover Fe65 overexpression in NIH3T3 cells results in highly condensed state (figure 15B) since chromatin from NIH3T3 overexpressing cells was quite completely undigested even after 10 minutes of incubation with micrococcal nuclease. These data revealed that the association of Fe65 with chromatin is functionally relevant since it determines the degree of chromatin decondensation in basal conditions.

**Figure 14: Fe65 KO and KD cells have more relaxed chromatin than WT**



Chromatin from the indicated cell lines, in which Fe65 was suppressed by gene KO or by RNA interference, was digested with 2 mM micrococcal nuclease for the indicated times. Digested DNA was examined by agarose gel electrophoresis. Fe65 KO or KD result in the accumulation of the smallest bands of nucleosomal ladder (arrows)

**Figure 15: Fe65 expression in KO cells restore the chromatin condensation state whereas its overexpression leads to high condensation state**



A: Retroviral-directed reexpression of wt Fe65 in KO MEFs restored the normal cleavage pattern in micrococcal nuclease assay as demonstrated by the absence of small bands even after 8 minutes of nuclease digestion.

B: Chromatin from Fe65 overexpressing NIH3T3 was resistant to micrococcal nuclease digestion compared to mock transfected cells as a consequence of high condensation state.

## **9. Fe65 mutants lacking the WW and the PTB1 domains or carrying C655F point mutation are unable to rescue the Fe65 KO MEFs phenotype**

Fe65 has the three protein-protein interaction domains interacting with several nuclear proteins. Among these two ligands are involved in chromatin remodelling functions. Indeed Fe65 interacts with the nucleosome assembly protein SET through a region that partially overlaps the WW domain and with the histone acetyl-transferase Tip60 and the transcription factor LSF through the PTB1 domain. Our findings on Fe65 involvement in regulation of chromatin state strongly support a possible mechanism involving SET and Tip60 proteins. Moreover Fe65 interacts with APP or AICD through the PTB2 domain. To explore the possible involvement of these known partners in the Fe65 nuclear function responsible for the phenotype observed in KO and KD cells, we cloned in the pBabe retroviral vector (see Materials and Methods) several mutants carrying deletion or point mutations in the three domains of the protein. In figure 16A the structural organization of wild type protein and its mutants is shown. The  $\Delta$ upWW mutant completely loses the N-terminus region of the protein until aminoacid residue 253.

This region is not involved in any known interaction but it contains a peculiar acidic region possibly involved in the association with chromatin.

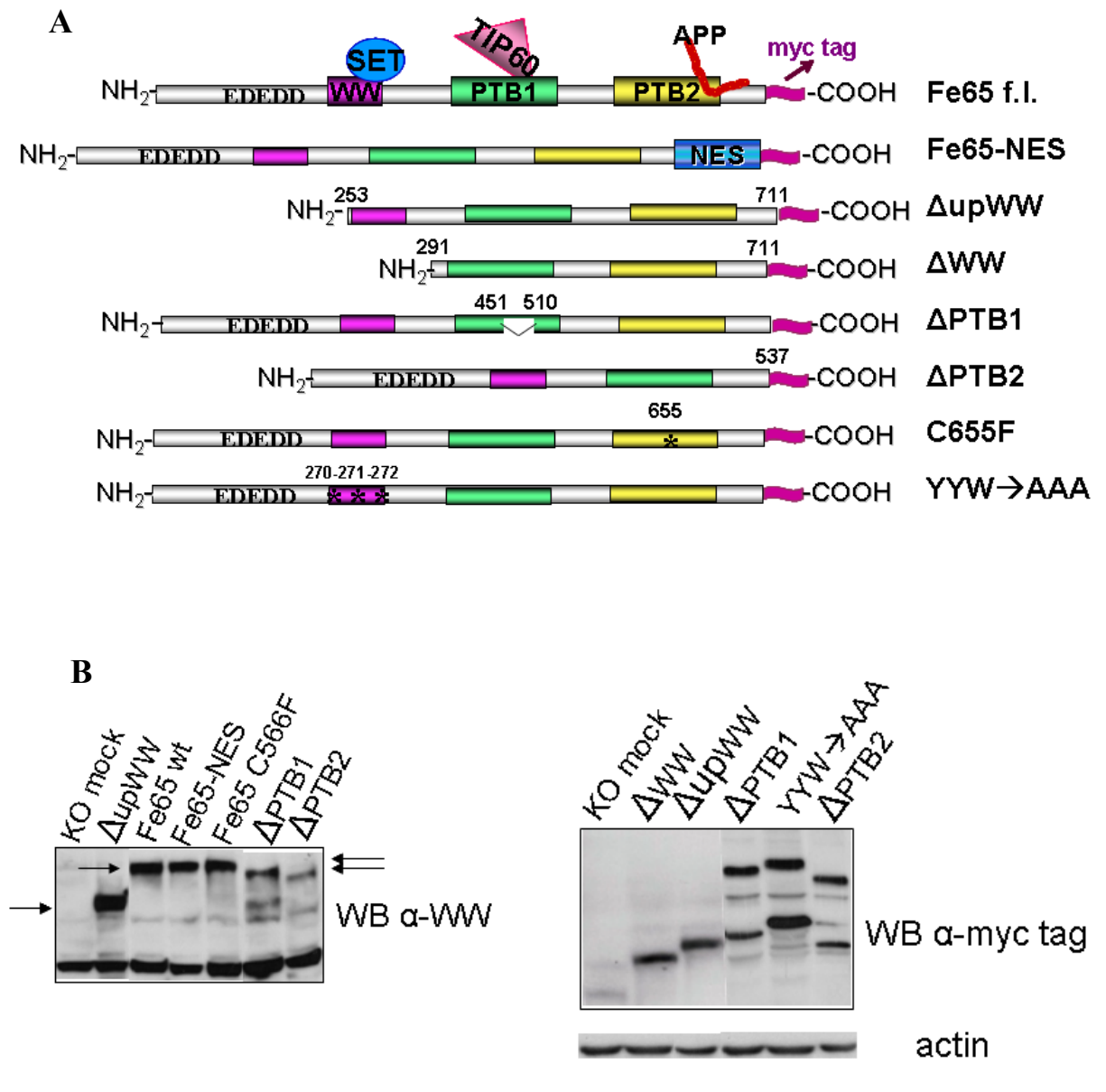
The  $\Delta$ WW loses the entire WW domain starting from aminoacid residue 291. The absence of WW domain has a profound effect on the protein since this mutant is unable to reach the nucleus. Moreover it is unable to interact with SET protein. The  $\Delta$ PTB1 mutant loses the region of the PTB1 domain between aminoacid 451-510 thus abolishing the interaction with Tip60.

The  $\Delta$ PTB2 mutant entirely loses the PTB2 domain that is involved in the APP/AICD binding. We generated also two mutants carrying specific point mutations. The first contains a triple mutation in the WW domain substituting the YYW sequence with AAA. This mutation specifically abolishes the interaction with SET protein and the

transactivation property of the protein. The second contains a single point mutation in the PTB2 domain (C655F) that specifically abolishes the interaction with APP and its paralogues APLP1 and APLP2.

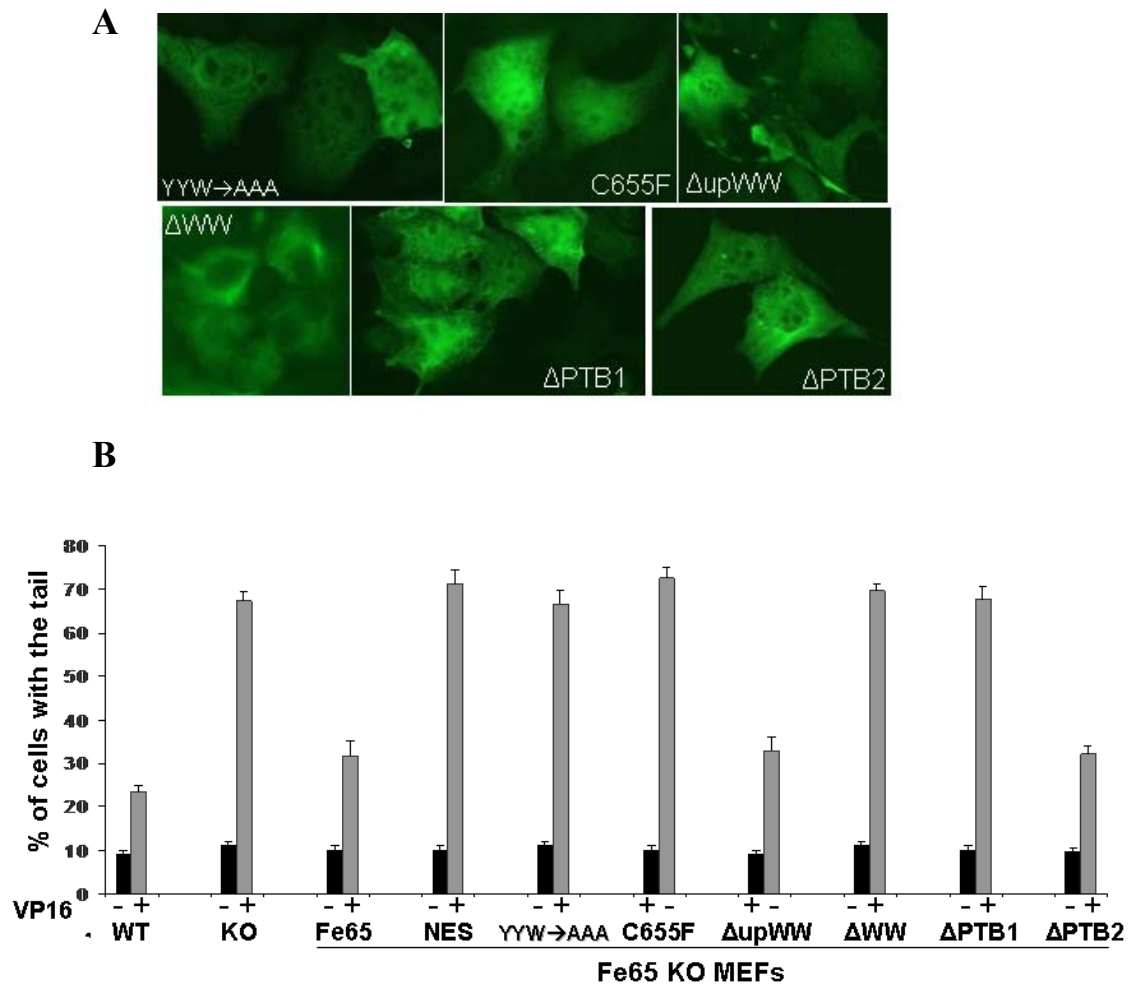
The expression level of wild type protein and its mutants were analyzed by western blot in Fe65 KO MEFs upon retroviral infection (figure 16B) using an anti-myc tag antibody or an antibody recognizing an epitope in the WW domain. Infected cells were also analyzed by immunostaining with an anti-myc antibody to evaluate the cellular localization of each Fe65 mutant. As shown in figure 17A, the  $\Delta$ PTB1,  $\Delta$ PTB2 and the  $\Delta$ upWW mutants showed the same cellular localization of the wild type protein since they accumulated in the nucleus upon overexpression. Also the C655F and the YYW $\rightarrow$ AAA mutants showed a proper nuclear localization thus suggesting that the loss of interaction with SET, Tip60 or APP/AICD do not alter the Fe65 nuclear localization. As expected, the  $\Delta$ WW mutant is unable to reach the nucleus and accumulates in the cytoplasm confirming that this region is necessary for protein nuclear localization. We performed a rescue experiment in Fe65 KO MEFs expressing each mutant protein. To this aim infected cells were exposed to 20 $\mu$ M etoposide and analyzed by comet assay counting the number of cells with the tail (figure 17B). As previously shown the wild type protein was able to rescue the phenotype whereas the protein fused to the nuclear export signal did not. As expected also the  $\Delta$ WW mutant was unable to rescue the phenotype being excluded from the nucleus. The  $\Delta$ upWW and the  $\Delta$ PTB2 mutants rescued the phenotype with the same extent of the wild type protein. Finally, despite their proper nuclear localization, the  $\Delta$ PTB1, the YYW $\rightarrow$ AAA and the C655F mutants were unable to rescue the phenotype suggesting that Fe65 interaction with Tip60, SET and APP/AICD is necessary for its nuclear function in DNA damage response. Interestingly the C655F mutant lacking the interaction with APP/AICD was unable to rescue the phenotype although the mutant lacking the entire PTB2 domain ( $\Delta$ PTB2) behaved like the wild type protein.

**Figure 16: Schematic representation and expression of Fe65 mutants**



A: Structural organization of wild type Fe65 protein and its mutants carrying specific deletions or point mutations. The number of aminoacid residues corresponding to deleted regions or mutated residues refers to rattus protein sequence. B: Western blots of Fe65 KO MEFs after infection with indicated Fe65 mutants were carried out with an antibody recognizing an epitope in the WW domain or with an anti-myc tag antibody.

**Figure 17: Dissection of Fe65 interaction domains necessary to rescue the Fe65 KO MEFs phenotype**



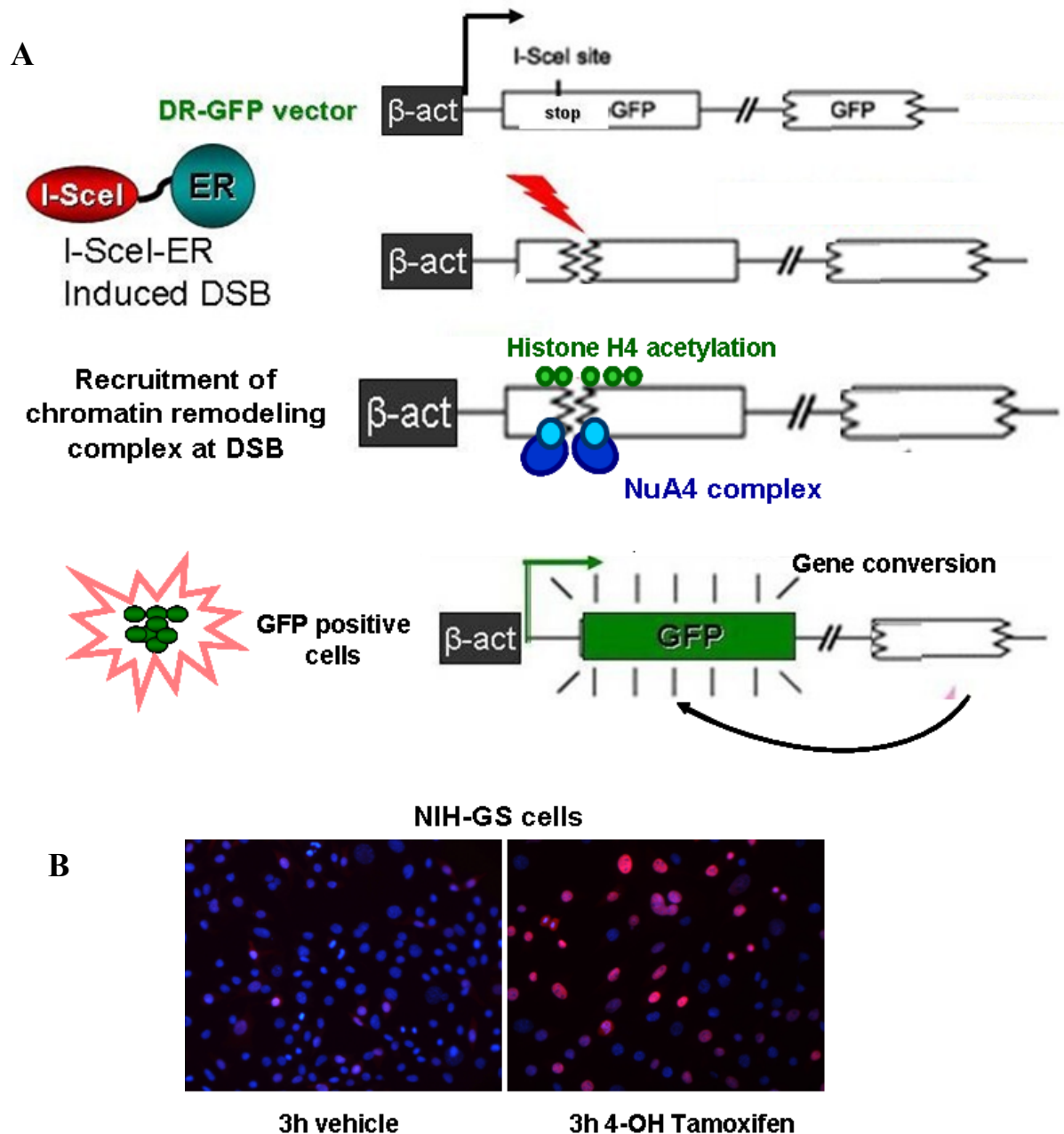
A : Fe65 KO MEFs were infected with corresponding mutants as reported under Materials and Methods and stained with an anti-myc tag antibody to reveal their cellular localization. B: Fe65 KO MEFs expressing indicated proteins and exposed to 20 $\mu$ M VP16 or to DMSO as a control were analyzed by comet assay counting the number of cells with the tail. A minimum of 50 cells per experiment were analyzed. All the experiments were done in triplicate.

## **10. Generation of the DR-GFP/ISce-I-ER system to study Fe65 involvement in chromatin remodelling during DNA repair**

The finding that the Fe65 mutant unable to bind Tip60 ( $\Delta$ PTB1) failed to rescue the high sensitivity to DNA damage observed in KO and KD cells, suggested us to focus on the possible involvement of Fe65/Tip60 complex in the cellular response to DNA damage. Indeed Tip60 is a well studied histone acetyl transferase involved in many cellular processes including chromatin remodelling during DNA repair of double strand breaks (DSBs). It has been shown that the NuA4 complex containing Tip60 and its cofactor TRRAP is rapidly recruited at DSBs during DNA repair to drive the acetylation of histone H4 in the surrounding region. Tip60 driven histone acetylation results in local chromatin decondensation that favours the loading of DNA repair machinery (Murr, Loizou et al. 2006). To analyze the possible involvement of Fe65 in Tip60 mediated chromatin remodelling during DNA damage response, we exploited the DRGFP/I-SceI experimental system (Richardson, Elliott et al. 1999) (see figure 18A). To this aim, we generated clones of NIH3T3 cells stably transfected with a DNA construct (*DR-GFP*) containing two non-functional *GFPs*. The upstream (5') *GFP* is under the control of the  $\beta$ -actin gene promoter and contains a single recognition site for the I-SceI endonuclease. Considering that no I-SceI sites are present in mammalian genomes, the expression of this enzyme results in generation of single DNA DSB only at *DR-GFP* sites (29, and figure 18A). We also generated an I-SceI-ER expression vector, in which the ISceI cDNA is fused in frame with the cDNA fragment encoding the hormone-binding site of the estrogen receptor alpha ( $ER\alpha$ ). The double stable clones NIH-GS bearing *DR-GFP* and I-SceI-ER were pooled and treated with 4-OH tamoxifen. Figure 18B shows the nuclear translocation of ISce-I-ER fusion protein upon 4-OH tamoxifen treatment. We performed chromatin immunoprecipitation experiments in our NIH-GS cells to evaluate Tip60/TRRAP recruitment and histone H4 acetylation upon I-SceI-ER driven DSBs generation,

amplifying with specific oligo pairs three regions located at 0.5, 2 and 10 Kb from I-SceI site respectively.

**Figure 18: The DR-GFP/ISce-I-ER system**

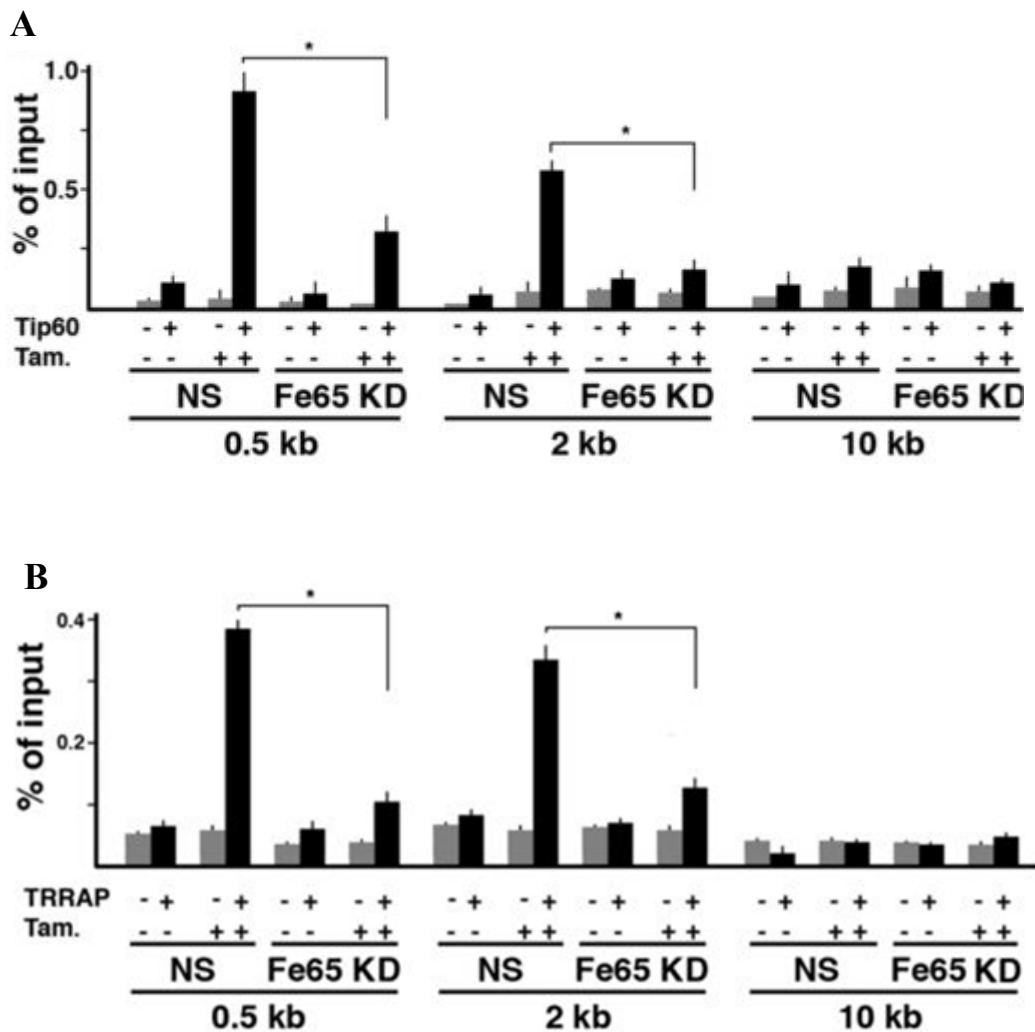


A: 5' *GFP* sequence was cleaved by I-SceI-ER upon the exposure of the NIH-GS cells to 1 $\mu$ M 4-Hydroxytamoxifen (tamoxifen) for 6 hours. Upon the cleavage, Tip60-TRRAP-containing complex was recruited at the DNA and histone H4 was acetylated by Tip60. Gene conversion events are able to repair the double strand break induced by I-SceI by using the downstream 3' *GFP* as donor that allow GFP expression. B: Immunostaining of NIH-GS cells with an anti-ER $\alpha$  monoclonal antibody that reveals the cellular localization of the ISce-I-ER fusion protein before and after 4-OH-tamoxifen treatment.

## **11. Fe65 suppression prevents the recruitment of Tip60-TRRAP at DNA double strand breaks**

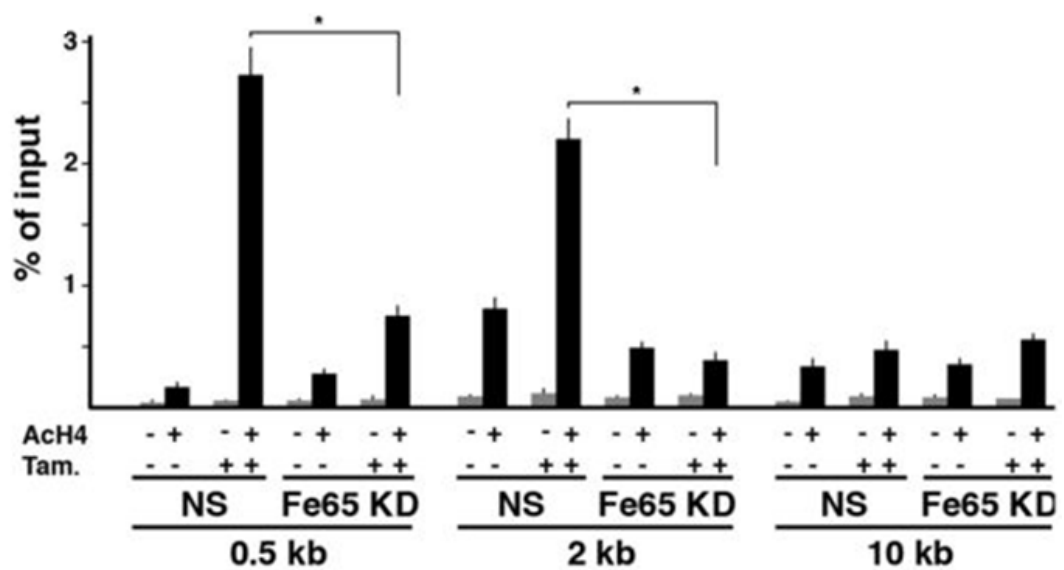
In agreement with that previously observed by others (Murr, Loizou et al. 2006), the cleavage induced by I-SceI-ER in NIH-GS cells resulted in the recruitment of Tip60 to the site of DNA damage. In fact, CHIP experiments with Tip60 antibody showed a significant enrichment of Tip60 at the 5' *GFP* site upon the induction of I-SceI-ER by tamoxifen. This enrichment was clearly detectable with oligonucleotide pairs amplifying DNA at 0.5 and 2 kb downstream of the cleavage site, but not with the control oligonucleotide pair targeting the region 10 kb downstream of the DSB (figure 19A). Interestingly, in cells where Fe65 was knocked down Tip60 recruitment to DSB was strongly decreased (figure 19A). Similar to Tip60, its partner TRRAP was recruited to DNA breaks in wt cells. Fe65 KD resulted again in a significant decrease of TRRAP recruitment (figure 19B). As a consequence of the impairment of Tip60-TRRAP recruitment to DNA strand breaks, CHIP experiments with an anti-acetyl-H4 antibody demonstrated that while in wt cells I-SceI-driven cleavage induced the histone H4 acetylation at the I-SceI site, the concomitant suppression of Fe65 significantly decreased H4 acetylation (figure 20) both at 0.5 and 2 Kb downstream regions.

**Figure 19: Fe65 suppression affects Tip60 and TRRAP recruitment at DNA double strand breaks.**



Fe65 knockdown is accompanied by a decreased recruitment of Tip60 at DNA double strand breaks. NIH-GS cells, stably transfected with the inducible form of I-SceI-ER restriction enzyme and with DR-GFP construct (see Materials and Methods) bearing a single I-SceI cleavage site, were treated with 1  $\mu$ M tamoxifen for 6 hours. ChIP was performed with Tip60 antibody (+) or control IgG (-). Immunoprecipitated chromatin was analyzed by real time PCR using three oligonucleotide pairs located at approximately 0.5, 2 and 10 Kb downstream of the I-SceI cleavage site. \*:  $p < 0.01$ . (C) TRRAP recruitment at DNA break induced by I-SceI was analyzed as described in panel B, by immunoprecipitating chromatin with TRRAP antibody.

**Figure 20: Fe65 suppression affects H4 acetylation at DNA double strand breaks**

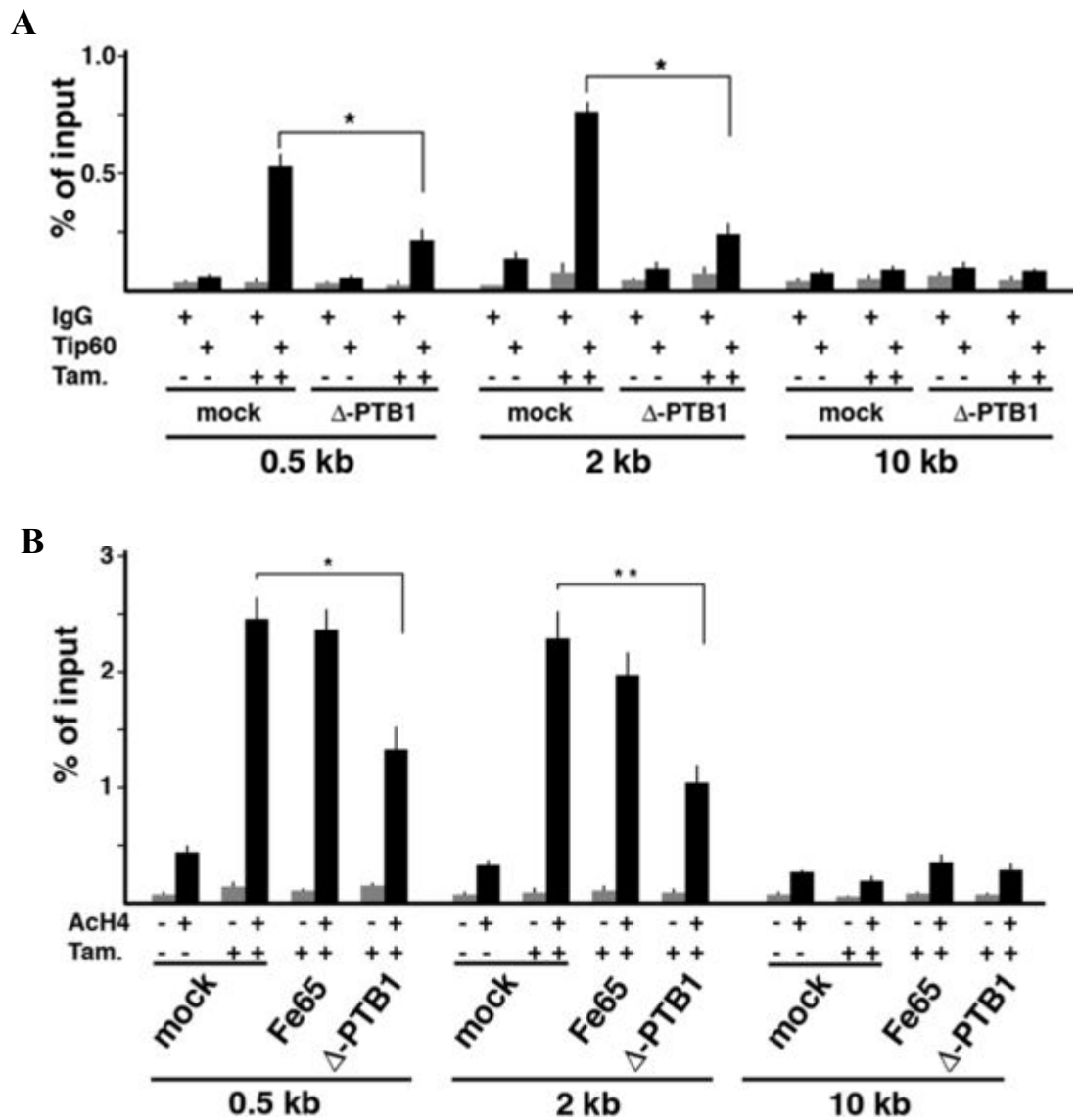


Chromatin, immunoprecipitated with an antibody recognizing acetylated histone H4, was analyzed in Fe65 KD NIH-GS cells before and after 4OH-tamoxifen induction of ISce-I-ER amplifying DNA regions located at approximately 0.5, 2 and 10 Kb downstream of the I-SceI cleavage site. Non silencing (NS) transfected NIH-GS cells were used as control. \*: p<0.01.

## **12. The $\Delta$ PTB1 mutant overexpression decreases Tip60 recruitment and histone H4 acetylation at DNA breaks.**

ChIP experiments in NIH-GS cells demonstrated that Fe65 is necessary for proper recruitment of Tip60 and its cofactor TRRAP at DNA double strand break suggesting that Tip60 could directly interact with the chromatin associated Fe65 in early steps of DNA repair. To further explore the role of Fe65/Tip60 interaction during DNA repair we analyzed the loading of Tip60 at DNA double stand break in NIH-GS cells expressing the  $\Delta$ PTB1 mutant by chromatin immunoprecipitation experiments. As shown in figure 21A the expression of  $\Delta$ -PTB1 mutant had a dominant negative effect strongly reducing Tip60 loading both at 0.5 and 2 Kb downstream regions. Accordingly H4 acetylation level was strongly reduced in  $\Delta$ PTB1 expressing NIH-GS cells compared to mock or wild type Fe65 transfected cells (figure 21B).

**Figure 21: The overexpression of  $\Delta$ PTB1 mutant impairs Tip60 loading and histone H4 acetylation at DNA double strand breaks**



A: NIH-GS cells were transfected with  $\Delta$ -PTB1 expression vector. After 24 hours, they were treated with 1  $\mu$ M tamoxifen or with vehicle (-) for 6 hours. ChIP was performed with Tip60 antibody or control IgG. Immunoprecipitated chromatin was analyzed by Real time PCR using three oligonucleotide pairs located at approximately 0.5, 2 and 10 Kb away from I-SceI cleavage site. \*:  $p < 0.01$  Overexpression of the Fe65 mutant  $\Delta$ -PTB1 decreases histone H4 acetylation at DNA breaks. NIH-GS cells were transfected with the indicated vector. ChIP experiments were performed as described in panel A. \*\*:  $p < 0.05$

### **13. The $\Delta$ PTB1 dominant negative effect depends on its interaction with chromatin**

To explain the dominant negative effect of  $\Delta$ PTB1 mutant on Tip60 loading and consequently on histone H4 acetylation at DNA double strand break, we analyzed the capability of this mutant to interact with intact and damaged chromatin using NIH-GS cellular system. We had previously demonstrated that endogenous Fe65 is widely associated with chromatin both in basal conditions and upon DNA damage induction (figure 12A and figure 13). To confirm these data we performed ChIP experiments in NIH-GS cells treated with vehicle or 4-OH tamixifen for 6 hours. Chromatin was immunoprecipitated with an anti-Fe65 antibody or control IgG and immunoprecipitated DNA was amplified by Real time PCR with the three oligo pairs described before. The endogenous Fe65 associated with chromatin in the regions surrounding the I-Sce-I site (0.5 and 2 Kb downstream regions). Moreover Fe65 was still detected 10 Kb downstream from I-SceI site confirming that it is widely associated with chromatin.

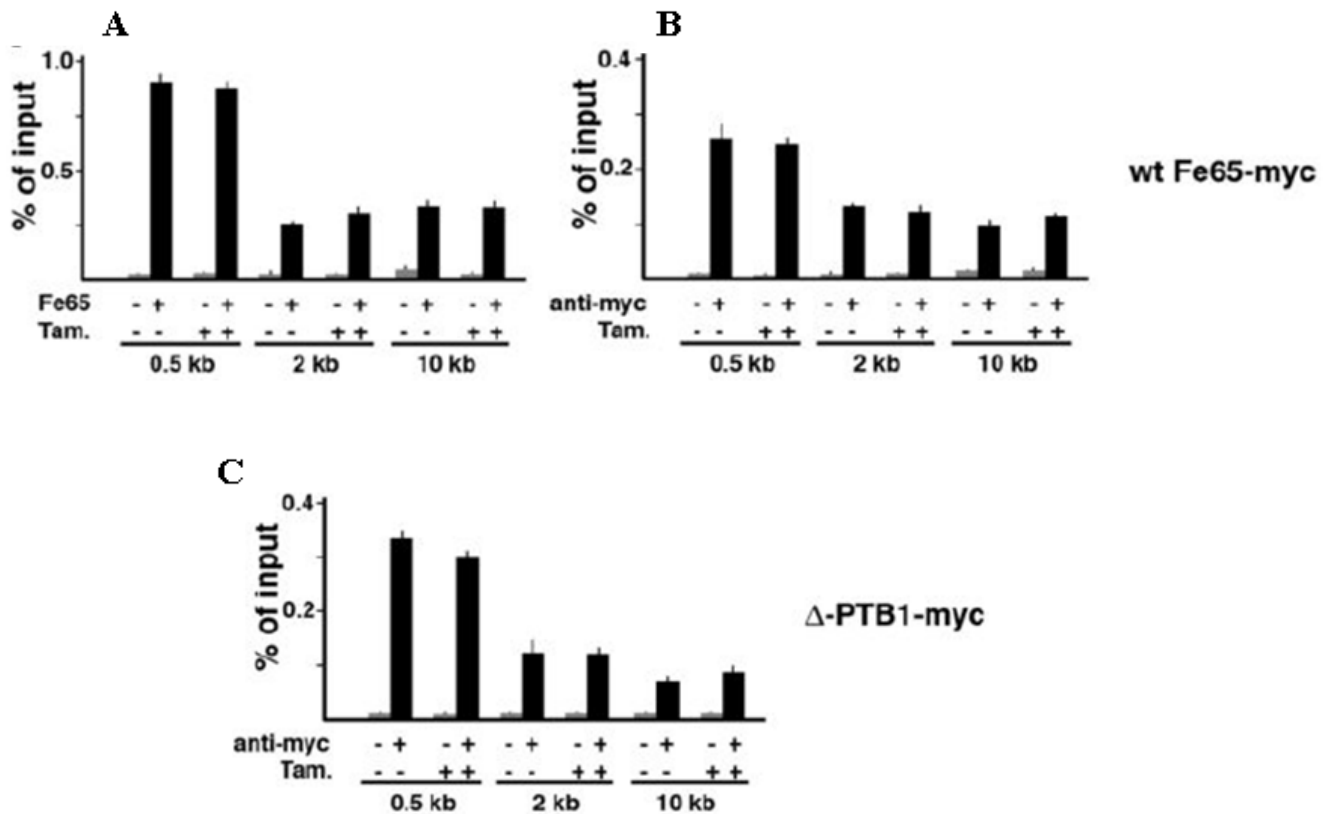
I-SceI-ER induction of double strand breaks did not alter the amount of associated protein at three analyzed sites confirming that Fe65 interacts both with intact and damaged chromatin (figure 22A).

ChIP experiments were carried out in NIH-GS cells transfected with the Fe65-myc encoding vector in which the wild type protein is fused to the myc tag. Chromatin was immunoprecipitated with an anti-myc tag antibody or control IgG and amplified with the three oligo pairs described before (figure 22B).

Similar to the endogenous protein, ectopically expressed Fe65-myc fusion protein was still able to interact with intact and damaged chromatin at three analyzed sites. Chromatin from NIH-GS cells expressing the  $\Delta$ PTB1-myc mutant was immunoprecipitated with an anti myc antibody or control IgG. The amplification of immunoprecipitated chromatin with the three oligo pairs described before, revealed that the  $\Delta$ PTB1 mutant was still able to interact with chromatin (figure 22C) thus explaining its dominant negative effect. Indeed the

$\Delta$ PTB1 mutant associated with chromatin could compete with the endogenous protein for the binding of some other partners of Fe65, which may be necessary for Fe65 proper function during chromatin remodelling associated to DNA repair.

**Figure 22: The  $\Delta$ PTB1 mutant is able to interact with intact and damaged chromatin**



A: Chromatin from NIH-GS cells were treated with 1  $\mu$ M tamoxifen or with vehicle (-) for 6 hours. ChIP was performed with an Fe65 antibody or control IgG. Immunoprecipitated chromatin was analyzed by Real time PCR using three oligonucleotide pairs located at approximately 0.5, 2 and 10 Kb away from I-SceI cleavage site. B: NIH-GS cells were transfected with an expression vector encoding the wild type Fe65 fused to the C-terminus with the myc tag. 48 hours upon transfection cells were treated with tamoxifen as in panel A and ChIP was carried out with an anti myc tag antibody or control IgG. Immunaprecipitated chromatin was amplified as in panel A. C: NIH-GS cells were transfected with an expression vector encoding the  $\Delta$ PTB1 mutant fused to the C-terminus with the myc tag. 48 hours upon transfection cells were treated with tamoxifen as in panel

A and B. ChIP was carried out with an anti myc tag antibody or control IgG. Immunoprecipitated chromatin was amplified as in panel A and B.

#### **14. Fe65 is necessary for efficient DNA repair**

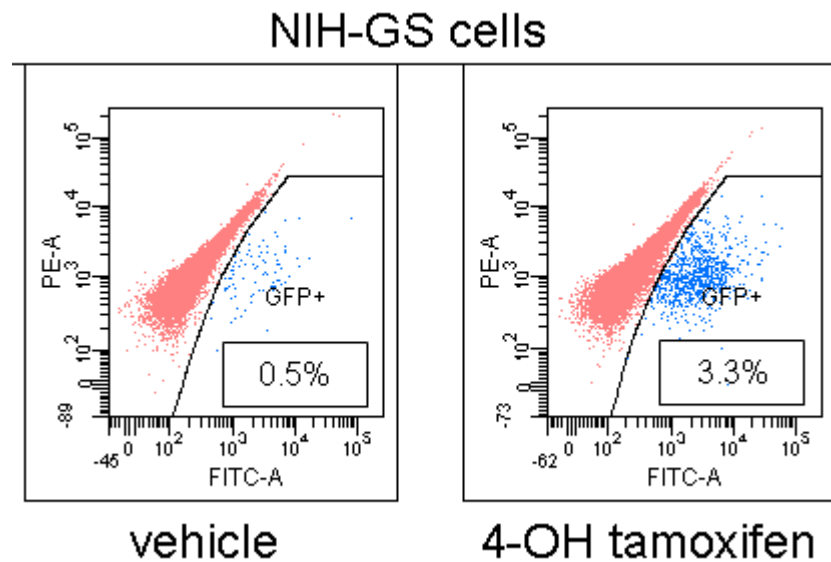
Chromatin immunoprecipitation experiments in NIH-GS cells clearly demonstrated the relevance of Fe65 in Tip60/TRRAP loading at DNA double strand breaks. As a consequence of Tip60/TRRAP decreased loading, acetylation of histone H4 was impaired in Fe65 KD cells or in  $\Delta$ PTB1 expressing cells compared to wild type.

To address the relevance of the Fe65 in DSB repair we measured the efficiency of repair in the same NIH-GS experimental system described before. These cells are stably transfected with DR-GFP and I-SceI-ER. The DR-GFP DNA fragment contains two non-functional *GFPs*. Indeed the 5' *GFP* gene in the DR-GFP sequence is under the control of the  $\beta$ -actin gene promoter, but it is mutated in order to generate two in-frame stop codons that terminate translation, thereby inactivating the GFP gene. The downstream (3') *GFP* is inactivated by upstream and downstream truncations, leaving only about 500 bp of the *GFP* sequence (see figure 18A).

When NIH-GS cells were treated with tamoxifen, the I-SceI-ER nuclear translocation results in DSBs generation. One possibility to repair these lesions is the homologous recombination repair that in this system induces intra chromosomal gene conversion leading to the reactivation of the 5' *GFP* gene. Indeed when the DSB is correctly repaired the frame of 5' *GFP* gene is restored allowing GFP expression. Thereby the extent of repair by homologous recombination was measured by counting GFP positive cells by FACS (see figure 23). In NIH-GS cells treated with 4-OH-tamoxifen the percentage of GFP positive analyzed 48 hours upon treatment, was about 3.5% whereas only few cells in the control expressed GFP. Under these conditions, we analyzed the effect of Fe65 KD on DNA repair

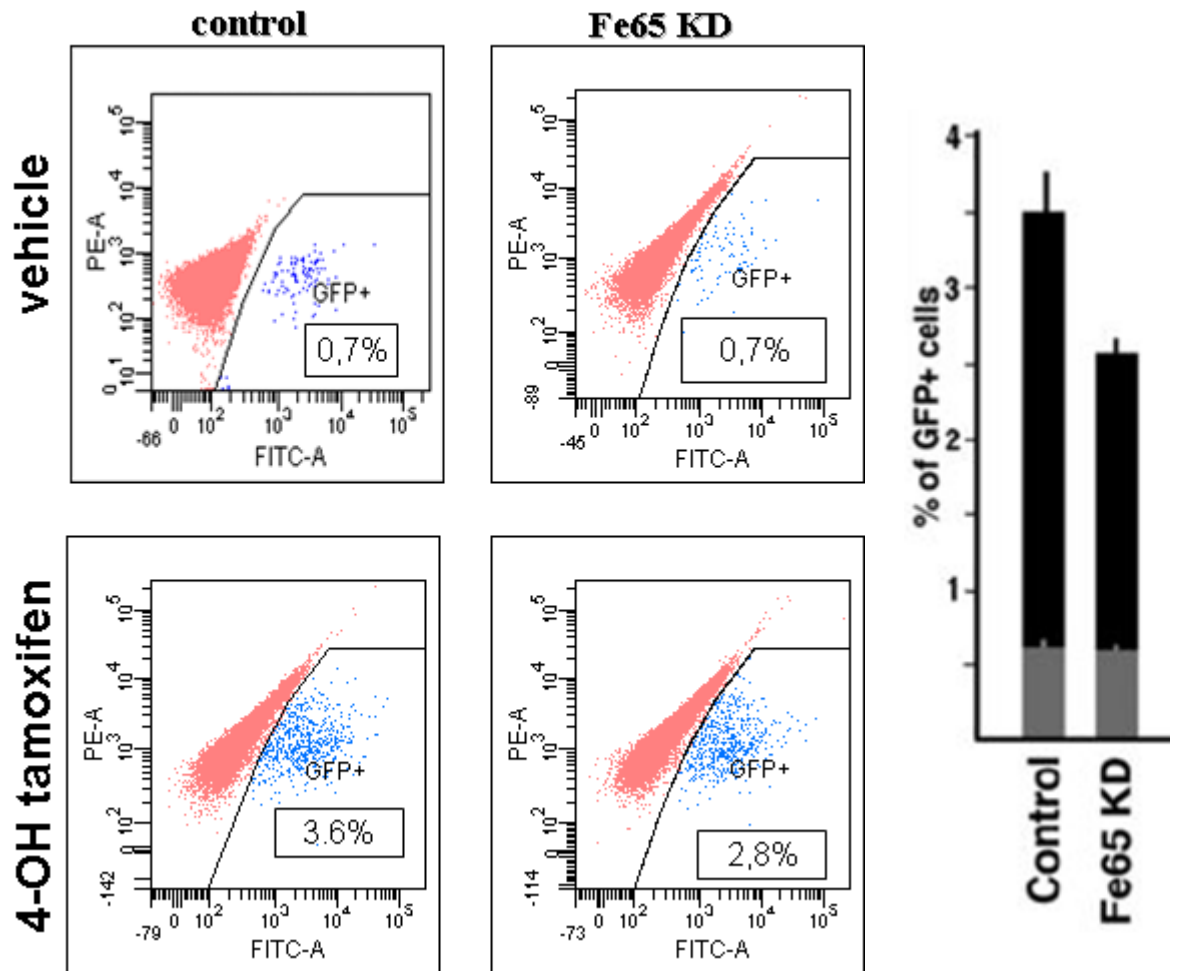
efficiency. To this aim NIH-GS cells were transfected with a pool of specific Fe65 siRNA or with non silencing siRNA as control. We measured the number of GFP positive cells by FACS analysis 48 hours after 4-OH tamoxifen exposure. As shown in figure 24 the Fe65 KD is accompanied by a significant decrease in GFP positive cells, thus clearly indicating that Fe65 KD reduced the efficiency of DNA repair. In agreement with CHIP experiments, a significant reduction of repair efficiency was also observed by transfecting NIH-GS cells the cells with the  $\Delta$ -PTB1 mutant, thus confirming the dominant negative effect of this protein (figure 25).

**Figure 23: Measurement of repair efficiency in NIH-GS cells by FACS analysis**



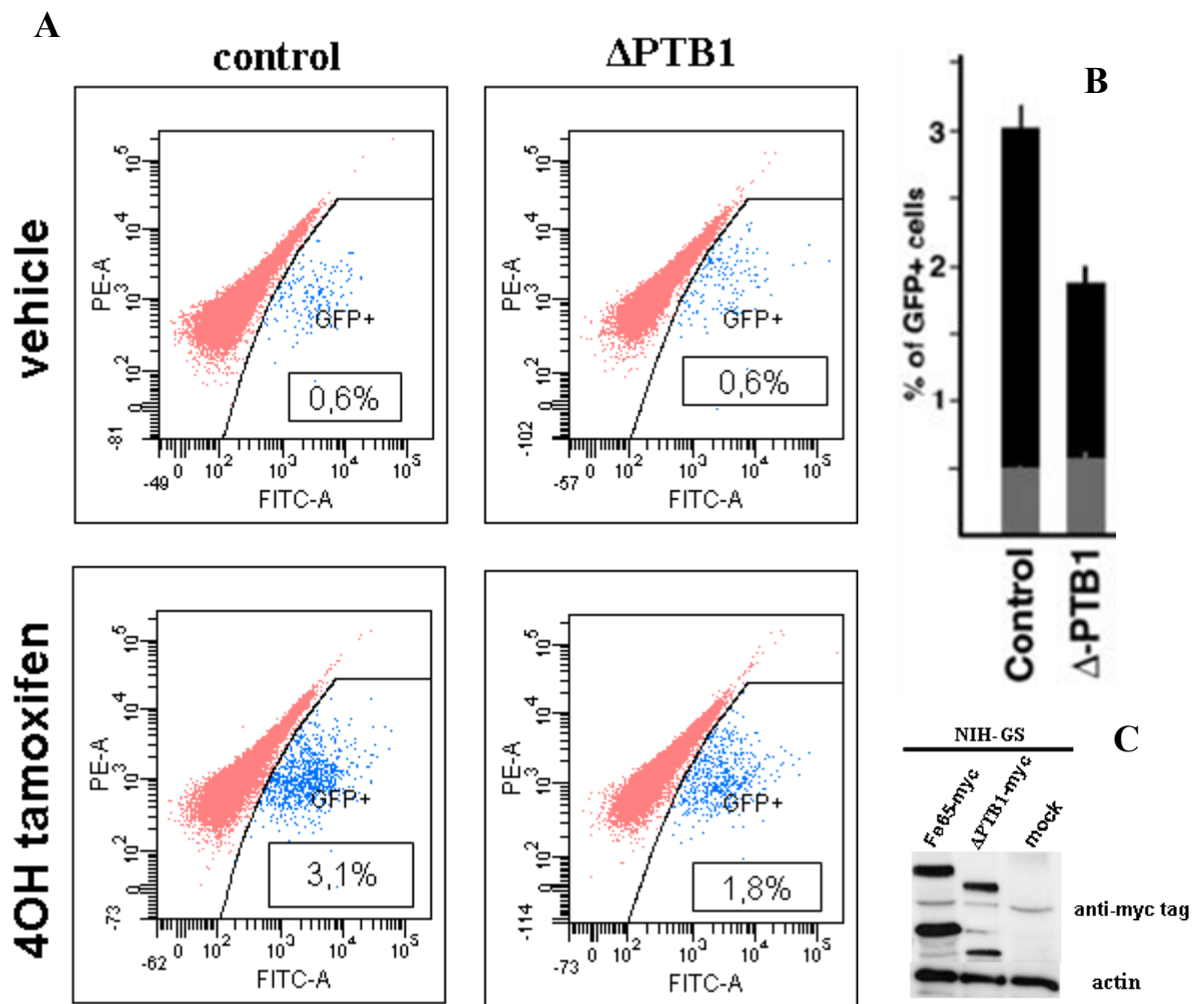
The upstream 5' *GFP* gene of DR-GFP construct, is under the control of the  $\beta$ -actin gene promoter, but it contains two in-frame stop codons that terminate translation, thereby inactivating the gene. The recombination event leads to the reactivation of the *GFP* gene, because the donor 3' *GFP* does not contain the above-mentioned stop codons. Therefore, a functional *GFP* is expressed in the cells where a successful repair takes place and the extent of repair can be measured by counting *GFP* positive cells by FACS. Two examples of FACS analyses are reported: in NIH-GS cells treated with vehicle the number of *GFP* positive cells was of about 0.5%, while it was of about 3.5% in the cells where I-SceI-ER was activated by tamoxifen.

**Figure 24: Fe65 suppression decreases DNA repair efficiency**



DNA repair efficiency in NIH-GS cells was measured by counting the percentage of GFP-positive cells 48 hours after the exposure of the cells to tamoxifen, which activates I-SceI ER. Representative FACS output of one experiment is shown: the upper panels refer to cells transfected with non-silencing control siRNA or Fe65 targeting siRNA and exposed to vehicle. The lower panels show the results obtained in cells treated with tamoxifen. The histogram reports the mean values of three independent experiments. Grey bars indicate the mean values obtained in the presence of vehicle. The difference between the two black bars is significant with a  $p < 0.01$ .

**Figure 25:  $\Delta$ PTB1 mutant overexpression impairs DNA repair efficiency**

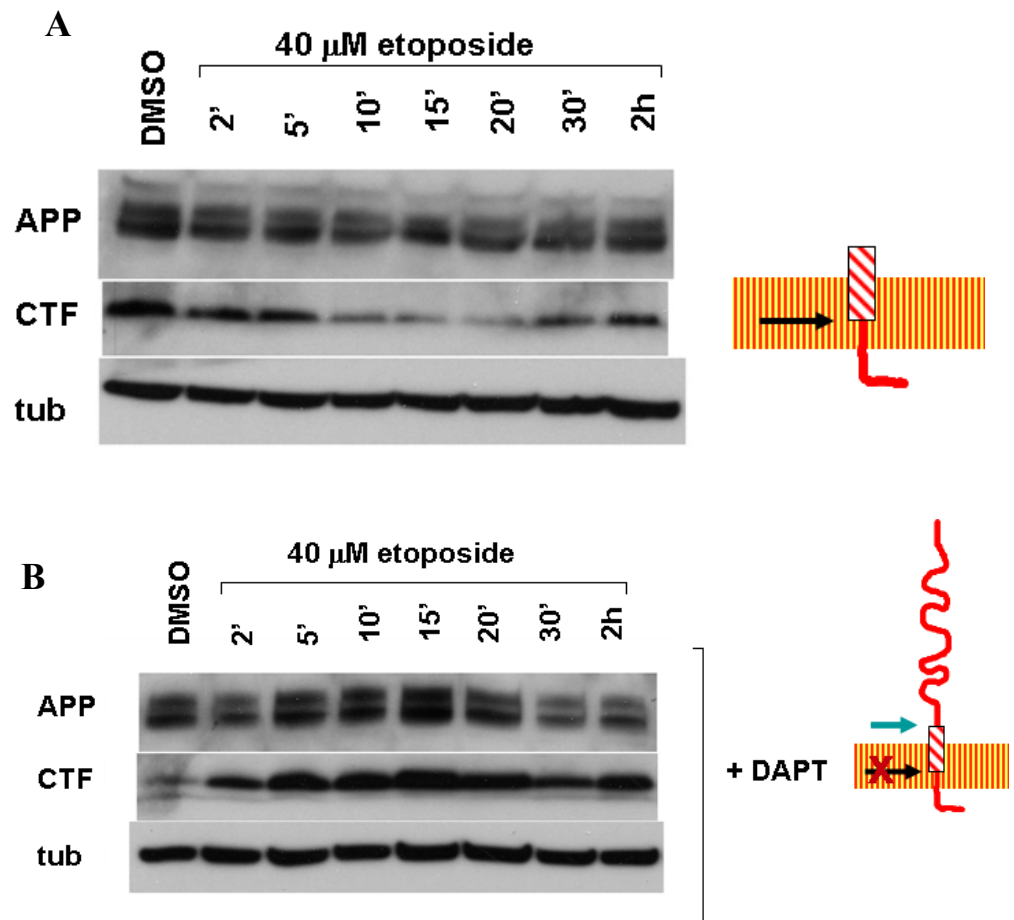


A: DNA repair efficiency in NIH-GS cells transfected with  $\Delta$ -PTB1 was measured by counting the percentage of GFP positive cells, 48 hours after the exposure of cells to tamoxifen or to vehicle for 6 hours. Representative FACS outputs of one experiment are shown: the upper panels refer to cells exposed for 6 hours to vehicle. The lower panels show the results obtained in cells treated with tamoxifen. B: The histogram reports the mean values of three independent experiments. Grey bars indicate the mean values obtained in the presence of vehicle. The difference between the two black bars is significant with a  $p < 0.01$ . C: Western blot analysis of  $\Delta$ PTB1 expression in NIH-GS cells. Actin was used for control of loading.

## **15. APP processing is induced by genotoxic stress in a $\gamma$ -secretase dependent manner**

The finding that Fe65 is a chromatin associated protein involved in Tip60 driven chromatin remodeling during DNA repair suggested us to explore the possibility that APP and its proteolytic processing could be involved in this nuclear function. Moreover we found that Fe65 undergoes rapid phosphorylation upon DNA damage induction suggesting that its phosphorylation could be the mechanism triggering NuA4 proper localization. Similar to Notch the final step of APP proteolytic processing involves the  $\gamma$ -secretase cleavage that generates the short C-terminal fragment AICD. Several data suggest that  $\gamma$ -secretase cleavage of APP could be a mechanism triggering the Fe65/AICD nuclear localization. We first analyzed the effect of etoposide treatment on APP proteolytic processing monitoring by western blot analysis the amount of the APP C-terminal fragments (CTF) derived from the cleavage of APP by  $\alpha$  - or  $\beta$ -secretase, C83 and C99, respectively. To this aim we used an APP antibody recognizing the C-terminal region of the protein that is able to detect both APP holoprotein and its CTFs. As shown in figure 26A, in the wild type, untreated MEFs, only the C83 band is clearly visible accordingly with the notion that APP ectodomain shedding is mainly due to  $\alpha$ -secretase cleavage. The treatment with 40  $\mu$ M etoposide resulted in a drastic decrease of the APP-CTF amount within few minutes and returned to basal levels two hours later. The observed decrease suggested us a possible induction of  $\gamma$ -secretase cleavage upon genotoxic stress induction. To asses this point we performed the same experiment in wild type MEFs pretreated with the  $\gamma$ -secretase inhibitor DAPT. As shown in figure 26B DAPT treatment prevents the decrease of APP-CTF clearly demonstrating that it depends on the induction of  $\gamma$ -secretase. Furthermore, both APP and APP-CTF in cells pretreated with DAPT and exposed to etoposide seemed to accumulate up to levels higher than those present in cells treated only with DAPT.

**Figure 26: Modifications of APP-CTF upon DNA damage**



APP and APP-CTF were analyzed by western blot in wild type MEFs used an antibody recognising an epitope in the C-terminal fragment of the protein (see Materials and Methods) A: Protein extracts were obtained from wild type MEFs exposed to 40μM etoposide for indicated time or to DMSO in control cells. 100μg of total protein extract was loaded per lane and tubulin was used for control of loading. The cartoon shows the APP-CTF stub in the membrane and the  $\gamma$ -secretase cleavage site (arrow).

B: Protein extracts were obtained from wild type MEFs pretreated chronically with 2μM DAPT for 24 hours and then exposed to 40μM etoposide for indicated time or to DMSO in control cells. As in A tubulin was used for control of loading. The cartoon shows the APP oloprotein, the first cleavage site that determines the shedding of the ectodomain and the inhibition of  $\gamma$ -secretase site by DAPT treatment.

These findings suggested a relationship between Fe65 modifications and the cleavage of the APP-CTF in response to DNA damage. To explore this point we analyzed the cleavage of APP-CTF in Fe65 KO MEFs. As shown in figure 27, in these cells the treatment with etoposide does not induce any changes in the amount of APP-CTF, thus further supporting that APP processing is dependent on Fe65 modification induced by genotoxic stress. Genotoxic stress induced activation of  $\gamma$ -secretase complex occurred with a little delay respect to Fe65 nuclear modification and Fe65 was necessary for the induction of  $\gamma$ -secretase cleavage of APP in response to etoposide treatment. Moreover the Fe65 mutant unable to interact with APP (C655F) did not rescue the Fe65 KO MEFs phenotype (figure 17B).

These data suggest that Fe65/APP interaction could be a crucial event in Fe65 nuclear function during DNA repair.

## **16. The interaction with APP is required for Fe65 function in DNA repair**

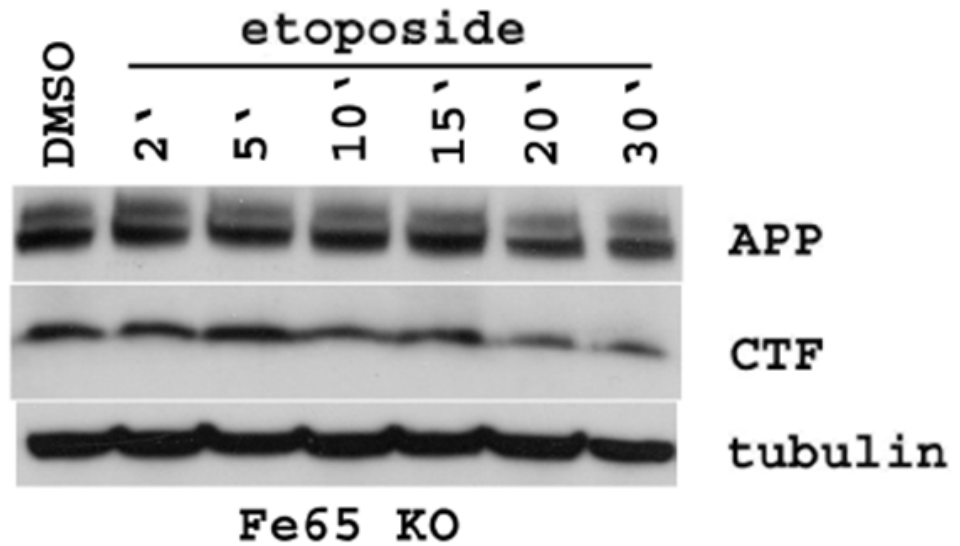
To better explore the molecular mechanism involving APP in Fe65 nuclear function during DNA repair we analyzed the effect of C655F mutant expression in NIH-GS cells.

Chromatin immunoprecipitation experiments in NIH-GS cells expressing C655F mutant demonstrated a strong decrease of Tip60 loading in the region surrounding the DSB (figure 28A) compared to control cells.

Accordingly the acetylation level of histone H4 was strongly reduced in C655F expressing cells (figure 28B).

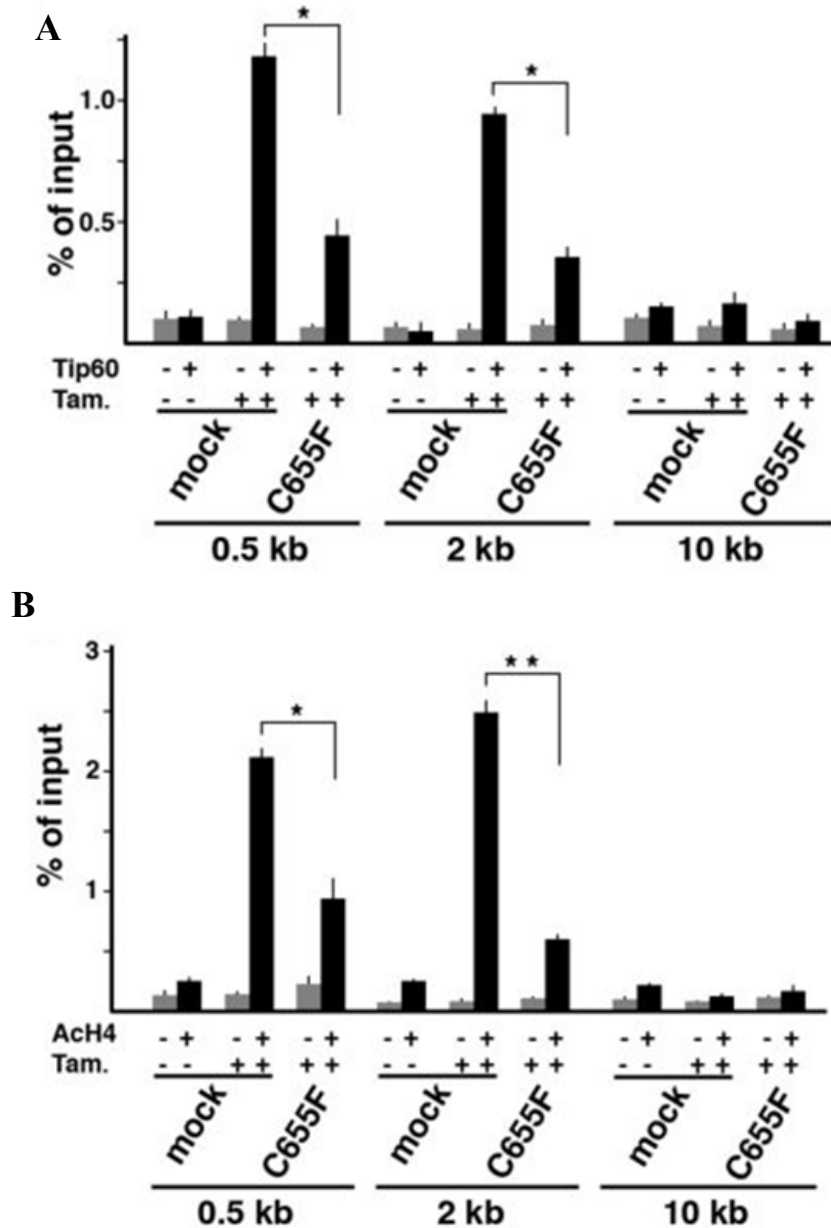
We further evaluated the effect of C655F mutant on DNA repair efficiency by FACS analysis counting the number of GFP positive cells (figure 29). As expected the expression of C655F mutant resulted in a strong dominant negative effect on DNA repair efficiency. These results suggest that the interaction with APP/AICD is necessary to allow Fe65 to adequately function during DNA repair.

**Figure 27: Genotoxic stress induced  $\gamma$ -secretase cleavage of APP depends on the presence of Fe65**



APP-CTF were analysed by western blot with an anti APP C-terminal antibody in Fe65 KO MEFs treated with etoposide at indicated time or with DMSO as control. 100 $\mu$ g of protein extract was loaded per lane. Tubulin was used for control of loading.

**Figure 28: Fe65 mutant unable to bind APP shows a dominant negative effect on Tip60 loading and histone H4 acetylation at DNA DSBs.**

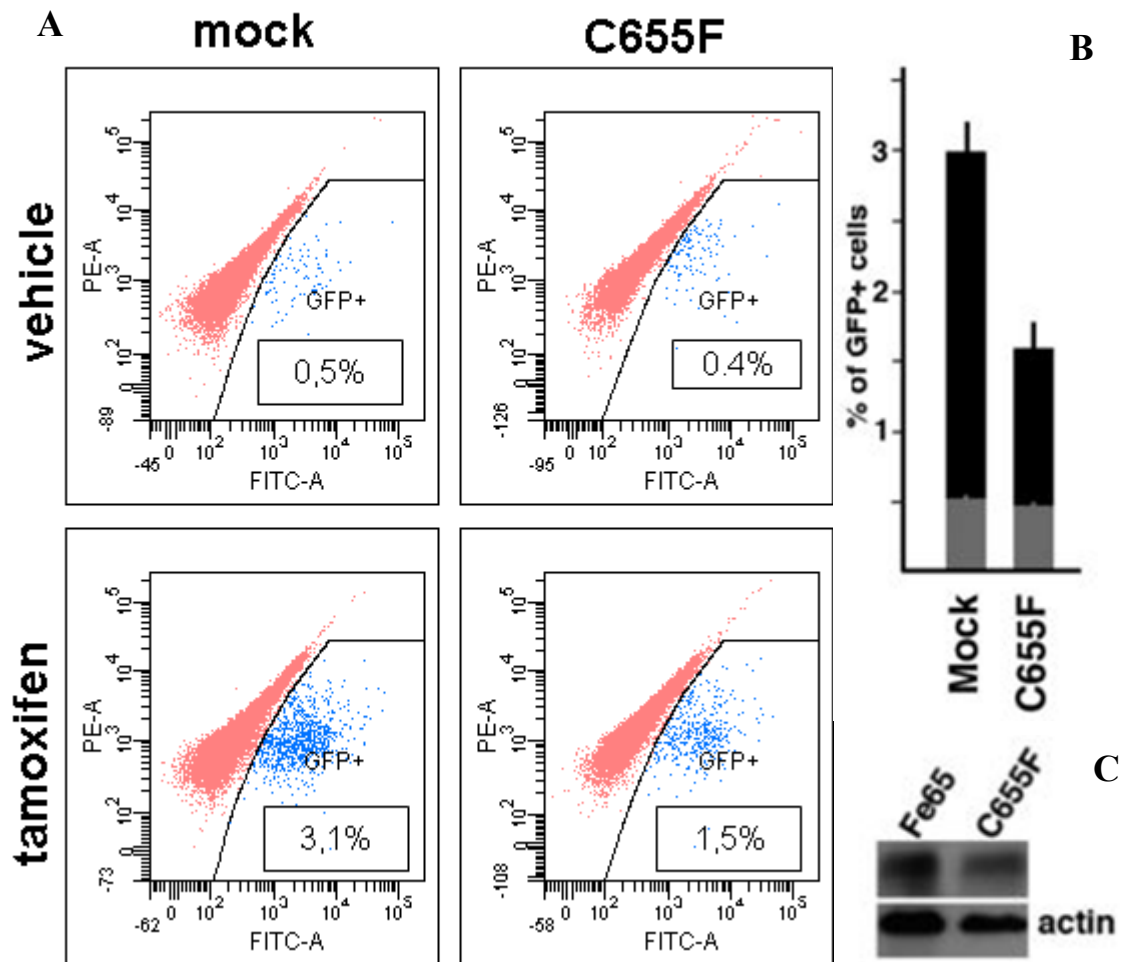


A: NIH-GS cells were transfected with C655F mutant or empty vector and exposed to tamoxifen as indicated. Chromatin was immunoprecipitated with an anti-Tip60 antibody and analyzed with the three oligo pairs described before.

B: ChIP experiments were performed as described in A using an anti-acetyl histone H4

\*\* $p < 0.001$

**Figure 29: C655F mutant has a dominant negative effect on DNA repair efficiency.**



A: DNA repair efficiency in NIH-GS cells transfected with C655F mutant was measured by counting the percentage of GFP positive cells, 48 hours after the exposure of cells to tamoxifen or to vehicle for 6 hours. Representative FACS outputs of one experiment are shown: the upper panels refer to cells exposed for 6 hours to vehicle. The lower panels show the results obtained in cells treated with tamoxifen. B: The histogram reports the mean values of three independent experiments. Grey bars indicate the mean values obtained in the presence of vehicle. The difference between the two black bars is significant with a  $p < 0.01$ . C: Western blot analysis of C655F mutant expression in NIH-GS cells. Actin was used for control of loading.

### **17. The dominant negative effect of C655F mutant depends on its inability to interact with chromatin.**

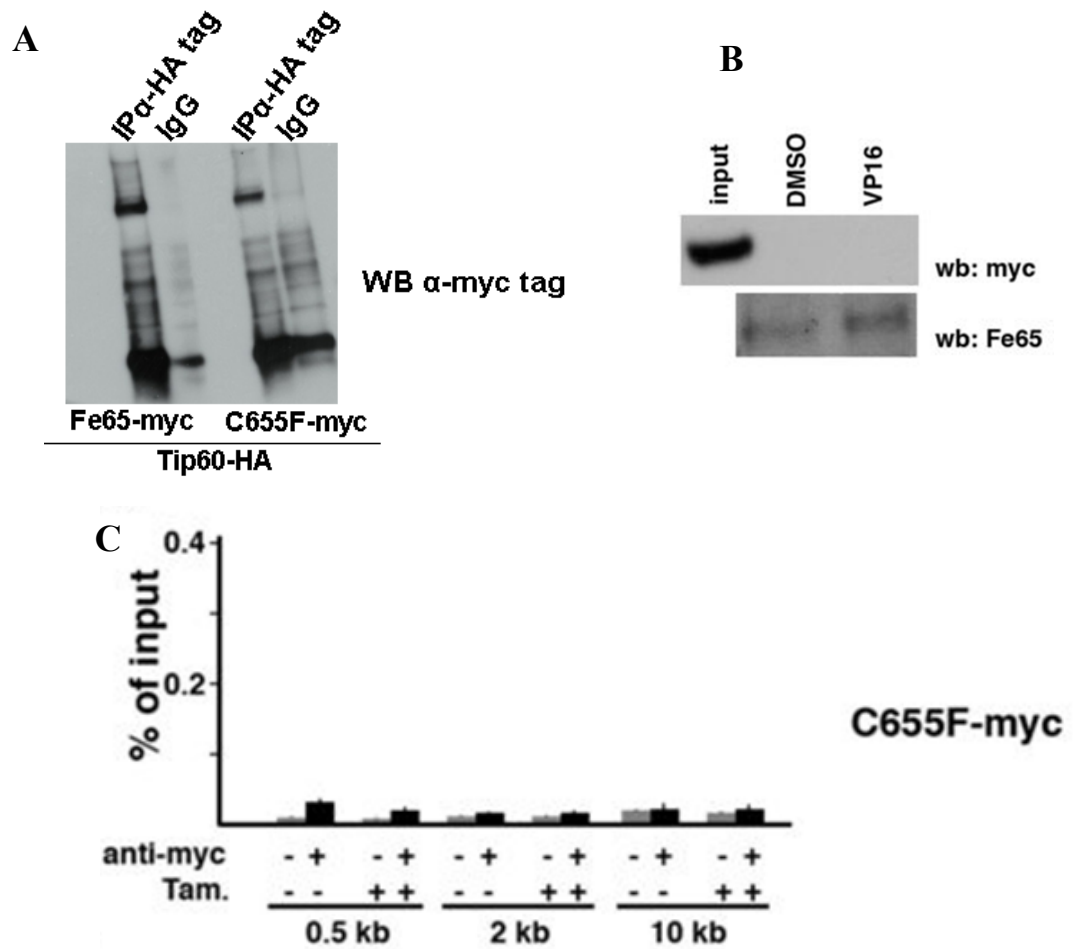
To better explore the mechanism by which the C655F mutant exerted a dominant negative effect on DNA repair we analyzed the capability of this protein to interact with Tip60. To this aim we performed co-immunoprecipitation experiments in NIH3T3 cells expressing both the Tip60-HA fusion protein and Fe65-myc in control cells or both Tip60-HA and C655F mutant. Nuclear protein extract from these cells were immunoprecipitated with an anti-HA tag antibody and immunoprecipitated protein were analyzed by western blot with an anti-myc tag antibody. As shown in figure 30A the C655F mutant binds Tip60 with the same extent of wild type protein. This result suggested that Fe65 interaction with APP is dispensable for Fe65 proper binding to Tip60.

Moreover, we analyzed the ability of C655F mutant to interact with chromatin before and after DNA damage induction in NIH-GS cellular system.

NIH-GS cells expressing the C655F-myc protein were exposed for 6 hours to tamoxifen or control vehicle. Chromatin was immunoprecipitated with an anti-myc tag antibody or control IgG. The amplification of immunoprecipitated chromatin with the three oligo pairs located at respectively 0.5, 2 and 10 Kb from I-Sce-I site revealed that C655F mutant was unable to interact with both intact and damaged chromatin (figure 30C).

These data suggested that C655F mutant exerts its dominant negative effect on DNA repair process sequestering NuA4 complex for the loading on chromatin associated Fe65 (figure 30B).

**Figure 30: The dominant negative effect of C655F mutant depends on its inability to interact with chromatin.**



A: NIH3T3 cells were transfected with both Fe65-myc and Tip60-HA expression vectors or with both C655F-myc and Tip60-HA. Nuclear protein extract were obtained from these cells 48 hours upon transfection and immunoprecipitated with an anti-HA tag antibody or with control IgG. Immunoprecipitated protein were resolved by SDS page and analysed by western blot with an anti-myc tag antibody. B: Association of C655F mutant with chromatin was analyzed as in figure 12A. The experiment shown in the upper panel demonstrated that C655F mutant was not associated to chromatin either in cells treated (VP16) or not treated (DMSO) with 100  $\mu$ M etoposide. The lower panel (re-blot of the filter shown in the upper panel) shows that endogenous Fe65 is associated with chromatin. C: ChIP experiments were carried out in NIH-GS cells expressing C655F-myc mutant as described in figure 21.

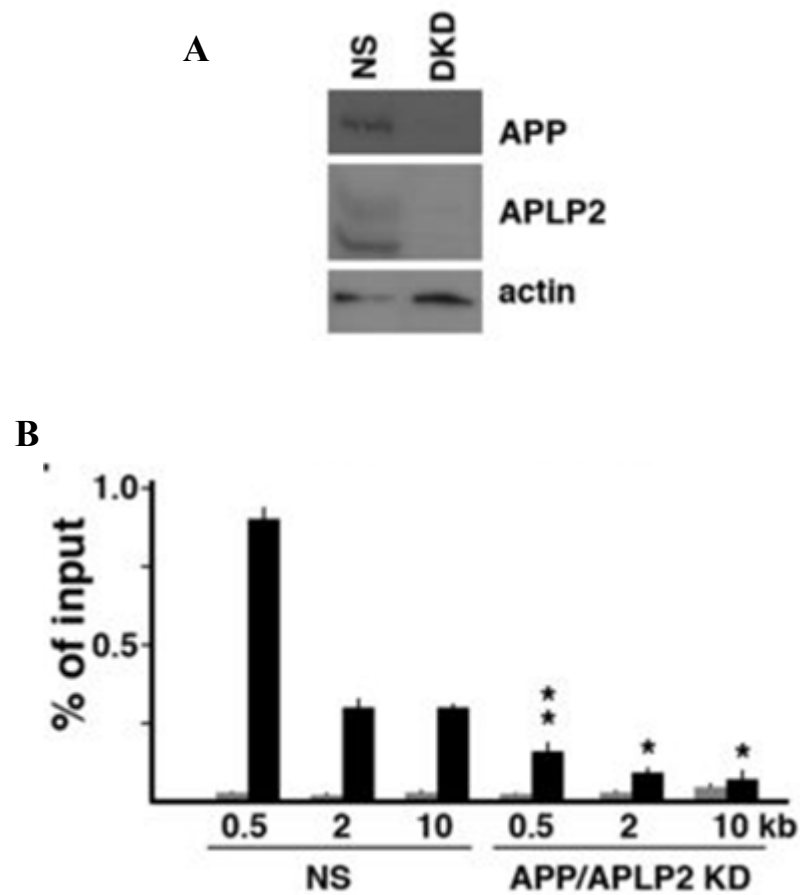
## **18. Fe65 interaction with APP is essential for its association with chromatin and in turn for its proper function in DNA repair.**

The finding that C655F mutant was unable to interact with chromatin suggested the possibility that Fe65 interaction with APP is necessary for its association with chromatin.

To better explore this point we evaluated the effect of APP/APLP2 KD on Fe65 function in DNA repair. NIH-GS cells were transfected with non silencing siRNA (NS) or with two siRNAs targeting APP and its paralogue APLP2 respectively. 48 hours upon transfection the level of both proteins was strongly reduced in APP/APLP2 double knock down cells (DKD) compared to NS (figure 31A). We first evaluated in these cells the association of Fe65 with chromatin by ChIP experiments (figure 31B).

APP/APLP2 KD abolished the association of Fe65 with chromatin at three analyzed sites thus clearly indicating that the interaction of Fe65 with APP/APLP2 is necessary to allow its association with chromatin. As expected the loading of Tip60 and TRRAP and the acetylation of histone H4 were drastically decreased in APP/APLP2 KD cells compared to non silencing cells (figure 32 A, B, C). Accordingly, DNA damage repair was less efficient in APP/APLP2 KD cells than in cells transfected with non-silencing siRNA (figure 33) as demonstrated by FACS analysis.

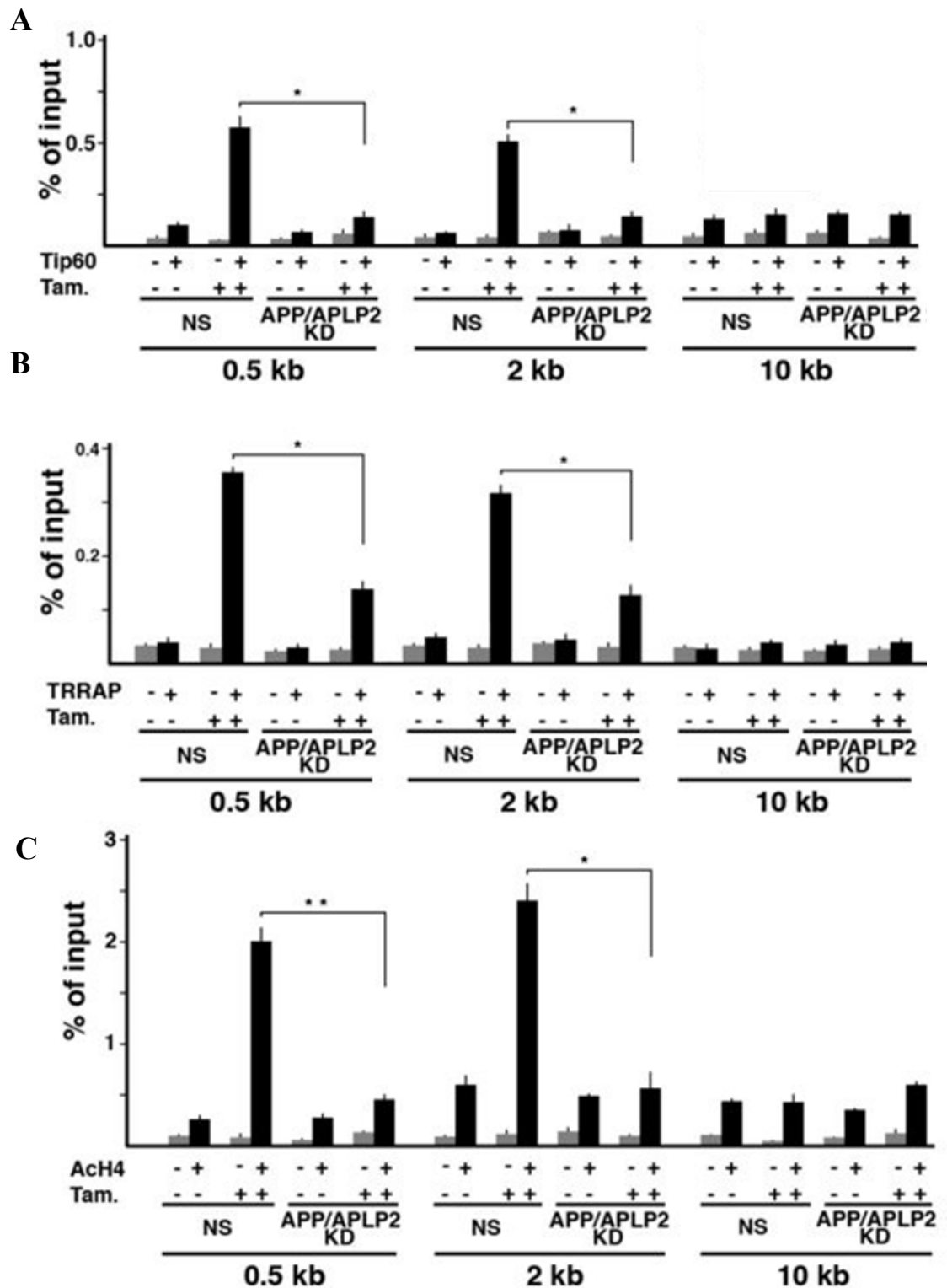
**Figure 31: APP/APLP2 KD impairs the association of Fe65 with chromatin.**



A: NIH-GS cells were transfected with non-silencing (NS) siRNA or with siRNAs targeting APP and APLP2 (double knock down; DKO). Western blot with APP or APLP2 antibodies was performed 48 hours upon transfection.

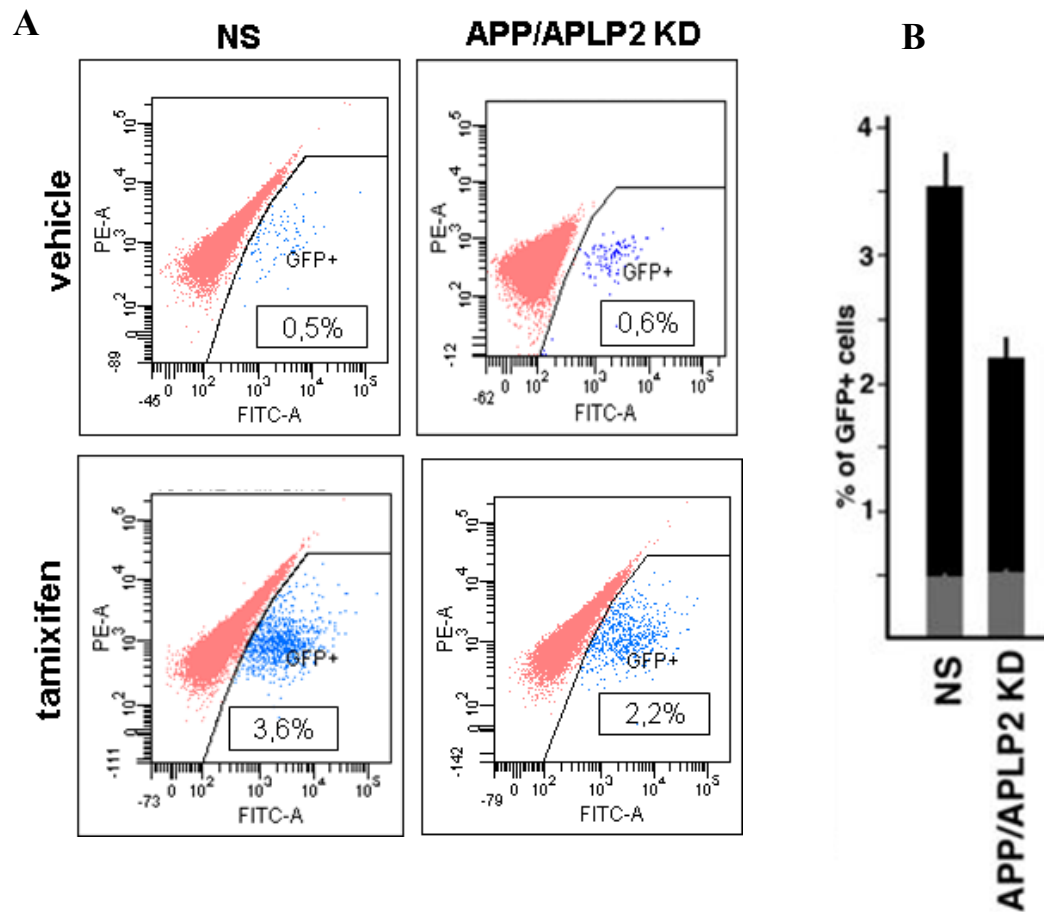
B: Chromatin from non silencing (NS) and APP/APLP2 knock down (KD) NIH-GS cells were immunoprecipitated with anti-Fe65 antibody and analyzed as described before.

**Figure 32: APP/APLP2 KD impairs the loading of NuA4 complex and histone H4 acetylation at DSBs**



Chromatin immunoprecipitation experiments were carried out as described before, in APP/APLP2 KD NIH-GS cells using anti-Tip60 (A), anti-TRRAP (B) and anti-acetyl H4 (C) antibodies.

**Figure 33: APP/APLP2 KD decreases the DNA repair efficiency in NIH-GS cells.**

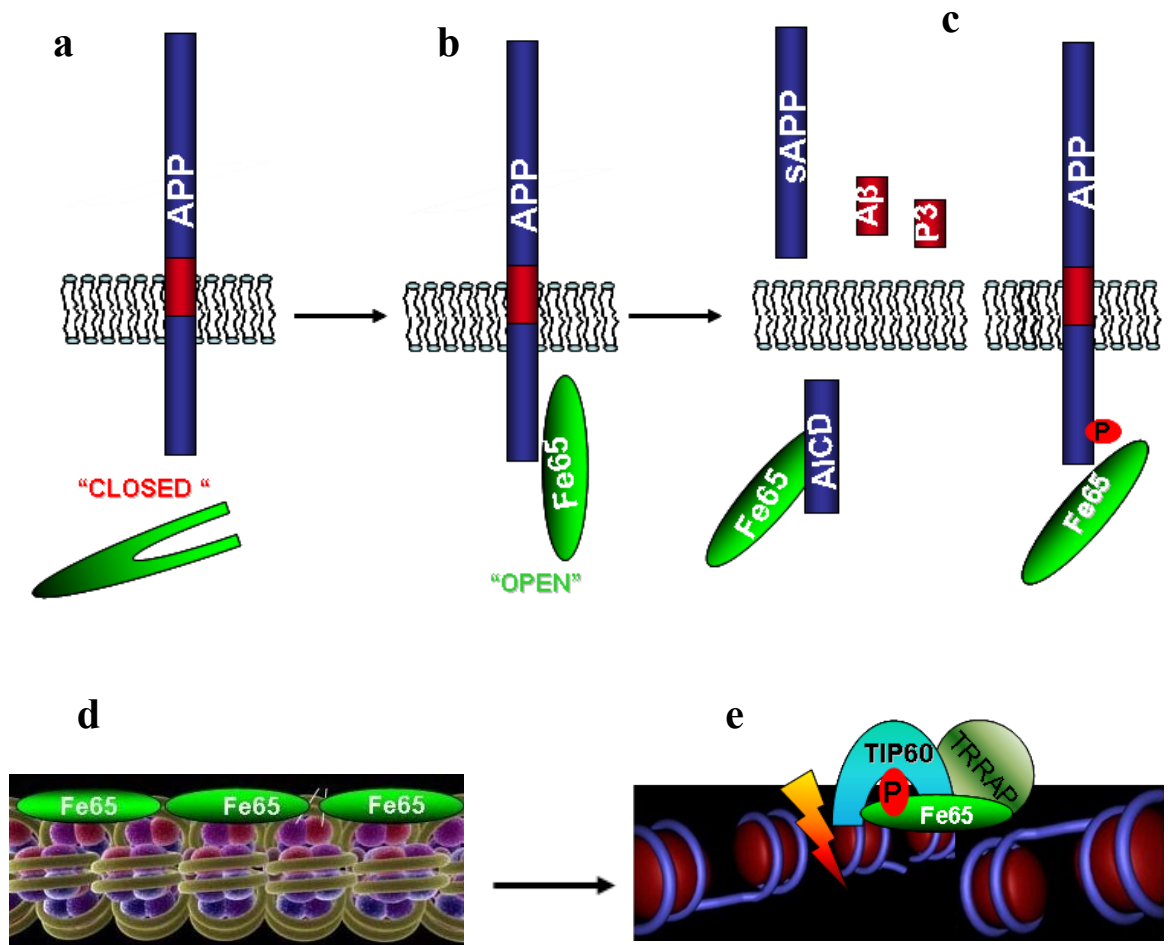


A: DNA repair efficiency in NIH-GS cells transfected with both APP and APLP2 targeting siRNAs was measured by counting the percentage of GFP positive cells, 48 hours after the exposure of cells to tamoxifen or to vehicle for 6 hours. Representative FACS outputs of one experiment are shown: the upper panels refer to cells exposed for 6 hours to vehicle. The lower panels show the results obtained in cells treated with tamoxifen. B: The histogram reports the mean values of three independent experiments. Grey bars indicate the mean values obtained in the presence of vehicle. The difference between the two black bars is significant with a  $p < 0.01$ .

## **DISCUSSION**

The phenotype of Fe65 KO cells and mice we observed at the beginning of my PhD project suggested us to explore the possible link between the function of this protein and the cellular machinery devoted to protect from and/or respond to DNA damages. Previous results suggested that Fe65 could have some nuclear functions, considering its presence in the nucleus and its interaction with several nuclear proteins. These results supported the hypothesis that Fe65 could be involved in the regulation of transcription, although most of them rely on the use of reporter gene assays. Fe65 appears to function as a key regulator of signals received and integrated at the membrane by APP holoprotein which modulates Fe65 nuclear localization and functions. Starting from the observation that the absence of Fe65 results in vivo and in vitro in high vulnerability to DNA damaging agents we tried to understand the molecular mechanism involving Fe65 and the Fe65/APP complex in this new biological function. We found for the first time that Fe65 is a chromatin bound protein that modulates the degree of chromatin condensation and is necessary for Tip60 proper function during DNA repair. Indeed the knockdown of Fe65 provokes a significant decrease in the recruitment of Tip60 and TRRAP to DNA double strand breaks. Accordingly, Fe65 suppression also provokes a dramatic decrease of histone H4 acetylation of lesioned chromatin and, in turn, the impairment of DNA repair efficiency. Furthermore, we demonstrated that the interaction of Fe65 with APP is necessary to allow Fe65 to associate with chromatin and therefore to play its role in the response to DNA damage. Based on these results we propose the hypothesis that Fe65 and its interaction with APP play a crucial role in the association of the NuA4 complex containing Tip60 and TRRAP to DNA lesion. Although further studies are necessary to definitively address the mechanisms of the Fe65 involvement in DNA repair and chromatin remodeling, available knowledge allow us to propose the model reported in Figure 34. The first step of this model is the interaction of Fe65 with APP. Our results demonstrate that a Fe65 mutant

**Figure 34: Fe65 involvement in chromatin remodelling during DNA damage repair.**



Available results support the hypothesis that Fe65 exists in two conformations. The interaction with the cytodomain of APP induces Fe65 from a “close” (a) to an “open” (b) conformation. The cleavage of APP or its phosphorylation may cause the release of Fe65 from the membrane anchor (c) thus allowing its association with chromatin (d). In basal conditions, chromatinized Fe65 appears to have a general role in favoring chromatin condensation. Chromatin associated Fe65 is necessary for the recruitment of Tip60-TRRAP-containing complex at DNA double strand breaks (e). Loss of function of the Fe65-APP machinery induces a significant decrease of DNA repair efficiency.

unable to interact with APP fails to rescue the phenotype induced by Fe65 KO. Moreover, the same mutant has a clear dominant negative effect on the recruitment of Tip60-TRRAP at the DNA lesion and, in turn, on the DNA repair efficiency of the cells (see figure 34). One possible explanation of the loss of function of the C655F mutant could be based on the model proposed by Cao and Sudhof (Cao and Sudhof 2004). This model suggests that the interaction of Fe65 with APP induces a conformational change leading Fe65 from a “closed” to an “open” conformation. The “closed” conformation could be due to an intramolecular interaction between the WW domain-containing region and the PTB domain region (Cao and Sudhof 2004). The APP cytodomain opens this structure by competing for the binding of the WW domain with the PTB2. A Fe65 deletion mutant, lacking the entire PTB2 domain, is, similarly to the C655F mutant, completely unable to interact with APP. However, this mutant protein, rescues the phenotype of Fe65 KO cells (data not shown). On this basis it could be speculated that this  $\Delta$ PTB2 mutant is in a constitutive “open” conformation, thus rescuing the absence of Fe65. On the contrary, the C655F mutant could be in a constitutive “closed” conformation, therefore being unable to rescue the effects of Fe65 suppression. The loss of the function of this C655F mutant is likely due to the fact that, opposite to what observed with wild type Fe65, it is unable to interact with the chromatin, while it is still able to interact with Tip60 (see figure 30), thus explaining why it exerts a strong dominant negative effect. Further evidence supporting the involvement of APP in the nuclear function of Fe65 comes from the results showing that the suppression of APP/APLP2 leads to the impairment of Fe65 functions. In fact, in APP/APLP2 KD cells the association of Fe65 to chromatin is strongly reduced and accordingly the recruitment of Tip60-TRRAP to damaged DNA, histone H4 acetylation and DNA damage repair are decreased. The second step of our model is the translocation of “active” Fe65 from its APP anchor site to the chromatin. One possible mechanism for this event implies the proteolytic processing of APP followed by the release of AICD-Fe65

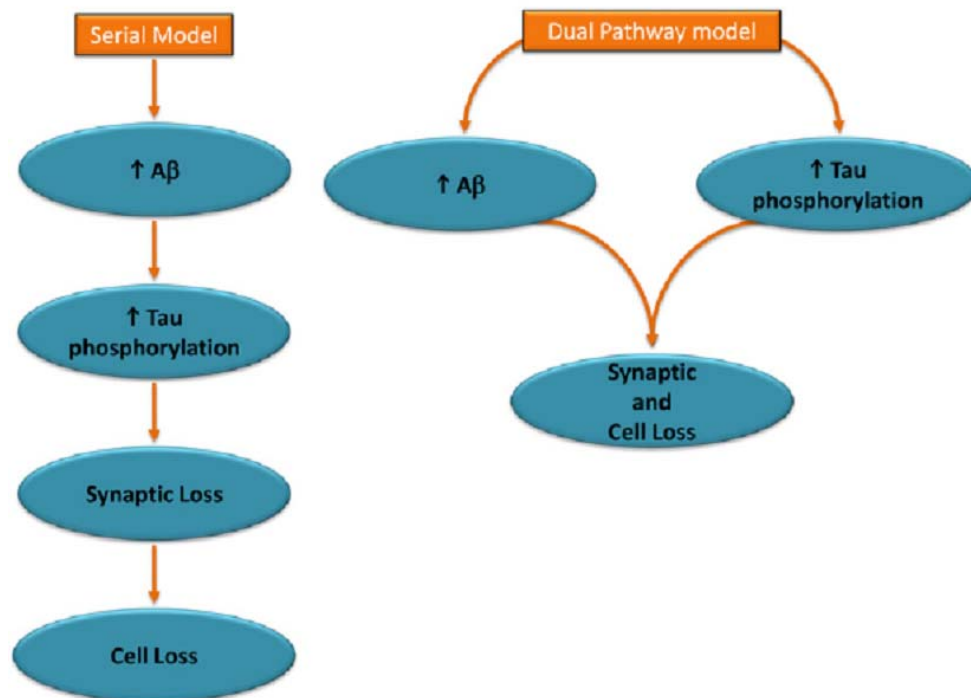
from the membrane. This possibility is supported by the induction of  $\gamma$ -secretase cleavage observed in response to DNA damaging agents (see figure 26). Another possibility is that post-translational modifications of APP and/or Fe65 cause the release of Fe65 and its nuclear translocation. For example, the phosphorylation of Thr668 of APP is an interesting candidate as a trigger mechanism inducing the release of Fe65 (Ando, Iijima et al. 2001). Our results indicate that, in basal conditions, nuclear Fe65 is associated to chromatin. As mentioned before, this association requires the interaction with APP, because a mutant Fe65 unable to interact with APP is not associated to chromatin and APP/APLP2 suppression decreases the association to chromatin of endogenous Fe65. The Fe65 KO or KD leads to a decondensation of the chromatin structure, therefore, at least in basal conditions, Fe65 seems to favor a condensed state of the chromatin. This Fe65 function remains to be studied in details. However, it seems to be distinct from that involved in the response of the cells to DNA damage and in the repair of the lesions. Chromatin fiber decompaction could be dependent at least in part on histone H4 acetylation, likely catalyzed by Tip60 (Shogren-Knaak, Ishii et al. 2006), thus Fe65 could also negatively regulate, via its interaction with Tip60, global histone acetylation and in turn the chromatin state. However, it is not expected that the phenotype observed in Fe65 KD cells, i.e. reduced efficiency of DNA repair, is a consequence of chromatin decompaction, considering that, at least in principle, decompacted chromatin should favor and not hamper DNA repair. This paradox could be explained by hypothesizing that Fe65 has two related but distinct effects on chromatin: on intact chromatin Fe65 favors the compaction of the chromatin, while, upon DNA double strand break, it stimulates the recruitment of Tip60, the acetylation of histone H4 and in turn the local relaxation of the chromatin. This possibility is reasonable if we consider that Fe65 is an adaptor molecule, which can interact with several different ligands. The  $\Delta$ PTB1 mutant has also a strong dominant negative effect. This dominant effect is in part due to the fact the this mutant was found

associated with chromatin (see figure 22) and could be the consequence of the titration of some other partners of Fe65, which may be necessary for the proper function of Fe65. Among these Fe65 partners, possibly involved in the phenomena we have described, there are the Set protein and the Abl tyrosine kinase. Both of them interact with the WW domain of Fe65 (Telese, Bruni et al. 2005) (Zambrano, Bruni et al. 2001) and could be involved in the nuclear functions of Fe65. Set is, in fact, a component of the INHAT complex (inhibitor of histone acetyl transferase) (Seo, McNamara et al. 2001) and nuclear Abl has a well-known role in the cellular response to DNA damage (Kharbanda, Ren et al. 1995). The third step concerns with the mechanisms through which Fe65 favors the recruitment of Tip60-TRRAP to the damaged DNA. Since Fe65 is associated to chromatin in basal conditions, one hypothesis is that Tip60-TRRAP containing complex is recruited to DNA lesion by binding Fe65 that is already on the chromatin. This hypothesis implies a signal inducing the interaction between Fe65 and Tip60- TRRAP. This signal could be the phosphorylation of Fe65, which was demonstrated to take place few minutes after the genotoxic stress (see figure 12). However, it cannot be definitively excluded that Fe65 suppression is affecting repair events upstream of the recruitment of Tip60-TRRAP, considering that Tip60 is involved in many different steps of DNA repair, either dependent or independent from NuA4 (Squatrito, Gorrini et al. 2006). For example, it is known that Tip60 associates with and acetylates ATM, thus promoting its activation (Sun, Jiang et al. 2005). The possibility that Fe65 suppression alters these events seems to be excluded by the finding that Fe65 KO does not affect ATM activation upon DNA damage (figure 10). The study of APP has tried to address the possible role of dysfunction of this molecule in the pathogenesis of AD. Our results suggest that the involvement of the Fe65-APP complex in the response of the cells to DNA damage and in the DNA repair machinery should be taken into account as a possible mechanism contributing to neuronal dysfunction observed in AD pathology.

In the Fe65; Fe65L1 double KO mice the phenotype observed (Guenette, Chang et al. 2006), mainly characterized by focal heterotopias of neurons likely due to the pial basement membrane disruption and intriguingly similar to that observed in APP; APLP1; APLP2 mice (Herms, Anliker et al. 2004), is very likely due to the impairment of an unknown Fe65 function different from that responsible for the phenotype we are describing. However, it should be considered that numerous human genetic diseases due to mutations of the DNA damage response machinery are also characterized by marked neurological defects (Rolig and McKinnon 2000). This close association has been interpreted either by hypothesizing a particular sensitivity of the neuronal cells to DNA damage or to the possibility that proteins involved in the response to DNA damage and cell cycle control also have additional and distinct functions in neurons. There are several observations that suggest exploring whether an altered processing of APP, and in turn a modification of its functions, could negatively affect the response of the neurons to DNA damage in AD brain, thus leading to chronic accumulation of DNA damages that could significantly contribute to the neuronal loss characteristics of AD pathology. In agreement with this possibility, it was reported that AD brains show high incidence of nuclei containing DNA strand breaks (Adamec, Vonsattel et al. 1999) and fibroblasts and lymphocytes from AD patients, exposed to DNA damaging agents, show more DNA strand breaks than the cells from normal subjects (Parshad, Sanford et al. 1996). Numerous results indicate that the neurotoxic effects of A $\beta$  could be dependent on its prooxidant activity (Reddy 2006), which could favour oxidative DNA damage. An altered response of neurons to DNA damage in AD is also suggested by the reexpression of cell cycle proteins observed in AD brain (Herrup, Neve et al. 2004). This reexpression occurs long time before the death of the neuron, thus it is hard to be considered part of a suicide mechanism to eliminate damaged cells. On the contrary, it could represent part of a mechanism to protect the cell by favoring the repair of DNA damages, also considering that cell cycle

reentry also occurs in neurons treated with DNA damaging agents (Kruman, Wersto et al. 2004). This possibility deserves further attention, also considering that numerous studies have pointed to the accumulation of DNA lesions, including double strand breaks mostly due to oxidative damage, in mild cognitive impairment and in AD. These observations indicate that DNA damage occurs in all the steps of the disease progression and DNA repair defects could significantly contribute to neurodysfunction and neurodegeneration observed in dementia (Lovell and Markesbery 2007). This hypothesis is in agreement with a new model proposed for Alzheimer disease pathogenesis. Indeed despite the unsolved questions linked to the “amyloid hypothesis”, emerging hypothesis such as the “dual pathways model” (Figure 35) (Small and Duff 2008) seems to better explain the relationship between A $\beta$  and tau abnormalities in Alzheimer disease. The “amyloid hypothesis” suggests a serial model of causality in which abnormal tau phosphorylation is a secondary disfunction due to the accumulation of A $\beta$  that leads to synaptic loss and neuronal death. The weakness of this hypothesis is mainly unmasked by the observation that although the lowering of A $\beta$  was achieved during anti-A $\beta$  immunotherapy trials, tau pathology, neuronal loss and cognitive impairment were still present in immunized AD patients. On the other hand the “dual pathways model” links the elevations of A $\beta$  peptide and tau hyperphosphorylation through common upstream molecular defects implicated in Alzheimer’s disease. Although many question remain to be addressed and many efforts are needed to demonstrate the causative role of DNA damage defects in Alzheimer disease neurodegeneration, our results open the possibility to explore the involvement of DNA damage response as the molecular defect contributing to the pathogenesis of Alzheimer’s disease.

**Figure 35: Two hypothesized models linking core features of Alzheimer's Disease**



The amyloid hypothesis assumes a serial model of causality, whereby abnormal elevations in  $A\beta$  drive tau hyperphosphorylation and other downstream manifestations of the disease. According to the dual pathway hypothesis,  $A\beta$  elevations and tau hyperphosphorylation can be linked by separate mechanisms driven by a common upstream molecular defect (from Scott A. Small 2008).

## REFERENCES

- Adamec, E., J. P. Vonsattel, et al. (1999). "DNA strand breaks in Alzheimer's disease." Brain Res **849**(1-2): 67-77.
- Agamanolis, D. P. and J. I. Greenstein (1979). "Ataxia-telangiectasia. Report of a case with Lewy bodies and vascular abnormalities within cerebral tissue." J Neuropathol Exp Neurol **38**(5): 475-89.
- Amtul, Z., P. A. Lewis, et al. (2002). "A presenilin 1 mutation associated with familial frontotemporal dementia inhibits gamma-secretase cleavage of APP and notch." Neurobiol Dis **9**(2): 269-73.
- Ando, K., K. I. Iijima, et al. (2001). "Phosphorylation-dependent regulation of the interaction of amyloid precursor protein with Fe65 affects the production of beta-amyloid." J Biol Chem **276**(43): 40353-61.
- Annaert, W. G., L. Levesque, et al. (1999). "Presenilin 1 controls gamma-secretase processing of amyloid precursor protein in pre-golgi compartments of hippocampal neurons." J Cell Biol **147**(2): 277-94.
- Atwood, C. S., G. M. Bishop, et al. (2002). "Amyloid-beta: a vascular sealant that protects against hemorrhage?" J Neurosci Res **70**(3): 356.
- Baki, L., J. Shioi, et al. (2004). "PS1 activates PI3K thus inhibiting GSK-3 activity and tau overphosphorylation: effects of FAD mutations." EMBO J **23**(13): 2586-96.
- Bakkenist, C. J. and M. B. Kastan (2004). "Initiating cellular stress responses." Cell **118**(1): 9-17.
- Barger, S. W. and A. D. Harmon (1997). "Microglial activation by Alzheimer amyloid precursor protein and modulation by apolipoprotein E." Nature **388**(6645): 878-81.
- Bartek, J. and J. Lukas (2007). "DNA damage checkpoints: from initiation to recovery or adaptation." Curr Opin Cell Biol **19**(2): 238-45.
- Barzilai, A., S. Biton, et al. (2008). "The role of the DNA damage response in neuronal development, organization and maintenance." DNA Repair (Amst) **7**(7): 1010-27.
- Beel, A. J. and C. R. Sanders (2008). "Substrate specificity of gamma-secretase and other intramembrane proteases." Cell Mol Life Sci **65**(9): 1311-34.
- Bentahir, M., O. Nyabi, et al. (2006). "Presenilin clinical mutations can affect gamma-secretase activity by different mechanisms." J Neurochem **96**(3): 732-42.
- Borchelt, D. R., G. Thinakaran, et al. (1996). "Familial Alzheimer's disease-linked presenilin 1 variants elevate Abeta1-42/1-40 ratio in vitro and in vivo." Neuron **17**(5): 1005-13.
- Borg, J. P., Y. Yang, et al. (1998). "The X11alpha protein slows cellular amyloid precursor protein processing and reduces Abeta40 and Abeta42 secretion." J Biol Chem **273**(24): 14761-6.
- Bressler, S. L., M. D. Gray, et al. (1996). "cDNA cloning and chromosome mapping of the human Fe65 gene: interaction of the conserved cytoplasmic domains of the human beta-amyloid precursor protein and its homologues with the mouse Fe65 protein." Hum Mol Genet **5**(10): 1589-98.
- Brion, J. P., A. M. Couck, et al. (1985). "Neurofibrillary tangles of Alzheimer's disease: an immunohistochemical study." J Submicrosc Cytol **17**(1): 89-96.
- Bruni, P., G. Minopoli, et al. (2002). "Fe65, a ligand of the Alzheimer's beta-amyloid precursor protein, blocks cell cycle progression by down-regulating thymidylate synthase expression." J Biol Chem **277**(38): 35481-8.
- Burstyn-Cohen, T., A. Frumkin, et al. (1998). "Accumulation of F-spondin in injured peripheral nerve promotes the outgrowth of sensory axons." J Neurosci **18**(21): 8875-85.

- Burstyn-Cohen, T., V. Tzarfaty, et al. (1999). "F-Spondin is required for accurate pathfinding of commissural axons at the floor plate." Neuron **23**(2): 233-46.
- Butz, S., M. Okamoto, et al. (1998). "A tripartite protein complex with the potential to couple synaptic vesicle exocytosis to cell adhesion in brain." Cell **94**(6): 773-82.
- Caille, I., B. Allinquant, et al. (2004). "Soluble form of amyloid precursor protein regulates proliferation of progenitors in the adult subventricular zone." Development **131**(9): 2173-81.
- Cao, X. and T. C. Sudhof (2001). "A transcriptionally [correction of transcriptively] active complex of APP with Fe65 and histone acetyltransferase Tip60." Science **293**(5527): 115-20.
- Cao, X. and T. C. Sudhof (2004). "Dissection of amyloid-beta precursor protein-dependent transcriptional transactivation." J Biol Chem **279**(23): 24601-11.
- Cappai, R., S. S. Mok, et al. (1999). "Recombinant human amyloid precursor-like protein 2 (APLP2) expressed in the yeast *Pichia pastoris* can stimulate neurite outgrowth." FEBS Lett **442**(1): 95-8.
- Cervantes, S., C. A. Saura, et al. (2004). "Functional implications of the presenilin dimerization: reconstitution of gamma-secretase activity by assembly of a catalytic site at the dimer interface of two catalytically inactive presenilins." J Biol Chem **279**(35): 36519-29.
- Chang, Y., G. Tesco, et al. (2003). "Generation of the beta-amyloid peptide and the amyloid precursor protein C-terminal fragment gamma are potentiated by FE65L1." J Biol Chem **278**(51): 51100-7.
- Citron, M., T. Oltersdorf, et al. (1992). "Mutation of the beta-amyloid precursor protein in familial Alzheimer's disease increases beta-protein production." Nature **360**(6405): 672-4.
- Conover, J. C. and R. L. Allen (2002). "The subventricular zone: new molecular and cellular developments." Cell Mol Life Sci **59**(12): 2128-35.
- Cotman, C. W. and J. H. Su (1996). "Mechanisms of neuronal death in Alzheimer's disease." Brain Pathol **6**(4): 493-506.
- Cullen, K. M., Z. Kocsi, et al. (2006). "Microvascular pathology in the aging human brain: evidence that senile plaques are sites of microhaemorrhages." Neurobiol Aging **27**(12): 1786-96.
- De Jonghe, C., C. Esselens, et al. (2001). "Pathogenic APP mutations near the gamma-secretase cleavage site differentially affect A $\beta$  secretion and APP C-terminal fragment stability." Hum Mol Genet **10**(16): 1665-71.
- Dermaut, B., S. Kumar-Singh, et al. (2004). "A novel presenilin 1 mutation associated with Pick's disease but not beta-amyloid plaques." Ann Neurol **55**(5): 617-26.
- Dickson, T. C., H. L. Saunders, et al. (1997). "Relationship between apolipoprotein E and the amyloid deposits and dystrophic neurites of Alzheimer's disease." Neuropathol Appl Neurobiol **23**(6): 483-91.
- Duilio, A., R. Faraonio, et al. (1998). "Fe65L2: a new member of the Fe65 protein family interacting with the intracellular domain of the Alzheimer's beta-amyloid precursor protein." Biochem J **330** ( Pt 1): 513-9.
- Duilio, A., N. Zambrano, et al. (1991). "A rat brain mRNA encoding a transcriptional activator homologous to the DNA binding domain of retroviral integrases." Nucleic Acids Res **19**(19): 5269-74.
- Eilam, R., Y. Peter, et al. (1998). "Selective loss of dopaminergic nigro-striatal neurons in brains of Atm-deficient mice." Proc Natl Acad Sci U S A **95**(21): 12653-6.
- Eilam, R., Y. Peter, et al. (2003). "Late degeneration of nigro-striatal neurons in ATM<sup>-/-</sup> mice." Neuroscience **121**(1): 83-98.

- Eisenhauer, P. B., R. J. Johnson, et al. (2000). "Toxicity of various amyloid beta peptide species in cultured human blood-brain barrier endothelial cells: increased toxicity of dutch-type mutant." J Neurosci Res **60**(6): 804-10.
- Ermekova, K. S., N. Zambrano, et al. (1997). "The WW domain of neural protein FE65 interacts with proline-rich motifs in Mena, the mammalian homolog of *Drosophila* enabled." J Biol Chem **272**(52): 32869-77.
- Esler, W. P. and M. S. Wolfe (2001). "A portrait of Alzheimer secretases--new features and familiar faces." Science **293**(5534): 1449-54.
- Essalmani, R., A. F. Macq, et al. (1996). "Missense mutations associated with familial Alzheimer's disease in Sweden lead to the production of the amyloid peptide without internalization of its precursor." Biochem Biophys Res Commun **218**(1): 89-96.
- Evin, G. and A. Weidemann (2002). "Biogenesis and metabolism of Alzheimer's disease Abeta amyloid peptides." Peptides **23**(7): 1285-97.
- Feinstein, Y., V. Borrell, et al. (1999). "F-spondin and mindin: two structurally and functionally related genes expressed in the hippocampus that promote outgrowth of embryonic hippocampal neurons." Development **126**(16): 3637-48.
- Feinstein, Y. and A. Klar (2004). "The neuronal class 2 TSR proteins F-spondin and Mindin: a small family with divergent biological activities." Int J Biochem Cell Biol **36**(6): 975-80.
- Ferri, C. P., M. Prince, et al. (2005). "Global prevalence of dementia: a Delphi consensus study." Lancet **366**(9503): 2112-7.
- Fiore, F., N. Zambrano, et al. (1995). "The regions of the Fe65 protein homologous to the phosphotyrosine interaction/phosphotyrosine binding domain of Shc bind the intracellular domain of the Alzheimer's amyloid precursor protein." J Biol Chem **270**(52): 30853-6.
- Fishel, M. L., M. R. Vasko, et al. (2007). "DNA repair in neurons: so if they don't divide what's to repair?" Mutat Res **614**(1-2): 24-36.
- Fluhrer, R., G. Multhaup, et al. (2003). "Identification of a beta-secretase activity, which truncates amyloid beta-peptide after its presenilin-dependent generation." J Biol Chem **278**(8): 5531-8.
- Frank, O., M. Heim, et al. (2002). "Real-time quantitative RT-PCR analysis of human bone marrow stromal cells during osteogenic differentiation in vitro." J Cell Biochem **85**(4): 737-46.
- Funamoto, S., M. Morishima-Kawashima, et al. (2004). "Truncated carboxyl-terminal fragments of beta-amyloid precursor protein are processed to amyloid beta-proteins 40 and 42." Biochemistry **43**(42): 13532-40.
- Gatei, M., D. Young, et al. (2000). "ATM-dependent phosphorylation of nibrin in response to radiation exposure." Nat Genet **25**(1): 115-9.
- Gatz, M., C. A. Reynolds, et al. (2006). "Role of genes and environments for explaining Alzheimer disease." Arch Gen Psychiatry **63**(2): 168-74.
- Ghersi, E., P. Vito, et al. (2004). "The intracellular localization of amyloid beta protein precursor (AbetaPP) intracellular domain associated protein-1 (AIDA-1) is regulated by AbetaPP and alternative splicing." J Alzheimers Dis **6**(1): 67-78.
- Gianni, D., N. Zambrano, et al. (2003). "Platelet-derived growth factor induces the beta-gamma-secretase-mediated cleavage of Alzheimer's amyloid precursor protein through a Src-Rac-dependent pathway." J Biol Chem **278**(11): 9290-7.
- Gibb, W. R. and A. J. Lees (1989). "The significance of the Lewy body in the diagnosis of idiopathic Parkinson's disease." Neuropathol Appl Neurobiol **15**(1): 27-44.
- Goldgaber, D., M. I. Lerman, et al. (1987). "Characterization and chromosomal localization of a cDNA encoding brain amyloid of Alzheimer's disease." Science **235**(4791): 877-80.

- Greenberg, S. M., E. H. Koo, et al. (1994). "Secreted beta-amyloid precursor protein stimulates mitogen-activated protein kinase and enhances tau phosphorylation." Proc Natl Acad Sci U S A **91**(15): 7104-8.
- Guenette, S., Y. Chang, et al. (2006). "Essential roles for the FE65 amyloid precursor protein-interacting proteins in brain development." EMBO J **25**(2): 420-31.
- Guenette, S. Y., J. Chen, et al. (1999). "hFE65L influences amyloid precursor protein maturation and secretion." J Neurochem **73**(3): 985-93.
- Guenette, S. Y., J. Chen, et al. (1996). "Association of a novel human FE65-like protein with the cytoplasmic domain of the beta-amyloid precursor protein." Proc Natl Acad Sci U S A **93**(20): 10832-7.
- Halliwell, B. (2006). "Oxidative stress and neurodegeneration: where are we now?" J Neurochem **97**(6): 1634-58.
- Handler, M., X. Yang, et al. (2000). "Presenilin-1 regulates neuronal differentiation during neurogenesis." Development **127**(12): 2593-606.
- Hardy, J. (1997). "Amyloid, the presenilins and Alzheimer's disease." Trends Neurosci **20**(4): 154-9.
- Hardy, J. and M. Hutton (1995). "Two new genes for Alzheimer's disease." Trends Neurosci **18**(10): 436.
- Harrison, J. C. and J. E. Haber (2006). "Surviving the breakup: the DNA damage checkpoint." Annu Rev Genet **40**: 209-35.
- Hayashi, Y., K. Kashiwagi, et al. (1994). "Alzheimer amyloid protein precursor enhances proliferation of neural stem cells from fetal rat brain." Biochem Biophys Res Commun **205**(1): 936-43.
- Heber, S., J. Herms, et al. (2000). "Mice with combined gene knock-outs reveal essential and partially redundant functions of amyloid precursor protein family members." J Neurosci **20**(21): 7951-63.
- Hebert, S. S., C. Godin, et al. (2003). "Dimerization of presenilin-1 in vivo: suggestion of novel regulatory mechanisms leading to higher order complexes." Biochem Biophys Res Commun **301**(1): 119-26.
- Heininger, K. (2000). "A unifying hypothesis of Alzheimer's disease. III. Risk factors." Hum Psychopharmacol **15**(1): 1-70.
- Helleday, T., J. Lo, et al. (2007). "DNA double-strand break repair: from mechanistic understanding to cancer treatment." DNA Repair (Amst) **6**(7): 923-35.
- Herms, J., B. Anliker, et al. (2004). "Cortical dysplasia resembling human type 2 lissencephaly in mice lacking all three APP family members." Embo J **23**(20): 4106-15.
- Herreman, A., L. Serneels, et al. (2000). "Total inactivation of gamma-secretase activity in presenilin-deficient embryonic stem cells." Nat Cell Biol **2**(7): 461-2.
- Herrup, K., R. Neve, et al. (2004). "Divide and die: cell cycle events as triggers of nerve cell death." J Neurosci **24**(42): 9232-9.
- Ho, A. and T. C. Sudhof (2004). "Binding of F-spondin to amyloid-beta precursor protein: a candidate amyloid-beta precursor protein ligand that modulates amyloid-beta precursor protein cleavage." Proc Natl Acad Sci U S A **101**(8): 2548-53.
- Hoe, H. S., L. A. Magill, et al. (2006). "FE65 interaction with the ApoE receptor ApoEr2." J Biol Chem **281**(34): 24521-30.
- Homayouni, R., D. S. Rice, et al. (1999). "Disabled-1 binds to the cytoplasmic domain of amyloid precursor-like protein 1." J Neurosci **19**(17): 7507-15.
- Howell, B. W., L. M. Lanier, et al. (1999). "The disabled 1 phosphotyrosine-binding domain binds to the internalization signals of transmembrane glycoproteins and to phospholipids." Mol Cell Biol **19**(7): 5179-88.
- Hu, Q., M. G. Hearn, et al. (1999). "Alternatively spliced isoforms of FE65 serve as neuron-specific and non-neuronal markers." J Neurosci Res **58**(5): 632-40.

- Huppert, S. S., M. X. Ilagan, et al. (2005). "Analysis of Notch function in presomitic mesoderm suggests a gamma-secretase-independent role for presenilins in somite differentiation." Dev Cell **8**(5): 677-88.
- Hutton, M., C. L. Lendon, et al. (1998). "Association of missense and 5'-splice-site mutations in tau with the inherited dementia FTDP-17." Nature **393**(6686): 702-5.
- Ikezu, T., B. D. Trapp, et al. (1998). "Caveolae, plasma membrane microdomains for alpha-secretase-mediated processing of the amyloid precursor protein." J Biol Chem **273**(17): 10485-95.
- Illenberger, S., Q. Zheng-Fischhofer, et al. (1998). "The endogenous and cell cycle-dependent phosphorylation of tau protein in living cells: implications for Alzheimer's disease." Mol Biol Cell **9**(6): 1495-512.
- Itzhaki, R. F. (1994). "Possible factors in the etiology of Alzheimer's disease." Mol Neurobiol **9**(1-3): 1-13.
- Jarrett, J. T., E. P. Berger, et al. (1993). "The carboxy terminus of the beta amyloid protein is critical for the seeding of amyloid formation: implications for the pathogenesis of Alzheimer's disease." Biochemistry **32**(18): 4693-7.
- Jeggo, P. A. and M. Lobrich (2006). "Contribution of DNA repair and cell cycle checkpoint arrest to the maintenance of genomic stability." DNA Repair (Amst) **5**(9-10): 1192-8.
- Jellinger, K. A. (2004). "Head injury and dementia." Curr Opin Neurol **17**(6): 719-23.
- Kakuda, N., S. Funamoto, et al. (2006). "Equimolar production of amyloid beta-protein and amyloid precursor protein intracellular domain from beta-carboxyl-terminal fragment by gamma-secretase." J Biol Chem **281**(21): 14776-86.
- Kang, J., H. G. Lemaire, et al. (1987). "The precursor of Alzheimer's disease amyloid A4 protein resembles a cell-surface receptor." Nature **325**(6106): 733-6.
- Katyal, S. and P. J. McKinnon (2007). "DNA repair deficiency and neurodegeneration." Cell Cycle **6**(19): 2360-5.
- Kay, B. K., M. P. Williamson, et al. (2000). "The importance of being proline: the interaction of proline-rich motifs in signaling proteins with their cognate domains." Faseb J **14**(2): 231-41.
- Kesavapany, S., S. J. Banner, et al. (2002). "Expression of the Fe65 adapter protein in adult and developing mouse brain." Neuroscience **115**(3): 951-60.
- Kharbanda, S., R. Ren, et al. (1995). "Activation of the c-Abl tyrosine kinase in the stress response to DNA-damaging agents." Nature **376**(6543): 785-8.
- Kim, H. S., E. M. Kim, et al. (2003). "C-terminal fragments of amyloid precursor protein exert neurotoxicity by inducing glycogen synthase kinase-3beta expression." Faseb J **17**(13): 1951-3.
- Kimberly, W. T., J. B. Zheng, et al. (2001). "The intracellular domain of the beta-amyloid precursor protein is stabilized by Fe65 and translocates to the nucleus in a notch-like manner." J Biol Chem **276**(43): 40288-92.
- King, G. D., K. Cherian, et al. (2004). "X11alpha impairs gamma- but not beta-cleavage of amyloid precursor protein." J Neurochem **88**(4): 971-82.
- King, G. D., R. G. Perez, et al. (2003). "X11alpha modulates secretory and endocytic trafficking and metabolism of amyloid precursor protein: mutational analysis of the YENPTY sequence." Neuroscience **120**(1): 143-54.
- Klein, J. A., C. M. Longo-Guess, et al. (2002). "The harlequin mouse mutation downregulates apoptosis-inducing factor." Nature **419**(6905): 367-74.
- Koo, E. H. and S. L. Squazzo (1994). "Evidence that production and release of amyloid beta-protein involves the endocytic pathway." J Biol Chem **269**(26): 17386-9.
- Kopan, R. and M. X. Ilagan (2004). "Gamma-secretase: proteasome of the membrane?" Nat Rev Mol Cell Biol **5**(6): 499-504.

- Kornilova, A. Y., J. Kim, et al. (2006). "Deducing the transmembrane domain organization of presenilin-1 in gamma-secretase by cysteine disulfide cross-linking." Biochemistry **45**(24): 7598-604.
- Kosik, K. S., C. L. Joachim, et al. (1986). "Microtubule-associated protein tau (tau) is a major antigenic component of paired helical filaments in Alzheimer disease." Proc Natl Acad Sci U S A **83**(11): 4044-8.
- Kruman, II, R. P. Wersto, et al. (2004). "Cell cycle activation linked to neuronal cell death initiated by DNA damage." Neuron **41**(4): 549-61.
- Kumar-Singh, S., D. Pirici, et al. (2005). "Dense-core plaques in Tg2576 and PSAPP mouse models of Alzheimer's disease are centered on vessel walls." Am J Pathol **167**(2): 527-43.
- Lai, M. T., E. Chen, et al. (2003). "Presenilin-1 and presenilin-2 exhibit distinct yet overlapping gamma-secretase activities." J Biol Chem **278**(25): 22475-81.
- Lamb, B. T., K. A. Bardel, et al. (1999). "Amyloid production and deposition in mutant amyloid precursor protein and presenilin-1 yeast artificial chromosome transgenic mice." Nat Neurosci **2**(8): 695-7.
- Laudon, H., B. Winblad, et al. (2007). "The Alzheimer's disease-associated gamma-secretase complex: functional domains in the presenilin 1 protein." Physiol Behav **92**(1-2): 115-20.
- LeBlanc, A. C. and P. Gambetti (1994). "Production of Alzheimer 4kDa beta-amyloid peptide requires the C-terminal cytosolic domain of the amyloid precursor protein." Biochem Biophys Res Commun **204**(3): 1371-80.
- LeDoux, S. P., N. M. Druzhyna, et al. (2007). "Mitochondrial DNA repair: a critical player in the response of cells of the CNS to genotoxic insults." Neuroscience **145**(4): 1249-59.
- Lee, H. G., R. J. Castellani, et al. (2005). "Amyloid-beta in Alzheimer's disease: the horse or the cart? Pathogenic or protective?" Int J Exp Pathol **86**(3): 133-8.
- Lee, J. H., K. F. Lau, et al. (2003). "The neuronal adaptor protein X11alpha reduces Abeta levels in the brains of Alzheimer's APPswe Tg2576 transgenic mice." J Biol Chem **278**(47): 47025-9.
- Lee, Y. and P. J. McKinnon (2007). "Responding to DNA double strand breaks in the nervous system." Neuroscience **145**(4): 1365-74.
- Levy-Lahad, E., A. Lahad, et al. (1995). "Apolipoprotein E genotypes and age of onset in early-onset familial Alzheimer's disease." Ann Neurol **38**(4): 678-80.
- Levy-Lahad, E., W. Wasco, et al. (1995). "Candidate gene for the chromosome 1 familial Alzheimer's disease locus." Science **269**(5226): 973-7.
- Liu, Y., Y. Wang, et al. (2008). "Involvement of xeroderma pigmentosum group A (XPA) in progeria arising from defective maturation of prelamin A." FASEB J **22**(2): 603-11.
- Lleo, A. (2008). "Activity of gamma-secretase on substrates other than APP." Curr Top Med Chem **8**(1): 9-16.
- Lovell, M. A. and W. R. Markesbery (2007). "Oxidative DNA damage in mild cognitive impairment and late-stage Alzheimer's disease." Nucleic Acids Res **35**(22): 7497-504.
- Lu, D. C., S. Rabizadeh, et al. (2000). "A second cytotoxic proteolytic peptide derived from amyloid beta-protein precursor." Nat Med **6**(4): 397-404.
- Luchsinger, J. A. and R. Mayeux (2004). "Dietary factors and Alzheimer's disease." Lancet Neurol **3**(10): 579-87.
- Lukas, C., J. Falck, et al. (2003). "Distinct spatiotemporal dynamics of mammalian checkpoint regulators induced by DNA damage." Nat Cell Biol **5**(3): 255-60.
- Margolis, B., J. P. Borg, et al. (1999). "The function of PTB domain proteins." Kidney Int **56**(4): 1230-7.

- Matsuda, S., T. Yasukawa, et al. (2001). "c-Jun N-terminal kinase (JNK)-interacting protein-1b/islet-brain-1 scaffolds Alzheimer's amyloid precursor protein with JNK." J Neurosci **21**(17): 6597-607.
- Mattson, M. P. (1997). "Cellular actions of beta-amyloid precursor protein and its soluble and fibrillogenic derivatives." Physiol Rev **77**(4): 1081-132.
- Mayeux, R. (2003). "Epidemiology of neurodegeneration." Annu Rev Neurosci **26**: 81-104.
- McCarthy, J. V. (2005). "Involvement of presenilins in cell-survival signalling pathways." Biochem Soc Trans **33**(Pt 4): 568-72.
- Minopoli, G., P. de Candia, et al. (2001). "The beta-amyloid precursor protein functions as a cytosolic anchoring site that prevents Fe65 nuclear translocation." J Biol Chem **276**(9): 6545-50.
- Minopoli, G., M. Stante, et al. (2007). "Essential roles for Fe65, Alzheimer amyloid precursor-binding protein, in the cellular response to DNA damage." J Biol Chem **282**(2): 831-5.
- Moehlmann, T., E. Winkler, et al. (2002). "Presenilin-1 mutations of leucine 166 equally affect the generation of the Notch and APP intracellular domains independent of their effect on Abeta 42 production." Proc Natl Acad Sci U S A **99**(12): 8025-30.
- Moller, H. J. and M. B. Graeber (1998). "The case described by Alois Alzheimer in 1911. Historical and conceptual perspectives based on the clinical record and neurohistological sections." Eur Arch Psychiatry Clin Neurosci **248**(3): 111-22.
- Murr, R., J. I. Loizou, et al. (2006). "Histone acetylation by Trrap-Tip60 modulates loading of repair proteins and repair of DNA double-strand breaks." Nat Cell Biol **8**(1): 91-9.
- Nakaya, T. and T. Suzuki (2006). "Role of APP phosphorylation in FE65-dependent gene transactivation mediated by AICD." Genes Cells **11**(6): 633-45.
- Noviello, C., P. Vito, et al. (2003). "Autosomal recessive hypercholesterolemia protein interacts with and regulates the cell surface level of Alzheimer's amyloid beta precursor protein." J Biol Chem **278**(34): 31843-7.
- Nukina, N. and Y. Ihara (1986). "One of the antigenic determinants of paired helical filaments is related to tau protein." J Biochem **99**(5): 1541-4.
- Nyborg, A. C., A. Y. Kornilova, et al. (2004). "Signal peptide peptidase forms a homodimer that is labeled by an active site-directed gamma-secretase inhibitor." J Biol Chem **279**(15): 15153-60.
- Oddo, S., L. Billings, et al. (2004). "Abeta immunotherapy leads to clearance of early, but not late, hyperphosphorylated tau aggregates via the proteasome." Neuron **43**(3): 321-32.
- Ohsawa, I., C. Takamura, et al. (1999). "Amino-terminal region of secreted form of amyloid precursor protein stimulates proliferation of neural stem cells." Eur J Neurosci **11**(6): 1907-13.
- Parisi, S., F. Passaro, et al. (2008). "Klf5 is involved in self-renewal of mouse embryonic stem cells." J Cell Sci **121**(Pt 16): 2629-34.
- Parks, A. L. and D. Curtis (2007). "Presenilin diversifies its portfolio." Trends Genet **23**(3): 140-50.
- Parshad, R. P., K. K. Sanford, et al. (1996). "Fluorescent light-induced chromatid breaks distinguish Alzheimer disease cells from normal cells in tissue culture." Proc Natl Acad Sci U S A **93**(10): 5146-50.
- Perkinton, M. S., C. L. Standen, et al. (2004). "The c-Abl tyrosine kinase phosphorylates the Fe65 adaptor protein to stimulate Fe65/amyloid precursor protein nuclear signaling." J Biol Chem **279**(21): 22084-91.

- Pietropaolo, S., J. Feldon, et al. (2008). "Age-dependent phenotypic characteristics of a triple transgenic mouse model of Alzheimer disease." *Behav Neurosci* **122**(4): 733-47.
- Pietropaolo, S., Y. Sun, et al. (2008). "The impact of voluntary exercise on mental health in rodents: a neuroplasticity perspective." *Behav Brain Res* **192**(1): 42-60.
- Poirier, J. (2003). "Apolipoprotein E and cholesterol metabolism in the pathogenesis and treatment of Alzheimer's disease." *Trends Mol Med* **9**(3): 94-101.
- Poirier, J., J. Davignon, et al. (1993). "Apolipoprotein E polymorphism and Alzheimer's disease." *Lancet* **342**(8873): 697-9.
- Qi-Takahara, Y., M. Morishima-Kawashima, et al. (2005). "Longer forms of amyloid beta protein: implications for the mechanism of intramembrane cleavage by gamma-secretase." *J Neurosci* **25**(2): 436-45.
- Raux, G., R. Gantier, et al. (2000). "Dementia with prominent frontotemporal features associated with L113P presenilin 1 mutation." *Neurology* **55**(10): 1577-8.
- Reddy, P. H. (2006). "Amyloid precursor protein-mediated free radicals and oxidative damage: implications for the development and progression of Alzheimer's disease." *J Neurochem* **96**(1): 1-13.
- Refolo, L. M., C. Eckman, et al. (1999). "Antisense-induced reduction of presenilin 1 expression selectively increases the production of amyloid beta42 in transfected cells." *J Neurochem* **73**(6): 2383-8.
- Richardson, C., B. Elliott, et al. (1999). "Chromosomal double-strand breaks introduced in mammalian cells by expression of I-Sce I endonuclease." *Methods Mol Biol* **113**: 453-63.
- Robbins, J. H. (1987). "Parkinson's disease, twins, and the DNA-damage hypothesis." *Ann Neurol* **21**(4): 412.
- Rogaev, E. I., R. Sherrington, et al. (1995). "Familial Alzheimer's disease in kindreds with missense mutations in a gene on chromosome 1 related to the Alzheimer's disease type 3 gene." *Nature* **376**(6543): 775-8.
- Roher, A. E. and T. A. Kokjohn (2002). "Of mice and men: The relevance of transgenic mice Abeta immunizations to Alzheimer's disease." *J Alzheimers Dis* **4**(5): 431-4.
- Rolig, R. L. and P. J. McKinnon (2000). "Linking DNA damage and neurodegeneration." *Trends Neurosci* **23**(9): 417-24.
- Roncarati, R., N. Sestan, et al. (2002). "The gamma-secretase-generated intracellular domain of beta-amyloid precursor protein binds Numb and inhibits Notch signaling." *Proc Natl Acad Sci U S A* **99**(10): 7102-7.
- Rovelet-Lecrux, A., D. Hannequin, et al. (2006). "APP locus duplication causes autosomal dominant early-onset Alzheimer disease with cerebral amyloid angiopathy." *Nat Genet* **38**(1): 24-6.
- Russo, C., V. Dolcini, et al. (2002). "Signal transduction through tyrosine-phosphorylated C-terminal fragments of amyloid precursor protein via an enhanced interaction with Shc/Grb2 adaptor proteins in reactive astrocytes of Alzheimer's disease brain." *J Biol Chem* **277**(38): 35282-8.
- Russo, T., R. Faraonio, et al. (1998). "Fe65 and the protein network centered around the cytosolic domain of the Alzheimer's beta-amyloid precursor protein." *FEBS Lett* **434**(1-2): 1-7.
- Rutten, B. P., H. Korr, et al. (2003). "The aging brain: less neurons could be better." *Mech Ageing Dev* **124**(3): 349-55.
- Rutten, B. P., C. Schmitz, et al. (2007). "The aging brain: accumulation of DNA damage or neuron loss?" *Neurobiol Aging* **28**(1): 91-8.
- Ryter, S. W., H. P. Kim, et al. (2007). "Mechanisms of cell death in oxidative stress." *Antioxid Redox Signal* **9**(1): 49-89.

- Sabo, S. L., A. F. Ikin, et al. (2003). "The amyloid precursor protein and its regulatory protein, FE65, in growth cones and synapses in vitro and in vivo." *J Neurosci* **23**(13): 5407-15.
- Sabo, S. L., L. M. Lanier, et al. (1999). "Regulation of beta-amyloid secretion by FE65, an amyloid protein precursor-binding protein." *J Biol Chem* **274**(12): 7952-7.
- Sato, T., N. Dohmae, et al. (2003). "Potential link between amyloid beta-protein 42 and C-terminal fragment gamma 49-99 of beta-amyloid precursor protein." *J Biol Chem* **278**(27): 24294-301.
- Sato, T., Y. Tanimura, et al. (2005). "Blocking the cleavage at midportion between gamma- and epsilon-sites remarkably suppresses the generation of amyloid beta-protein." *FEBS Lett* **579**(13): 2907-12.
- Saura, C. A., S. Y. Choi, et al. (2004). "Loss of presenilin function causes impairments of memory and synaptic plasticity followed by age-dependent neurodegeneration." *Neuron* **42**(1): 23-36.
- Scheinfeld, M. H., R. Roncarati, et al. (2002). "Jun NH2-terminal kinase (JNK) interacting protein 1 (JIP1) binds the cytoplasmic domain of the Alzheimer's beta-amyloid precursor protein (APP)." *J Biol Chem* **277**(5): 3767-75.
- Scheuner, D., C. Eckman, et al. (1996). "Secreted amyloid beta-protein similar to that in the senile plaques of Alzheimer's disease is increased in vivo by the presenilin 1 and 2 and APP mutations linked to familial Alzheimer's disease." *Nat Med* **2**(8): 864-70.
- Schroeter, E. H., M. X. Ilagan, et al. (2003). "A presenilin dimer at the core of the gamma-secretase enzyme: insights from parallel analysis of Notch 1 and APP proteolysis." *Proc Natl Acad Sci U S A* **100**(22): 13075-80.
- Selkoe, D. and R. Kopan (2003). "Notch and Presenilin: regulated intramembrane proteolysis links development and degeneration." *Annu Rev Neurosci* **26**: 565-97.
- Selkoe, D. J. (2001). "Alzheimer's disease: genes, proteins, and therapy." *Physiol Rev* **81**(2): 741-66.
- Seo, S. B., P. McNamara, et al. (2001). "Regulation of histone acetylation and transcription by INHAT, a human cellular complex containing the set oncoprotein." *Cell* **104**(1): 119-30.
- Shen, J., R. T. Bronson, et al. (1997). "Skeletal and CNS defects in Presenilin-1-deficient mice." *Cell* **89**(4): 629-39.
- Sherrington, R., E. I. Rogaev, et al. (1995). "Cloning of a gene bearing missense mutations in early-onset familial Alzheimer's disease." *Nature* **375**(6534): 754-60.
- Shiloh, Y. (2003). "ATM and related protein kinases: safeguarding genome integrity." *Nat Rev Cancer* **3**(3): 155-68.
- Shiloh, Y. (2006). "The ATM-mediated DNA-damage response: taking shape." *Trends Biochem Sci* **31**(7): 402-10.
- Shogren-Knaak, M., H. Ishii, et al. (2006). "Histone H4-K16 acetylation controls chromatin structure and protein interactions." *Science* **311**(5762): 844-7.
- Simeone, A., A. Duilio, et al. (1994). "Expression of the neuron-specific FE65 gene marks the development of embryo ganglionic derivatives." *Dev Neurosci* **16**(1-2): 53-60.
- Small, S. A. and K. Duff (2008). "Linking Abeta and tau in late-onset Alzheimer's disease: a dual pathway hypothesis." *Neuron* **60**(4): 534-42.
- Song, W., P. Nadeau, et al. (1999). "Proteolytic release and nuclear translocation of Notch-1 are induced by presenilin-1 and impaired by pathogenic presenilin-1 mutations." *Proc Natl Acad Sci U S A* **96**(12): 6959-63.
- Squatrito, M., C. Gorrini, et al. (2006). "Tip60 in DNA damage response and growth control: many tricks in one HAT." *Trends Cell Biol* **16**(9): 433-42.

- St George-Hyslop, P. H., J. L. Haines, et al. (1990). "Genetic linkage studies suggest that Alzheimer's disease is not a single homogeneous disorder. FAD Collaborative Study Group." *Nature* **347**(6289): 194-7.
- Stante, M., G. Minopoli, et al. (2009). "Fe65 is required for Tip60-directed histone H4 acetylation at DNA strand breaks." *Proc Natl Acad Sci U S A* **106**(13): 5093-8.
- Sun, Y., X. Jiang, et al. (2005). "A role for the Tip60 histone acetyltransferase in the acetylation and activation of ATM." *Proc Natl Acad Sci U S A* **102**(37): 13182-7.
- Suzuki, N., T. T. Cheung, et al. (1994). "An increased percentage of long amyloid beta protein secreted by familial amyloid beta protein precursor (beta APP717) mutants." *Science* **264**(5163): 1336-40.
- Tanzi, R. E. and L. Bertram (2005). "Twenty years of the Alzheimer's disease amyloid hypothesis: a genetic perspective." *Cell* **120**(4): 545-55.
- Tarr, P. E., R. Roncarati, et al. (2002). "Tyrosine phosphorylation of the beta-amyloid precursor protein cytoplasmic tail promotes interaction with Shc." *J Biol Chem* **277**(19): 16798-804.
- Telese, F., P. Bruni, et al. (2005). "Transcription regulation by the adaptor protein Fe65 and the nucleosome assembly factor SET." *EMBO Rep* **6**(1): 77-82.
- Terry, R. D., L. A. Hansen, et al. (1987). "Senile dementia of the Alzheimer type without neocortical neurofibrillary tangles." *J Neuropathol Exp Neurol* **46**(3): 262-8.
- Thinakaran, G. and A. T. Parent (2004). "Identification of the role of presenilins beyond Alzheimer's disease." *Pharmacol Res* **50**(4): 411-8.
- Tomita, T. and T. Iwatsubo (1999). "[Molecular cell biology of presenilins]." *Nippon Yakurigaku Zasshi* **114**(6): 337-46.
- Trommsdorff, M., J. P. Borg, et al. (1998). "Interaction of cytosolic adaptor proteins with neuronal apolipoprotein E receptors and the amyloid precursor protein." *J Biol Chem* **273**(50): 33556-60.
- van Gent, D. C. and M. van der Burg (2007). "Non-homologous end-joining, a sticky affair." *Oncogene* **26**(56): 7731-40.
- Van Nostrand, W. E., J. P. Melchor, et al. (2001). "Pathogenic effects of D23N Iowa mutant amyloid beta -protein." *J Biol Chem* **276**(35): 32860-6.
- von Koch, C. S., H. Zheng, et al. (1997). "Generation of APLP2 KO mice and early postnatal lethality in APLP2/APP double KO mice." *Neurobiol Aging* **18**(6): 661-9.
- Wang, P., G. Yang, et al. (2005). "Defective neuromuscular synapses in mice lacking amyloid precursor protein (APP) and APP-Like protein 2." *J Neurosci* **25**(5): 1219-25.
- Wang, Z., R. Natta, et al. (2000). "Toxicity of Dutch (E22Q) and Flemish (A21G) mutant amyloid beta proteins to human cerebral microvessel and aortic smooth muscle cells." *Stroke* **31**(2): 534-8.
- Wasco, W., K. Bupp, et al. (1992). "Identification of a mouse brain cDNA that encodes a protein related to the Alzheimer disease-associated amyloid beta protein precursor." *Proc Natl Acad Sci U S A* **89**(22): 10758-62.
- Weissman, L., N. C. de Souza-Pinto, et al. (2007). "DNA repair, mitochondria, and neurodegeneration." *Neuroscience* **145**(4): 1318-29.
- Weller, R. O., M. Subash, et al. (2008). "Perivascular drainage of amyloid-beta peptides from the brain and its failure in cerebral amyloid angiopathy and Alzheimer's disease." *Brain Pathol* **18**(2): 253-66.
- Wines-Samuelson, M. and J. Shen (2005). "Presenilins in the developing, adult, and aging cerebral cortex." *Neuroscientist* **11**(5): 441-51.
- Wolfe, M. S. (2006). "Alzheimer protease hitches a ride." *Nat Med* **12**(12): 1352-4.
- Wolfe, M. S., J. De Los Angeles, et al. (1999). "Are presenilins intramembrane-cleaving proteases? Implications for the molecular mechanism of Alzheimer's disease." *Biochemistry* **38**(35): 11223-30.

- Wolfe, M. S., W. Xia, et al. (1999). "Two transmembrane aspartates in presenilin-1 required for presenilin endoproteolysis and gamma-secretase activity." *Nature* **398**(6727): 513-7.
- Wong, P. C., H. Zheng, et al. (1997). "Presenilin 1 is required for Notch1 and DII1 expression in the paraxial mesoderm." *Nature* **387**(6630): 288-92.
- Wood, J. G., S. S. Mirra, et al. (1986). "Neurofibrillary tangles of Alzheimer disease share antigenic determinants with the axonal microtubule-associated protein tau (tau)." *Proc Natl Acad Sci U S A* **83**(11): 4040-3.
- Wu, X., V. Ranganathan, et al. (2000). "ATM phosphorylation of Nijmegen breakage syndrome protein is required in a DNA damage response." *Nature* **405**(6785): 477-82.
- Wyman, C. and R. Kanaar (2006). "DNA double-strand break repair: all's well that ends well." *Annu Rev Genet* **40**: 363-83.
- Xu, F., J. Davis, et al. (2005). "Protease nexin-2/amyloid beta-protein precursor limits cerebral thrombosis." *Proc Natl Acad Sci U S A* **102**(50): 18135-40.
- Yagishita, S., M. Morishima-Kawashima, et al. (2006). "DAPT-induced intracellular accumulations of longer amyloid beta-proteins: further implications for the mechanism of intramembrane cleavage by gamma-secretase." *Biochemistry* **45**(12): 3952-60.
- Yasuoka, K., K. Hirata, et al. (2004). "Expression of amyloid precursor protein-like molecule in astroglial cells of the subventricular zone and rostral migratory stream of the adult rat forebrain." *J Anat* **205**(2): 135-46.
- Yu, C., S. H. Kim, et al. (2001). "Characterization of a presenilin-mediated amyloid precursor protein carboxyl-terminal fragment gamma. Evidence for distinct mechanisms involved in gamma -secretase processing of the APP and Notch1 transmembrane domains." *J Biol Chem* **276**(47): 43756-60.
- Zambrano, N., P. Bruni, et al. (2001). "The beta-amyloid precursor protein APP is tyrosine-phosphorylated in cells expressing a constitutively active form of the Abl protooncogene." *J Biol Chem* **276**(23): 19787-92.
- Zambrano, N., J. D. Buxbaum, et al. (1997). "Interaction of the phosphotyrosine interaction/phosphotyrosine binding-related domains of Fe65 with wild-type and mutant Alzheimer's beta-amyloid precursor proteins." *J Biol Chem* **272**(10): 6399-405.
- Zambrano, N., G. Minopoli, et al. (1998). "The Fe65 adaptor protein interacts through its PID1 domain with the transcription factor CP2/LSF/LBP1." *J Biol Chem* **273**(32): 20128-33.
- Zhang, Y., C. Goodyer, et al. (2000). "Selective and protracted apoptosis in human primary neurons microinjected with active caspase-3, -6, -7, and -8." *J Neurosci* **20**(22): 8384-9.
- Zhou, D., C. Novello, et al. (2004). "Growth factor receptor-bound protein 2 interaction with the tyrosine-phosphorylated tail of amyloid beta precursor protein is mediated by its Src homology 2 domain." *J Biol Chem* **279**(24): 25374-80.